

# A second-order direct Eulerian GRP scheme for ten-moment Gaussian closure equations with source terms

Jiangfu Wang<sup>a</sup>, Huazhong Tang<sup>b,a,\*</sup>

<sup>a</sup>Center for Applied Physics and Technology, HEDPS and LMAM, School of Mathematical Sciences, Peking University, Beijing, 100871, PR China.

<sup>b</sup>Nanchang Hangkong University, Nanchang, 330000, Jiangxi Province, PR China.

---

## Abstract

This paper proposes a second-order accurate direct Eulerian generalized Riemann problem (GRP) scheme for the ten-moment Gaussian closure equations with source terms. The generalized Riemann invariants associated with the rarefaction waves, the contact discontinuity and the shear waves are given, and the 1D exact Riemann solver is obtained. After that, the generalized Riemann invariants and the Rankine-Hugoniot jump conditions are directly used to resolve the left and right nonlinear waves (rarefaction wave and shock wave) of the local GRP in Eulerian formulation, and then the 1D direct Eulerian GRP scheme is derived. They are much more complicated, technical and nontrivial due to more physical variables and elementary waves. Some 1D and 2D numerical experiments are presented to check the accuracy and high resolution of the proposed GRP schemes, where the 2D direct Eulerian GRP scheme is given by using the Strang splitting method for simplicity. It should be emphasized that several examples of 2D Riemann problems are constructed for the first time.

*Keywords:* Ten-moment equations; exact Riemann solver; generalized Riemann problem; generalized Riemann invariants; Rankine-Hugoniot jump conditions.

---

## 1. Introduction

It is well-known that the compressible Euler equations of gas dynamics can be derived from the Boltzmann equation [21] by assuming local thermodynamic equilibrium. However, for many problems, such as collisionless plasma [13, 33, 18, 47, 11] and the non-equilibrium gas dynamics [9], the local thermodynamic equilibrium assumption does not hold and anisotropic effects are often present, so that the Euler equations are less suitable. The ten-moment Gaussian closure equations [22] provide an alternative for such applications, where the pressure is described by an anisotropic and symmetric tensor.

Some numerical schemes have been proposed for solving the ten-moment equations in the past decades. A second-order upwind finite volume scheme was introduced in [9]. First-order relaxation numerical schemes were employed to approximate the weak solutions of those equations, see [6, 7]. A Harten–Lax–van Leer–contact (HLLC) approximate Riemann solver was applied in [37] to solve the ten-moment equations coupled with magnetic field. In recent years, some high-order numerical methods were also developed, including high-order positivity-preserving discontinuous Galerkin (DG) methods [31], finite difference weighted essentially non-oscillatory (WENO) schemes [32], and high-order entropy stable finite difference methods [39] as well as DG methods [8]. Besides, a second-order robust monotone upwind scheme was formulated in [28], and a second-order well-balanced (WB) scheme to handle equilibrium states was constructed in [29]. Additionally, a robust finite volume scheme for the two-fluid ten-moment plasma flow equations was proposed in [30]. The high-order accurate positivity-preserving and well-balanced discontinuous Galerkin schemes for ten-moment equations were also developed in [46], where a special modification to the numerical HLLC flux was imposed to enforce the well-balancedness and the geometric quasilinearization approach [50] was applied to simplify the positivity analysis.

---

\*Corresponding author.

Email addresses: 2101110034@stu.pku.edu.cn (Jiangfu Wang), hztang@math.pku.edu.cn (Huazhong Tang)

The generalized Riemann problem (GRP) scheme, which serves as an analytic second-order extension of the Godunov method, was initially developed for the study of compressible fluid dynamics [2]. This approach employs a piecewise linear function to approximate the “initial” data. Subsequently, it resolves a local GRP analytically at each cell interface to determine the numerical flux. For a detailed description, the readers are referred to [3]. There are two versions of the original GRP scheme: the Lagrangian and the Eulerian. Typically, the Eulerian version is derived through a transformation based on the Lagrangian framework, which can be particularly intricate, especially when dealing with sonic and multi-dimensional scenarios. To circumvent those difficulties, second-order accurate direct Eulerian GRP schemes were respectively developed for the shallow water equations [23], the Euler equations [5], and a more general weakly coupled system [4]. Those schemes directly resolve the local GRPs in the Eulerian formulation by using generalized Riemann invariants and Rankine-Hugoniot jump conditions.

Up to now, the GRP methodology has been widely implemented in many physically interesting cases, including the reactive flows [1], the motion of elastic strings [42], the shallow water equations [23], the radially symmetric compressible flows [26], the one-dimensional (1D) and two-dimensional (2D) special relativistic hydrodynamics (RHD) [55, 56], the gas-liquid two-phase flow in high-temperature and high-pressure transient wells [54], the spherically symmetric general RHD [51], the radiation hydrodynamical equations [19], the Baser-Nunziato two-phase model [20], the blood flow model in arteries [40], the compressible flows of real materials [48], the Kapila model of compressible multiphase flows [12], the laminar two-phase flow model with two-velocities [58] and so on. Besides, a comparison between the GRP scheme and the gas-kinetic scheme revealed the good performance of the GRP solver in simulating some inviscid flows [25]. By integrating the GRP scheme with the moving mesh method [43], the adaptive direct Eulerian GRP scheme was effectively developed in [14], resulting in enhanced resolution and accuracy. The adaptive GRP scheme was further studied in simulating 2D complex wave configurations formulated with the 2D Riemann problems of Euler equations [15] and was also extended to unstructured triangular meshes [27]. There are also many works on the high-order GRP schemes, such as the third-order GRP schemes for the Euler equations [53], 1D RHD [52] and the general hyperbolic balance law [35, 36]. Moreover, a two-stage fourth order time-accurate GRP scheme was also proposed for hyperbolic conservation laws [24] and for the special RHD [57]. Arbitrary high-order DG schemes based on the GRP solver were developed [49], where the reconstruction steps were halved compared with the existing high-order Runge-Kutta DG (RKDG) schemes. The two-stage fourth-order DG method based on the GRP solver was also developed in [10], and the computational cost can be considerably reduced by more than 50% compared with the same order multi-stage strong-stability-preserving (SSP) RKDG method. The GRP-based high resolution schemes for the multi-medium flows [17, 16] and the axisymmetric hydrodynamics [59] were recently developed.

This paper develops the second-order direct Eulerian GRP scheme for the ten-moment Gaussian closure equations with source terms. The generalized Riemann invariants and the exact solutions of the 1D Riemann problem are given. Compared to the Euler equations [5], the shallow water equations [23] and the blood flow in arteries [40] etc., the ten-moment equations have more physical variables and more elementary waves (e.g. the left and the right shear waves which are linearly degenerate and separated by the contact discontinuity). More physical variables means that more linear algebra equations should be derived to compute the instantaneous time derivatives. Two more elementary waves means that four different solution states between the left and right nonlinear waves should be resolved technically. All these features make the derivation of the direct Eulerian GRP scheme for the ten-moment equations much more complicated and nontrivial.

This paper is organized as follows. Section 2 introduces the 1D ten-moment equations and gives corresponding eigenvalues, eigenvectors and generalized Riemann invariants. Section 3 introduces the outline of the 1D direct GRP scheme and its extension to 2D case. Section 4 presents the exact solver for the classical Riemann problem, and Section 5 resolves the generalized Riemann problems. Some 1D and 2D numerical experiments are conducted in Section 6 to demonstrate the accuracy and performance of the proposed GRP scheme. It should be emphasized that several examples of 2D Riemann problems are constructed for the first time. Section 7 concludes this paper.

## 2. Preliminaries and notations

This section introduces the 1D ten-moment equations, and corresponding eigenvalues as well as eigenvectors, discusses the characteristic fields, and gives generalized Riemann invariants.

### 2.1. 1D ten-moment equations

The 1D ten-moment Gaussian closure equations with source term may be written into the form of balance laws as

$$\frac{\partial \mathbf{U}}{\partial t} + \frac{\partial \mathbf{F}(\mathbf{U})}{\partial x} = \mathbf{S}^x(\mathbf{U}), \quad (2.1)$$

where the solution vector  $\mathbf{U} = (\rho, m_1, m_2, E_{11}, E_{12}, E_{22})^\top$ ,  $\rho$ ,  $\mathbf{m} = (m_1, m_2)^\top$ , and  $E_{ij}$  denote the density, the momentum vector, and the component of the symmetric energy tensor  $\mathbf{E} = (E_{ij})$ , respectively,  $1 \leq i, j \leq 2$ . The flux  $\mathbf{F}(\mathbf{U})$  and the source term  $\mathbf{S}^x(\mathbf{U})$  are respectively given by

$$\begin{aligned} \mathbf{F}(\mathbf{U}) &= \left( \rho u_1, \rho u_1^2 + p_{11}, \rho u_1 u_2 + p_{12}, (E_{11} + p_{11})u_1, E_{12}u_1 + \frac{1}{2}(p_{11}u_2 + p_{12}u_1), E_{22}u_1 + p_{12}u_2 \right)^\top, \\ \mathbf{S}^x(\mathbf{U}) &= \left( 0, -\frac{1}{2}\rho \partial_x W, 0, -\frac{1}{2}\rho u_1 \partial_x W, -\frac{1}{4}\rho u_2 \partial_x W, 0 \right)^\top, \end{aligned} \quad (2.2)$$

where  $\mathbf{u} = (u_1, u_2)^\top = \mathbf{m}/\rho$  denotes the velocity vector, and the function  $W(x)$  is a given potential, which may denote the electron quiver energy in laser light (see e.g. [33, 38]). The system (2.1) is closed by the following ‘‘equation of state’’

$$\mathbf{p} = (p_{ij})_{2 \times 2} = 2\mathbf{E} - \rho \mathbf{u} \otimes \mathbf{u}, \quad (2.3)$$

where the symbol  $\otimes$  denotes the tensor product, and its solution  $\mathbf{U}$  should stay in the physically admissible state set

$$\mathcal{G} := \{ \mathbf{U} \in \mathbb{R}^6 : \rho > 0, \mathbf{x}^\top \mathbf{p} \mathbf{x} > 0 \quad \forall \mathbf{x} \in \mathbb{R}^2 \setminus \{ \mathbf{0} \} \}, \quad (2.4)$$

which means that  $\rho > 0$ ,  $p_{11} > 0$  and  $\det(\mathbf{p}) := p_{11}p_{22} - p_{12}^2 > 0$ .

Rewrite (2.1) into the following quasi-linear form

$$\frac{\partial \rho}{\partial t} + u_1 \frac{\partial \rho}{\partial x} + \rho \frac{\partial u_1}{\partial x} = 0, \quad (2.5a)$$

$$\frac{\partial u_1}{\partial t} + u_1 \frac{\partial u_1}{\partial x} + \frac{1}{\rho} \frac{\partial p_{11}}{\partial x} = -\frac{1}{2} W_x, \quad (2.5b)$$

$$\frac{\partial u_2}{\partial t} + u_1 \frac{\partial u_2}{\partial x} + \frac{1}{\rho} \frac{\partial p_{12}}{\partial x} = 0, \quad (2.5c)$$

$$\frac{\partial p_{11}}{\partial t} + 3p_{11} \frac{\partial u_1}{\partial x} + u_1 \frac{\partial p_{11}}{\partial x} = 0, \quad (2.5d)$$

$$\frac{\partial p_{12}}{\partial t} + 2p_{12} \frac{\partial u_1}{\partial x} + p_{11} \frac{\partial u_2}{\partial x} + u_1 \frac{\partial p_{12}}{\partial x} = 0, \quad (2.5e)$$

$$\frac{\partial p_{22}}{\partial t} + p_{22} \frac{\partial u_1}{\partial x} + 2p_{12} \frac{\partial u_2}{\partial x} + u_1 \frac{\partial p_{22}}{\partial x} = 0. \quad (2.5f)$$

It is obvious that (2.5d) and (2.5b) imply that

$$\frac{\partial u_1}{\partial x} = -\frac{1}{3p_{11}} \frac{\mathcal{D}p_{11}}{\mathcal{D}t}, \quad (2.6)$$

$$\frac{\partial p_{11}}{\partial x} = -\rho \left( \frac{\mathcal{D}u_1}{\mathcal{D}t} + \frac{1}{2} W_x \right), \quad (2.7)$$

respectively, where  $\frac{\mathcal{D}}{\mathcal{D}t} := \frac{\partial}{\partial t} + u_1 \frac{\partial}{\partial x}$  is the material derivative. Then it follows that

$$\begin{aligned} \frac{\partial u_1}{\partial t} &= \frac{u_1}{3p_{11}} \frac{\mathcal{D}p_{11}}{\mathcal{D}t} + \frac{\mathcal{D}u_1}{\mathcal{D}t}, \\ \frac{\partial p_{11}}{\partial t} &= \frac{\mathcal{D}p_{11}}{\mathcal{D}t} + \rho u_1 \frac{\mathcal{D}u_1}{\mathcal{D}t} + \frac{1}{2} \rho u_1 W_x. \end{aligned} \quad (2.8)$$

Besides, (2.5e) and (2.5c) imply that

$$\frac{\partial u_2}{\partial x} = -\frac{1}{p_{11}} \left( \frac{\mathcal{D}p_{12}}{\mathcal{D}t} - \frac{2p_{12}}{3p_{11}} \frac{\mathcal{D}p_{11}}{\mathcal{D}t} \right), \quad (2.9)$$

$$\frac{\partial p_{12}}{\partial x} = -\rho \frac{\mathcal{D}u_2}{\mathcal{D}t}, \quad (2.10)$$

respectively, where (2.6) has been used in (2.9). It follows that

$$\begin{aligned} \frac{\partial u_2}{\partial t} &= \frac{\mathcal{D}u_2}{\mathcal{D}t} + \frac{u_1}{p_{11}} \left( \frac{\mathcal{D}p_{12}}{\mathcal{D}t} - \frac{2p_{12}}{3p_{11}} \frac{\mathcal{D}p_{11}}{\mathcal{D}t} \right), \\ \frac{\partial p_{12}}{\partial t} &= \frac{\mathcal{D}p_{12}}{\mathcal{D}t} + \rho u_1 \frac{\mathcal{D}u_2}{\mathcal{D}t}. \end{aligned} \quad (2.11)$$

Moreover, (2.5f) implies that

$$\frac{\mathcal{D}p_{22}}{\mathcal{D}t} = \frac{p_{11}p_{22} - 4p_{12}^2}{3p_{11}^2} \frac{\mathcal{D}p_{11}}{\mathcal{D}t} + \frac{2p_{12}}{p_{11}} \frac{\mathcal{D}p_{12}}{\mathcal{D}t}, \quad (2.12)$$

where (2.6) and (2.9) have been used.

## 2.2. Eigenvalues, eigenvectors and generalized Riemann invariants

The eigenvalues of the system (2.1) or (2.5) are given (see e.g. [9]) by

$$\lambda_1 = u_1 - c, \quad \lambda_2 = u_1 - \frac{c}{\sqrt{3}}, \quad \lambda_3 = \lambda_4 = u_1, \quad \lambda_5 = u_1 + \frac{c}{\sqrt{3}}, \quad \lambda_6 = u_1 + c,$$

where  $c := \sqrt{3p_{11}/\rho}$  denotes the sound speed, and the linearly independent six associated right eigenvectors for (2.5) may be chosen (see e.g. [39]) as follows

$$\begin{aligned} \tilde{\mathbf{r}}_1 &= (\rho p_{11}, -c p_{11}, -c p_{12}, 3p_{11}^2, 3p_{11}p_{12}, p_{11}p_{22} + 2p_{12}^2)^\top, \\ \tilde{\mathbf{r}}_2 &= \left( 0, 0, -\frac{c}{\sqrt{3}}, 0, p_{11}, 2p_{12} \right)^\top, \\ \tilde{\mathbf{r}}_3 &= (0, 0, 0, 0, 0, 1)^\top, \quad \tilde{\mathbf{r}}_4 = (1, 0, 0, 0, 0, 0)^\top, \\ \tilde{\mathbf{r}}_5 &= \left( 0, 0, \frac{c}{\sqrt{3}}, 0, p_{11}, 2p_{12} \right)^\top, \\ \tilde{\mathbf{r}}_6 &= (\rho p_{11}, c p_{11}, c p_{12}, 3p_{11}^2, 3p_{11}p_{12}, p_{11}p_{22} + 2p_{12}^2)^\top. \end{aligned}$$

Denote the primitive variables vector by  $\mathbf{V} := (\rho, u_1, u_2, p_{11}, p_{12}, p_{22})^\top$ . The associated right eigenvector matrix  $\mathbf{R}(\mathbf{U}) = \frac{\partial \mathbf{U}}{\partial \mathbf{V}} \cdot (\tilde{\mathbf{r}}_1, \dots, \tilde{\mathbf{r}}_6)$  for (2.1) is given in Appendix A.

By simple calculations, one can find that for any physically admissible  $\mathbf{V}$ ,  $\nabla_{\mathbf{V}} \lambda_i(\mathbf{V}) \cdot \tilde{\mathbf{r}}_i(\mathbf{V}) \neq 0$  for  $i = 1, 6$  and  $\nabla_{\mathbf{V}} \lambda_i(\mathbf{V}) \cdot \tilde{\mathbf{r}}_i(\mathbf{V}) = 0$  for  $i = 2, 3, 4, 5$ . Hence, only the first and the sixth characteristic fields are genuinely nonlinear, and the other characteristic fields are linearly degenerate. Possible wave patterns associated with those characteristic fields are

$$\begin{aligned} \text{for } \lambda_1 = u_1 - c: & \quad 1\text{-shock or 1-rarefaction wave,} \\ \text{for } \lambda_2 = u_1 - \frac{c}{\sqrt{3}}: & \quad 2\text{-shear wave,} \\ \text{for } \lambda_3 = \lambda_4 = u_1: & \quad 3, 4\text{-contact wave,} \\ \text{for } \lambda_5 = u_1 + \frac{c}{\sqrt{3}}: & \quad 5\text{-shear wave,} \\ \text{for } \lambda_6 = u_1 + c: & \quad 6\text{-shock or 6-rarefaction wave.} \end{aligned}$$

Note that the characteristic fields of the 1D ten-moment equations are similar to those of the 1D shear shallow

water model [34]. According to the following relations

$$\frac{d\rho}{\tilde{r}_i^{(1)}} = \frac{du_1}{\tilde{r}_i^{(2)}} = \frac{du_2}{\tilde{r}_i^{(3)}} = \frac{dp_{11}}{\tilde{r}_i^{(4)}} = \frac{dp_{12}}{\tilde{r}_i^{(5)}} = \frac{dp_{22}}{\tilde{r}_i^{(6)}}, \quad i = 1, 2, \dots, 6,$$

where  $\tilde{r}_i^{(k)}$  denotes the  $k$ -th component of  $\tilde{\mathbf{r}}_i$ ,  $k = 1, 2, \dots, 6$ , one can derive the following generalized Riemann invariants for six characteristic fields

$$\begin{aligned} \text{for } \lambda_1 = u_1 - c : \quad & \frac{p_{11}}{\rho^3}, \frac{p_{12}}{\rho^3}, u_1 + c, u_2 + \frac{\sqrt{3}p_{12}}{\sqrt{\rho p_{11}}}, \frac{\det(\mathbf{p})}{\rho^4}, \\ \text{for } \lambda_2 = u_1 - \frac{c}{\sqrt{3}} : \quad & \rho, u_1, p_{11}, u_2 + \frac{p_{12}}{\sqrt{\rho p_{11}}}, \det(\mathbf{p}), \\ \text{for } \lambda_3 = u_1 : \quad & \rho, u_1, u_2, p_{11}, p_{12}, \\ \text{for } \lambda_4 = u_1 : \quad & u_1, u_2, p_{11}, p_{12}, p_{22}, \\ \text{for } \lambda_5 = u_1 + \frac{c}{\sqrt{3}} : \quad & \rho, u_1, p_{11}, u_2 - \frac{p_{12}}{\sqrt{\rho p_{11}}}, \det(\mathbf{p}), \\ \text{for } \lambda_6 = u_1 + c : \quad & \frac{p_{11}}{\rho^3}, \frac{p_{12}}{\rho^3}, u_1 - c, u_2 - \frac{\sqrt{3}p_{12}}{\sqrt{\rho p_{11}}}, \frac{\det(\mathbf{p})}{\rho^4}, \end{aligned}$$

which are constant across corresponding linearly degenerate wave or rarefaction wave.

### 3. Numerical schemes

This section introduces the 1D direct Eulerian GRP scheme and its extension to the 2D case by the Strang splitting method.

#### 3.1. Outline of 1D GRP scheme

For the sake of simplicity, the space domain is divided into a uniform mesh  $\{x_{j+\frac{1}{2}}, j \in \mathbb{Z}\}$  with  $\Delta x := x_{j+\frac{1}{2}} - x_{j-\frac{1}{2}}$ , denote the  $j$ th cell by  $I_j := [x_{j-\frac{1}{2}}, x_{j+\frac{1}{2}}]$ . Assume that  $\Delta t := t_{n+1} - t_n$ , and at the time  $t = t_n$ , the approximate solution is piecewisely linear with the slope  $\sigma_j^n$ ,  $n \geq 0$ , and reconstructed as

$$\mathbf{V}(x, t_n) = \mathbf{V}_j^n + \sigma_j^n(x - x_j) \quad \forall x \in I_j, \quad (3.1)$$

where  $\mathbf{V}_j^n$  approximates the cell average of  $\mathbf{V}(x, t_n)$  over the cell  $I_j$ . Hence the second-order Godunov-type scheme to solve (2.1) is

$$\mathbf{U}_j^{n+1} = \mathbf{U}_j^n - \frac{\Delta t}{\Delta x} \left( \mathbf{F}_{j+\frac{1}{2}}^{n+\frac{1}{2}} - \mathbf{F}_{j-\frac{1}{2}}^{n+\frac{1}{2}} \right) + \frac{\Delta t}{2} \left( \mathbf{S}_{j+\frac{1}{2}}^{x, n+\frac{1}{2}} + \mathbf{S}_{j-\frac{1}{2}}^{x, n+\frac{1}{2}} \right), \quad (3.2)$$

where  $\mathbf{F}_{j+\frac{1}{2}}^{n+\frac{1}{2}} = \mathbf{F}(\mathbf{U}(\mathbf{V}_{j+\frac{1}{2}}^{n+\frac{1}{2}}))$  and  $\mathbf{S}_{j+\frac{1}{2}}^{x, n+\frac{1}{2}} = \mathbf{S}^x(\mathbf{U}(\mathbf{V}_{j+\frac{1}{2}}^{n+\frac{1}{2}}))$ ,  $\mathbf{V}_{j+\frac{1}{2}}^{n+\frac{1}{2}}$  denotes a second-order accurate approximation of  $\mathbf{V}(x_{j+\frac{1}{2}}, t_n + \frac{1}{2}\Delta t)$  and is analytically derived by resolving the local GRP at each point  $(x_{j+\frac{1}{2}}, t_n)$ , i.e.,

$$\mathbf{V}(x, t_n) = \begin{cases} (2.1), & t - t_n > 0, \\ \mathbf{V}_j^n + \sigma_j^n(x - x_j), & x < x_{j+\frac{1}{2}}, \\ \mathbf{V}_{j+1}^n + \sigma_{j+1}^n(x - x_{j+1}), & x > x_{j+\frac{1}{2}}. \end{cases} \quad (3.3)$$

More specifically,  $\mathbf{V}_{j+\frac{1}{2}}^{n+\frac{1}{2}}$  is usually calculated by

$$\mathbf{V}_{j+\frac{1}{2}}^{n+\frac{1}{2}} = \mathbf{V}_{j+\frac{1}{2}}^n + \frac{\Delta t}{2} \left( \frac{\partial \mathbf{V}}{\partial t} \right)_{j+\frac{1}{2}}^n, \quad (3.4)$$

where  $\left(\frac{\partial \mathbf{V}}{\partial t}\right)_{j+\frac{1}{2}}^n$  is obtained by resolving the problem (3.3), according to those theorems in Section 5, and  $\mathbf{V}_{j+\frac{1}{2}}^n := \omega\left(0; \mathbf{V}_{j+\frac{1}{2},L}^n, \mathbf{V}_{j+\frac{1}{2},R}^n\right)$ , here  $\omega\left(\frac{x-x_j}{t-t_n}; \mathbf{V}_{j+\frac{1}{2},L}^n, \mathbf{V}_{j+\frac{1}{2},R}^n\right)$  is the exact solution of the associated Riemann problem for (2.1) centered at  $(x_{j+\frac{1}{2}}, t_n)$ , i.e., the Cauchy problem

$$\begin{cases} \frac{\partial \mathbf{U}(\mathbf{V})}{\partial t} + \frac{\partial \mathbf{F}(\mathbf{U}(\mathbf{V}))}{\partial x} = 0, & t - t_n > 0 \\ \mathbf{V}(x, t_n) = \begin{cases} \mathbf{V}_{j+\frac{1}{2},L}^n, & x < x_{j+\frac{1}{2}}, \\ \mathbf{V}_{j+\frac{1}{2},R}^n, & x > x_{j+\frac{1}{2}}, \end{cases} \end{cases} \quad (3.5)$$

where  $\mathbf{V}_{j+\frac{1}{2},L}^n = \mathbf{V}_j^n + \frac{\Delta x}{2} \boldsymbol{\sigma}_j^n$  and  $\mathbf{V}_{j+\frac{1}{2},R}^n = \mathbf{V}_{j+1}^n - \frac{\Delta x}{2} \boldsymbol{\sigma}_{j+1}^n$  are the left and right limiting values of  $\mathbf{V}(x, t_n)$  at  $x_{j+\frac{1}{2}}$ . The exact solution of Riemann problem (3.5) is given in Section 4, while the approximate slope  $\boldsymbol{\sigma}_j^n$  is evolved by some slope limiter.

After obtaining  $\mathbf{U}_j^{n+1}$  by the scheme (3.2), applying some slope limiter to get the slope of  $\mathbf{U}$ , denoted by  $\hat{\boldsymbol{\sigma}}_j^{n+1}$ , and then the slope  $\boldsymbol{\sigma}_j^{n+1}$  of  $\mathbf{V}$  can be obtained by the chain rule. The minmod type and van Leer limiters are utilized here. With the minmod type limiter,  $\hat{\boldsymbol{\sigma}}_j^{n+1}$  is calculated componentwisely by

$$\hat{\boldsymbol{\sigma}}_j^{n+1} = \mathbf{R}_j \cdot \text{minmod} \left( \frac{\theta}{\Delta x} \mathbf{R}_j^{-1} (\mathbf{U}_j^{n+1} - \mathbf{U}_{j-1}^{n+1}), \frac{1}{\Delta x} \mathbf{R}_j^{-1} (\mathbf{U}_{j+\frac{1}{2}}^{n+1,-} - \mathbf{U}_{j-\frac{1}{2}}^{n+1,-}), \frac{\theta}{\Delta x} \mathbf{R}_j^{-1} (\mathbf{U}_{j+1}^{n+1} - \mathbf{U}_j^{n+1}) \right), \quad (3.6)$$

where  $\mathbf{R}_j := \mathbf{R}(\mathbf{U}_j^{n+1})$ , the parameter  $\theta \in [1, 2)$ , and  $\mathbf{U}_{j+\frac{1}{2}}^{n+1,-} := \mathbf{U}(\mathbf{V}_{j+\frac{1}{2}}^{n+1,-})$  with  $\mathbf{V}_{j+\frac{1}{2}}^{n+1,-} := \mathbf{V}_{j+\frac{1}{2}}^n + \Delta t \left(\frac{\partial \mathbf{V}}{\partial t}\right)_{j+\frac{1}{2}}^n$ .  $\mathbf{R}(\mathbf{U})$  is the right eigenvector matrix of the Jacobian matrix  $\frac{\partial \mathbf{F}(\mathbf{U})}{\partial \mathbf{U}}$  and given in Appendix A. With the van Leer limiter,  $\hat{\boldsymbol{\sigma}}_j^{n+1}$  is calculated componentwise by

$$\hat{\boldsymbol{\sigma}}_j^{n+1} = \mathbf{R}_j \cdot \text{vanLeer} (\mathbf{R}_j^{-1} \mathbf{U}_{j-1}^{n+1}, \mathbf{R}_j^{-1} \mathbf{U}_j^{n+1}, \mathbf{R}_j^{-1} \mathbf{U}_{j+1}^{n+1}), \quad (3.7)$$

where the van Leer limiter function is defined as [45, 60]

$$\text{vanLeer}(a_L, a_M, a_R) = \begin{cases} 0, & \text{if } a_L = a_R \text{ or } f \leq 0 \text{ or } f \geq 1, \\ 4f(1-f)s, & \text{if } a_L \neq a_R \text{ and } 0 < f < 1, \end{cases}$$

where  $f = \frac{\Delta_{ML}}{\Delta_{RL}}$ ,  $s = \frac{\Delta_{RL}}{2\Delta x}$ ,  $\Delta_{ML} = a_M - a_L$  and  $\Delta_{RL} = a_R - a_L$ .

In summary, the second-order direct Eulerian GRP scheme for the 1D ten-moment equations (2.1) is implemented in the following four steps:

**Step 1:** Give the piecewise initial data (3.1), and solve the local Riemann problem (3.5) to get the solution  $\mathbf{V}_{j+\frac{1}{2}}^n$  by using the exact Riemann solver stated in Section 4.

**Step 2:** Calculate  $\left(\frac{\partial \mathbf{V}}{\partial t}\right)_{j+\frac{1}{2}}^n$  by those theorems in Section 5, and  $\mathbf{V}_{j+\frac{1}{2}}^{n+\frac{1}{2}}$  in (3.4), then the numerical flux  $\mathbf{F}_{j+\frac{1}{2}}^{n+\frac{1}{2}}$  and the source term  $\mathbf{S}_{j+\frac{1}{2}}^{n+\frac{1}{2}}$  can be obtained.

**Step 3:** Evaluate the cell averages  $\mathbf{U}_j^{n+1}$  by the scheme (3.2).

**Step 4:** Update the slope  $\hat{\boldsymbol{\sigma}}_j^{n+1}$  of the conservative variables by the slope limiter (3.6) or (3.7), and calculate the slope  $\boldsymbol{\sigma}_j^{n+1}$  of the primitive variables by the chain rule, then go to Step 1 by replacing  $n$  with  $n+1$ .

### 3.2. 2D extension of GRP scheme

For simplicity, this work is limited to a 2D uniform Cartesian grid and uses the Strang splitting method to extend the above GRP scheme to the 2D case. Consider the 2D ten-moment equations

$$\frac{\partial \mathbf{U}}{\partial t} + \frac{\partial \mathbf{F}(\mathbf{U})}{\partial x} + \frac{\partial \mathbf{G}(\mathbf{U})}{\partial y} = \mathbf{S}^x(\mathbf{U}) + \mathbf{S}^y(\mathbf{U}), \quad (3.8)$$

where  $\mathbf{U}$ ,  $\mathbf{F}(\mathbf{U})$ , and  $\mathbf{S}^x(\mathbf{U})$  are the same as those in Section 2.1, and the flux  $\mathbf{G}(\mathbf{U})$  and the source term  $\mathbf{S}^y(\mathbf{U})$  are defined by

$$\begin{aligned}\mathbf{G}(\mathbf{U}) &= \left( \rho u_2, \rho u_1 u_2 + p_{12}, \rho u_2^2 + p_{22}, E_{11} u_2 + p_{12} u_1, E_{12} u_2 + \frac{1}{2}(p_{12} u_2 + p_{22} u_1), (E_{22} + p_{22}) u_2 \right)^\top, \\ \mathbf{S}^y(\mathbf{U}) &= \left( 0, 0, -\frac{1}{2} \rho \partial_y W, 0, -\frac{1}{4} \rho u_1 \partial_y W, -\frac{1}{2} \rho u_2 \partial_y W \right)^\top.\end{aligned}$$

The 2D ten-moment equations (3.8) are split into two 1D subsystems

$$\frac{\partial \mathbf{U}}{\partial t} + \frac{\partial \mathbf{F}(\mathbf{U})}{\partial x} = \mathbf{S}^x(\mathbf{U}) \quad \text{and} \quad \frac{\partial \mathbf{U}}{\partial t} + \frac{\partial \mathbf{G}(\mathbf{U})}{\partial x} = \mathbf{S}^y(\mathbf{U}).$$

Hence it suffices to consider the derivation of the GRP scheme for the subsystem in the  $x$ -direction in Section 3.1. If denoting the 1D GRP evolution operators for the above two subsystems by  $\mathcal{L}_x(\Delta t)$  and  $\mathcal{L}_y(\Delta t)$ , respectively, for one time step  $\Delta t$ , then by using the Strang splitting method, the simple 2D GRP scheme can be given by

$$\mathbf{U}^{n+1} = \mathcal{L}_x \left( \frac{\Delta t}{2} \right) \mathcal{L}_y(\Delta t) \mathcal{L}_x \left( \frac{\Delta t}{2} \right) \mathbf{U}^n.$$

#### 4. Exact Riemann solver

This section gives the exact Riemann solver for the associated Riemann problem

$$\begin{cases} \frac{\partial \mathbf{U}(\mathbf{V})}{\partial t} + \frac{\partial \mathbf{F}(\mathbf{U}(\mathbf{V}))}{\partial x} = 0, & t > 0, \\ \mathbf{V}(x, 0) = \begin{cases} \mathbf{V}_L, & x < 0, \\ \mathbf{V}_R, & x > 0. \end{cases} \end{cases} \quad (4.1)$$

As an example, a special local wave configuration shown in Figure 1 for the associated Riemann problem is only considered here, where there is a 1-rarefaction wave, a 2-shear wave, a 3,4-contact discontinuity, a 5-shear wave and a 6-shock wave. Other local wave configurations may be similarly treated. One can see from Figure 1 that there are five solution states between the given left and right states  $\mathbf{V}_L$  and  $\mathbf{V}_R$  to be determined, that is, the state inside the 1-rarefaction wave denoted by  $\mathbf{V}_{\text{Lfan}}$  and four solution states between the  $i$ -wave and the  $(i+1)$ -wave ( $1 \leq i < 6$ ) denoted by

$$\begin{cases} \mathbf{V}_{*L} = (\rho_{*L}, u_{1,*}, u_{2,*L}, p_{11,*}, p_{12,*L}, p_{22,*L})^\top, \\ \mathbf{V}_{**L} = (\rho_{*L}, u_{1,*}, u_{2,**}, p_{11,*}, p_{12,**}, p_{22,**L})^\top, \\ \mathbf{V}_{**R} = (\rho_{*R}, u_{1,*}, u_{2,**}, p_{11,*}, p_{12,**}, p_{22,**R})^\top, \\ \mathbf{V}_{*R} = (\rho_{*R}, u_{1,*}, u_{2,*R}, p_{11,*}, p_{12,*R}, p_{22,*R})^\top. \end{cases}$$

To determine them, the generalized Riemann invariants will be used for the rarefaction wave, the shear waves and the contact discontinuity, while the Rankine-Hugoniot jump conditions will be used for the shock wave. For the sake of convenience, the main steps of the exact Riemann solver for (4.1) is shown in Figure 2.

##### 4.1. Computations of $u_{1,*}$ and $p_{11,*}$

Analogous to the derivation for the Euler equations in [44, Proposition 4.1], one can prove the following results for the 1D ten-moment equations.

**Theorem 4.1** (Computing  $p_{11,*}$  and  $u_{1,*}$ ). *The pressure component  $p_{11,*}$  of the Riemann problem (4.1) is given by the root of the algebraic equation*

$$f(p_{11}, \mathbf{V}_L, \mathbf{V}_R) := f_L(p_{11}, \mathbf{V}_L) + f_R(p_{11}, \mathbf{V}_R) + u_{1,R} - u_{1,L} = 0, \quad (4.2)$$

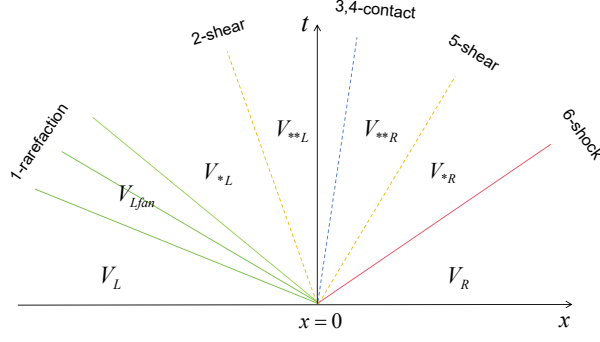


Figure 1: The schematic description of a local wave configuration of the associated Riemann problem (4.1).

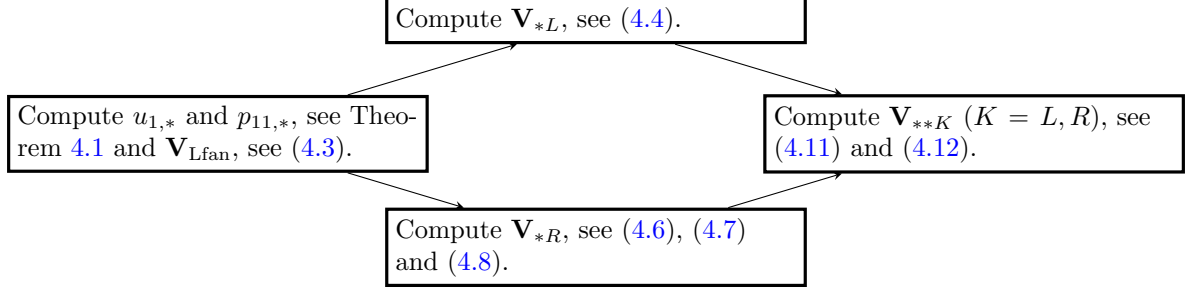


Figure 2: The main steps of the exact Riemann solver in Section 4.

where the function  $f_L$  is given by

$$f_L(p_{11}, \mathbf{V}_L) = \begin{cases} (p_{11} - p_{11,L}) \left[ \frac{1}{\rho_L(2p_{11} + p_{11,L})} \right]^{\frac{1}{2}}, & \text{if } p_{11} > p_{11,L} \text{ (1-shock)}, \\ c_L \left[ \left( \frac{p_{11}}{p_{11,L}} \right)^{\frac{1}{3}} - 1 \right], & \text{if } p_{11} \leq p_{11,L} \text{ (1-rarefaction)}, \end{cases}$$

and the function  $f_R$  is given by

$$f_R(p_{11}, \mathbf{V}_R) = \begin{cases} (p_{11} - p_{11,R}) \left[ \frac{1}{\rho_R(2p_{11} + p_{11,R})} \right]^{\frac{1}{2}}, & \text{if } p_{11} > p_{11,R} \text{ (6-shock)}, \\ c_R \left[ \left( \frac{p_{11}}{p_{11,R}} \right)^{\frac{1}{3}} - 1 \right], & \text{if } p_{11} \leq p_{11,R} \text{ (6-rarefaction)}. \end{cases}$$

Moreover, the velocity  $u_{1,*}$  may be given by

$$u_{1,*} = \frac{1}{2}(u_{1,L} + u_{1,R}) + \frac{1}{2}[f_R(p_{11,*}, \mathbf{V}_R) - f_L(p_{11,*}, \mathbf{V}_L)].$$

*Proof.* The proof is similar to that of the Euler equations, see [44, Subsection 4.2], with replacing the adiabatic index  $\gamma$  with 3.  $\square$

To find the root of the nonlinear equation (4.2), the Newton-Raphson iterative method is applied, where the initial guess value may be obtained in an adaptive way, similar to that for the Euler equations [44, Section 9.5 and Figure 9.4].

#### 4.2. Computations of $\mathbf{V}_{Lfan}$

The 1-rarefaction wave, which is identified by the condition  $p_{11,*} \leq p_{11,L}$ , is enclosed by the head and the tail, whose characteristic speeds are given respectively by

$$S_{HL} = u_{1,L} - c_L, \quad S_{TL} = u_{1,*} - c_{*L},$$



where  $c_{*L} = c_L \left( \frac{p_{11,*}}{p_{11,L}} \right)^{\frac{1}{3}}$ . The solution  $\mathbf{V}_{\text{Lfan}}$  inside the 1-rarefaction fan is easily obtained by considering the characteristic ray through the origin  $(0, 0)$  and a general point  $(x, t)$  inside the fan. The slope of the characteristic line is

$$\frac{dx}{dt} = \frac{x}{t} = u_1 - c.$$

Using the generalized Riemann invariants associated with the 1-rarefaction wave yields

$$\mathbf{V}_{\text{Lfan}} \begin{cases} \rho = \frac{\rho_L}{2} \left[ 1 + \frac{1}{c_L} \left( u_{1,L} - \frac{x}{t} \right) \right], \\ u_1 = \frac{1}{2} \left( c_L + u_{1,L} + \frac{x}{t} \right), \\ u_2 = u_{2,L} + \frac{\sqrt{3}p_{12,L}}{\sqrt{\rho_L p_{11,L}}} - \frac{\sqrt{3}p_{12}}{\sqrt{\rho p_{11}}}, \\ p_{11} = \frac{p_{11,L}}{8} \left[ 1 + \frac{1}{c_L} \left( u_{1,L} - \frac{x}{t} \right) \right]^3, \\ p_{12} = p_{12,L} \frac{\rho^3}{\rho_L^3}, \\ p_{22} = \left[ \frac{\det(\mathbf{p}_L)}{\rho_L^4} \rho^4 + p_{12}^2 \right] / p_{11}. \end{cases} \quad (4.3)$$

**Remark 4.2.** For the 6-rarefaction wave, which is identified by the condition  $p_{11,*} \leq p_{11,R}$  and enclosed by the characteristic speeds given respectively by  $S_{HR} = u_{1,R} + c_R$  and  $S_{TR} = u_{1,*} + c_{*R}$  with  $c_{*R} = c_R \left( \frac{p_{11,*}}{p_{11,R}} \right)^{\frac{1}{3}}$ , the solution  $\mathbf{V}_{\text{Rfan}}$  is given by

$$\mathbf{V}_{\text{Rfan}} \begin{cases} \rho = \frac{\rho_R}{2} \left[ 1 + \frac{1}{c_R} \left( \frac{x}{t} - u_{1,R} \right) \right], \\ u_1 = \frac{1}{2} \left( u_{1,R} - c_R + \frac{x}{t} \right), \\ u_2 = u_{2,R} - \frac{\sqrt{3}p_{12,R}}{\sqrt{\rho_R p_{11,R}}} + \frac{\sqrt{3}p_{12}}{\sqrt{\rho p_{11}}}, \\ p_{11} = \frac{p_{11,R}}{8} \left[ 1 + \frac{1}{c_R} \left( \frac{x}{t} - u_{1,R} \right) \right]^3, \\ p_{12} = p_{12,R} \frac{\rho^3}{\rho_R^3}, \\ p_{22} = \left[ \frac{\det(\mathbf{p}_R)}{\rho_R^4} \rho^4 + p_{12}^2 \right] / p_{11}. \end{cases}$$

#### 4.3. Computing $\mathbf{V}_{*L}$

For the state  $\mathbf{V}_{*L}$ , which is between the 1-rarefaction wave and the 2-shear wave, utilizing the generalized Riemann invariants across the 1-rarefaction wave can obtain

$$\begin{aligned} \rho_{*L} &= \rho_L \left( \frac{p_{11,*}}{p_{11,L}} \right)^{\frac{1}{3}}, & u_{2,*L} &= u_{2,L} + \frac{\sqrt{3}p_{12,L}}{\sqrt{\rho_L p_{11,L}}} - \frac{\sqrt{3}p_{12,*L}}{\sqrt{\rho_{*L} p_{11,*}}}, \\ p_{12,*L} &= p_{12,L} \frac{\rho_{*L}^3}{\rho_L^3}, & p_{22,*L} &= \left[ \frac{\det(\mathbf{p}_L)}{\rho_L^4} \rho_{*L}^4 + p_{12,*L}^2 \right] / p_{11,*}. \end{aligned} \quad (4.4)$$

**Remark 4.3.** For the state  $\mathbf{V}_{*R}$ , which is between the 6-rarefaction wave and the 5-shear wave, use of the generalized Riemann invariants across the 6-rarefaction wave may give

$$\begin{aligned} \rho_{*R} &= \rho_R \left( \frac{p_{11,*}}{p_{11,R}} \right)^{\frac{1}{3}}, & u_{2,*R} &= u_{2,R} - \frac{\sqrt{3}p_{12,R}}{\sqrt{\rho_R p_{11,R}}} + \frac{\sqrt{3}p_{12,*R}}{\sqrt{\rho_{*R} p_{11,*}}}, \\ p_{12,*R} &= p_{12,R} \frac{\rho_{*R}^3}{\rho_R^3}, & p_{22,*R} &= \left[ \frac{\det(\mathbf{p}_R)}{\rho_R^4} \rho_{*R}^4 + p_{12,*R}^2 \right] / p_{11,*}. \end{aligned}$$

#### 4.4. Computing $\mathbf{V}_{*R}$

The solution state  $\mathbf{V}_{*R}$  is between the 5-shear wave and the 6-shock wave, while the 6-shock wave with the following speed

$$\sigma_R = u_{1,R} + c_R \sqrt{\frac{2p_{11,*}}{3p_{11,R}} + \frac{1}{3}} = u_{1,*} + \frac{1}{\rho_{*R}} \sqrt{(2p_{11,*} + p_{11,R})\rho_R} \quad (4.5)$$

is identified by the condition  $p_{11,*} > p_{11,R}$ . The derivation of (4.5) is similar to that of the shock speed for the Euler equations, see Section 3.1.3 in [44]. Moreover, (4.5) implies that  $u_{1,*} < \sigma_R$ . By applying the Rankine-

Hugoniot jump conditions for the variables  $\rho$ ,  $m_1$  and  $E_{11}$ , similar to the discussion for the Euler equations in [44], one can obtain

$$\rho_{*R} = \rho_R \frac{2p_{11,*} + p_{11,R}}{p_{11,*} + 2p_{11,R}}. \quad (4.6)$$

The condition  $p_{11,*} > p_{11,R}$  implies that  $\rho_{*R} \in (\rho_R, 2\rho_R)$ .

Using the Rankine-Hugoniot jump conditions for the variables  $m_2$  and  $E_{12}$  yields

$$\mathbf{A}^R \begin{pmatrix} u_{2,*R} \\ p_{12,*R} \end{pmatrix} = \begin{pmatrix} a_1^R \\ a_2^R \end{pmatrix}, \quad (4.7)$$

where

$$\begin{aligned} \mathbf{A}^R &:= \begin{pmatrix} \rho_{*R}(u_{1,*} - \sigma_R) & 1 \\ E_{11,*R} - \frac{1}{2}\rho_{*R}u_{1,*}\sigma_R & u_{1,*} - \frac{1}{2}\sigma_R \end{pmatrix}, \\ a_1^R &:= \rho_R(u_{1,R} - \sigma_R)u_{2,R} + p_{12,R}, \\ a_2^R &:= E_{12,R}(u_{1,R} - \sigma_R) + \frac{1}{2}(p_{11,R}u_{2,R} + p_{12,R}u_{1,R}). \end{aligned}$$

Due to

$$\det(\mathbf{A}^R) = \frac{p_{11,*}(2\rho_R - \rho_{*R}) + p_{11,R}\rho_R}{2\rho_{*R}} > 0,$$

the solution of (4.7) exists and is unique.

By the Rankine-Hugoniot jump conditions for the variable  $E_{22}$ , one has

$$E_{22,*R}u_{1,*} + p_{12,*R}u_{2,*R} - (E_{22,R}u_{1,R} + p_{12,R}u_{2,R}) = \sigma_R(E_{22,*R} - E_{22,R}),$$

which implies that

$$E_{22,*R} = \frac{E_{22,R}u_{1,R} + p_{12,R}u_{2,R} - \sigma_R E_{22,R} - p_{12,*R}u_{2,*R}}{u_{1,*} - \sigma_R},$$

and then using the ‘‘equation of state’’ yields

$$p_{22,*R} = 2E_{22,*R} - \rho_{*R}u_{2,*R}^2. \quad (4.8)$$

**Remark 4.4.** For the 1-shock wave with the speed

$$\sigma_L = u_{1,L} - c_L \sqrt{\frac{2p_{11,*}}{3p_{11,L}} + \frac{1}{3}} = u_{1,*} - \frac{1}{\rho_{*L}} \sqrt{(2p_{11,*} + p_{11,L})\rho_L},$$

which is identified by the condition  $p_{11,*} > p_{11,L}$ , one can obtain

$$\rho_{*L} = \rho_L \frac{2p_{11,*} + p_{11,L}}{p_{11,*} + 2p_{11,L}}.$$

The variables  $u_{2,*L}$  and  $p_{12,*L}$  are obtained by solving the following system

$$\mathbf{A}^L \begin{pmatrix} u_{2,*L} \\ p_{12,*L} \end{pmatrix} = \begin{pmatrix} a_1^L \\ a_2^L \end{pmatrix},$$

where

$$\begin{aligned} \mathbf{A}^L &:= \begin{pmatrix} \rho_{*L}(u_{1,*} - \sigma_L) & 1 \\ E_{11,*L} - \frac{1}{2}\rho_{*L}u_{1,*}\sigma_L & u_{1,*} - \frac{1}{2}\sigma_L \end{pmatrix}, \\ a_1^L &:= \rho_L(u_{1,L} - \sigma_L)u_{2,L} + p_{12,L}, \end{aligned}$$

$$a_2^L := E_{12,L}(u_{1,L} - \sigma_L) + \frac{1}{2}(p_{11,L}u_{2,L} + p_{12,L}u_{1,L}).$$

The variable  $p_{22,*L}$  is given by

$$p_{22,*L} = 2E_{22,*L} - \rho_{*L}u_{2,*L}^2,$$

where

$$E_{22,*L} = \frac{E_{22,L}u_{1,L} + p_{12,L}u_{2,L} - \sigma_L E_{22,L} - p_{12,*L}u_{2,*L}}{u_{1,*} - \sigma_L}.$$

#### 4.5. Computing $\mathbf{V}_{**L}$ and $\mathbf{V}_{**R}$

The solution state  $\mathbf{V}_{**L}$  is between the 2-shear wave and the contact discontinuity, while  $\mathbf{V}_{**R}$  is between the 5-shear wave and the contact discontinuity. Across the 2-shear wave, utilizing the generalized Riemann invariant  $u_2 + \frac{p_{12}}{\sqrt{\rho p_{11}}}$  gives

$$u_{2,**} + \frac{p_{12,**}}{\sqrt{\rho_{*L}p_{11,*}}} = a_3^L, \quad (4.9)$$

with  $a_3^L := u_{2,*L} + \frac{p_{12,*L}}{\sqrt{\rho_{*L}p_{11,*}}}$ . For the 5-shear wave, using the generalized Riemann invariant  $u_2 - \frac{p_{12}}{\sqrt{\rho p_{11}}}$  yields

$$u_{2,**} - \frac{p_{12,**}}{\sqrt{\rho_{*R}p_{11,*}}} = a_3^R, \quad (4.10)$$

with  $a_3^R := u_{2,*R} - \frac{p_{12,*R}}{\sqrt{\rho_{*R}p_{11,*}}}$ . Solving (4.9) and (4.10) gives

$$\begin{aligned} u_{2,**} &= \frac{a_3^L \sqrt{\rho_{*L}} + a_3^R \sqrt{\rho_{*R}}}{\sqrt{\rho_{*L}} + \sqrt{\rho_{*R}}}, \\ p_{12,**} &= \frac{(a_3^L - a_3^R) \sqrt{\rho_{*L} \rho_{*R} p_{11,*}}}{\sqrt{\rho_{*L}} + \sqrt{\rho_{*R}}}. \end{aligned} \quad (4.11)$$

Moreover, the fact that  $\det(\mathbf{p})$  is the generalized Riemann invariant of both the 2-shear wave and the 5-shear wave implies that

$$p_{22,**K} = \frac{\det(\mathbf{p}_{*K}) + p_{12,**}^2}{p_{11,*}}, \quad K = L, R. \quad (4.12)$$

## 5. Resolution of the GRP

This section resolves the following GRP problem

$$\begin{cases} (2.1), & t > 0, \\ \mathbf{V}(x, 0) = \begin{cases} \mathbf{V}_L + x \mathbf{V}'_L, & x < 0, \\ \mathbf{V}_R + x \mathbf{V}'_R, & x > 0, \end{cases} \end{cases} \quad (5.1)$$

to derive the limiting value of  $\frac{\partial \mathbf{V}}{\partial t}$  at  $x = 0$ , as  $t \rightarrow 0+$ , where  $\mathbf{V}'_K := (\rho'_K, u'_{1,K}, u'_{2,K}, p'_{11,K}, p'_{12,K}, p'_{22,K})^\top$ ,  $K = L, R$ , are the constant slope vectors. The initial structure of the solution  $\mathbf{V}^{\text{GRP}}(x, t)$  of (5.1) is determined by the exact solution  $\boldsymbol{\omega}(\frac{x}{t}; \mathbf{V}_L, \mathbf{V}_R)$  of the Riemann problem (4.1) and

$$\lim_{t \rightarrow 0+} \mathbf{V}^{\text{GRP}}(\lambda t, t) = \boldsymbol{\omega}(0; \mathbf{V}_L, \mathbf{V}_R) =: \mathbf{V}^{\text{RP}}, \quad x = \lambda t.$$

The local wave pattern around the singularity point  $(x, t) = (0, 0)$  of the GRP (5.1) typically exhibits piecewise smoothness and comprises elementary wave types, including the rarefaction wave, the shock wave, the shear wave, and the contact discontinuity, as depicted schematically in Figure 3.

The rarefaction waves in the solution of the Riemann problem (4.1) exhibit isentropic flow properties, making the generalized Riemann invariants constant with vanishing derivatives within  $i$ th-rarefaction wave ( $i = 1, 6$ ), but unfortunately, those properties do not generally hold for the generalized Riemann problem (5.1) due to the

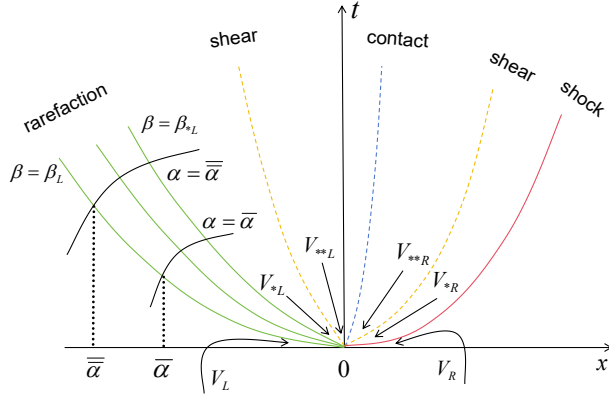


Figure 3: The schematic description of a local wave configuration of the GRP (5.1) with  $0 \leq t \ll 1$ .

need to consider the curved rarefaction waves. Nonetheless, for a short time period  $0 \leq t \ll 1$ , the solution of (5.1) may be considered as a perturbation of the solution of (4.1), allowing us to expect that the generalized Riemann invariants remain regular within the  $i$ th-rarefaction waves ( $i = 1, 6$ ) of the solution  $\mathbf{V}^{\text{GRP}}(x, t)$  near the singularity point  $(x, t) = (0, 0)$ . Consequently, the generalized Riemann invariants are still utilized to resolve the rarefaction waves around this singularity point.

From this, as an example, we will continue to focus our attention on the specific local wave configuration depicted in Figure 3, corresponding to Figure 1. In this configuration, a rarefaction wave propagates to the left, while a shock wave moves to the right. The intermediate region between them is separated by two shear waves and a contact discontinuity. It is worth noting that other local wave configurations can be analyzed in a similar manner. In the subsequent subsections, the nonsonic case (see Subsection 5.1), the sonic case (see Subsection 5.2), and the acoustic case (see Subsection 5.3) will be separately discussed in detail to compute the limiting value of  $\frac{\partial \mathbf{V}}{\partial t}(0, t)$  as  $t \rightarrow 0+$ .

### 5.1. Nonsonic case

If the  $t$ -axis is located between the 1-wave and the 6-wave, the nonsonic case happens. Denote the limiting values of  $\frac{\partial \mathbf{V}}{\partial t}(0, t)$  when  $t \rightarrow 0+$  in the four middle domains by  $(\frac{\partial \mathbf{V}}{\partial t})_{*L}$ ,  $(\frac{\partial \mathbf{V}}{\partial t})_{**L}$ ,  $(\frac{\partial \mathbf{V}}{\partial t})_{**R}$  and  $(\frac{\partial \mathbf{V}}{\partial t})_{*R}$ , respectively. The derivations of those limiting values are very long-winded and tedious, and for the sake of convenience, the main steps in this subsection are outlined in Figure 4.

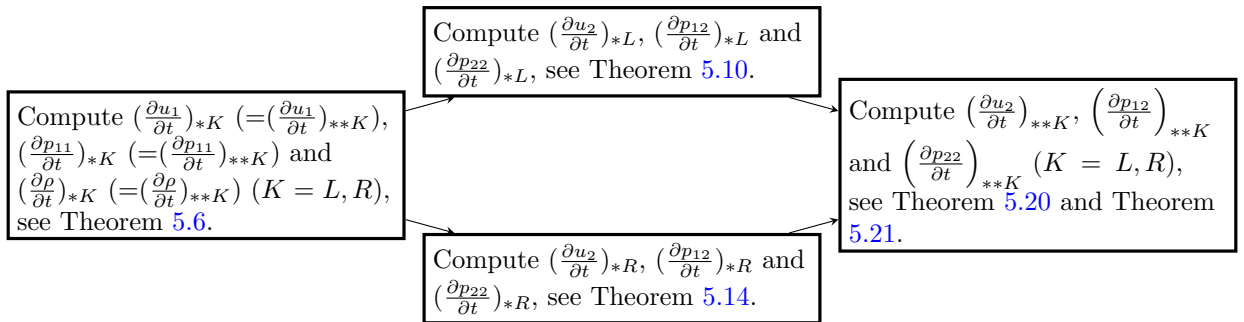


Figure 4: The main steps for the nonsonic case in Subsection 5.1.

#### 5.1.1. Computing $(\frac{\partial u_1}{\partial t})_{*K}$ , $(\frac{\partial p_{11}}{\partial t})_{*K}$ and $(\frac{\partial p}{\partial t})_{*K}$ ( $K = L, R$ )

Similar to the second-order accurate GRP scheme in [5, 55, 56, 19], the region of the 1-rarefaction wave associated with  $\lambda_1 = u_1 - c$  can be described by the characteristic coordinates  $(\alpha, \beta)$ , where  $\alpha \in [-\infty, 0]$ ,  $\beta \in [\beta_L, \beta_{*L}]$  with  $\beta_L = \lambda_1(\mathbf{V}_L)$  and  $\beta_{*L} = \lambda_1(\mathbf{V}_{*L})$ , see Figure 3, and  $\beta = \beta(x, t)$  and  $\alpha = \alpha(x, t)$  are the integral curves of the following two equations

$$\frac{dx}{dt} = u_1 - c, \quad \frac{dx}{dt} = u_1 + c, \quad (5.2)$$

respectively. Here,  $\beta$  represents the initial value of the slope  $\lambda_1 = u_1 - c$  at the singularity point  $(0,0)$ , and  $\alpha$  denotes the  $x$ -coordinate of the intersection point between the transversal characteristic curve and the leading  $\beta$ -curve, as illustrated in Figure 3. Two equations in (5.2) may give

$$\frac{\partial x}{\partial \alpha} = (u_1 - c) \frac{\partial t}{\partial \alpha}, \quad \frac{\partial x}{\partial \beta} = (u_1 + c) \frac{\partial t}{\partial \beta}, \quad (5.3)$$

which further imply that

$$\frac{\partial^2 t}{\partial \alpha \partial \beta} = \frac{1}{2c} \left( \frac{\partial(u_1 - c)}{\partial \beta} \frac{\partial t}{\partial \alpha} - \frac{\partial(u_1 + c)}{\partial \alpha} \frac{\partial t}{\partial \beta} \right). \quad (5.4)$$

Similarly, for the associated Riemann problem, there exists a local coordinate transformation  $x_{\text{ass}} = x(\alpha, \beta)$ ,  $t_{\text{ass}} = t(\alpha, \beta)$ . Both local coordinate transformations satisfy the properties [5]

$$\frac{\partial \lambda_1}{\partial t}(0, \beta) = 1, \quad \frac{\partial t}{\partial \alpha}(0, \beta) = \frac{\partial t_{\text{ass}}}{\partial \alpha}(0, \beta), \quad \frac{\partial t}{\partial \beta}(0, \beta) = 0, \quad \beta_L \leq \beta \leq \beta_{*L}. \quad (5.5)$$

It follows from (5.4) that

$$\frac{\partial^2 t}{\partial \alpha \partial \beta}(0, \beta) = \frac{1}{2c(0, \beta)} \frac{\partial t}{\partial \alpha}(0, \beta). \quad (5.6)$$

Let  $\psi_1 := u_1 + c$  and  $S_1 := \frac{p_{11}}{\rho^3}$ . Following the same derivation in [5], one has the following explicit expressions of the local coordinate transformation in the 1-rarefaction wave of the associated Riemann problem

$$t_{\text{ass}}(\alpha, \beta) = \frac{\alpha}{\psi_{1,L} - \beta}, \quad x_{\text{ass}}(\alpha, \beta) = \frac{\alpha\beta}{\psi_{1,L} - \beta}. \quad (5.7)$$

Because  $\psi_1 = u_1 + c$ ,  $\beta = u_1(0, \beta) - c(0, \beta)$  and  $\psi_1$  is a generalized Riemann invariant across the 1-rarefaction wave, one has

$$c(0, \beta) = \frac{1}{2}(\psi_{1,L} - \beta), \quad u_1(0, \beta) = \frac{1}{2}(\psi_{1,L} + \beta). \quad (5.8)$$

Combining (5.5), (5.7) with (5.8) gives

$$\frac{\partial t}{\partial \alpha}(0, \beta) = \frac{1}{2c(0, \beta)}. \quad (5.9)$$

Due to  $d\psi_1 = du_1 - \frac{c}{2\rho} d\rho + \frac{3}{2\rho c} dp_{11}$  and  $dS_1 = \frac{-3p_{11}}{\rho^4} d\rho + \frac{1}{\rho^3} dp_{11}$ , using (2.5a), (2.5b) and (2.5d) yields

$$\frac{\partial \psi_1}{\partial t} + (u_1 + c) \frac{\partial \psi_1}{\partial x} = \Pi_1, \quad (5.10)$$

$$\frac{\partial S_1}{\partial t} + u_1 \frac{\partial S_1}{\partial x} = 0, \quad (5.11)$$

where  $\Pi_1 := -\frac{c^2}{2\rho} \frac{\partial \rho}{\partial x} + \frac{1}{2\rho} \frac{\partial p_{11}}{\partial x} - \frac{1}{2} W_x$ . Besides, one has

$$dp_{11} = c^2 d\rho + \rho^3 dS_1. \quad (5.12)$$

It follows that

$$\Pi_1 = \frac{1}{2\rho} \left( \frac{\partial p_{11}}{\partial x} - c^2 \frac{\partial \rho}{\partial x} \right) - \frac{1}{2} W_x = \frac{1}{2} \rho^2 \frac{\partial S_1}{\partial x} - \frac{1}{2} W_x. \quad (5.13)$$

For  $\psi_1$ , by the total differentials of  $\psi_1$  and  $S_1$ , one has

$$d\psi_1 = du_1 + \frac{1}{\rho c} dp_{11} + \frac{\rho^2}{2c} dS_1. \quad (5.14)$$

The following lemma gives the expressions of  $(\rho^2 \frac{\partial S_1}{\partial t})(0, \beta)$  and  $\frac{\partial \psi_1}{\partial t}(0, \beta)$ .

**Lemma 5.1.** *If assuming that the 1-rarefaction wave associated with  $u_1 - c$  moves to the left, and considering the generalized Riemann invariants  $\psi_1, S_1$  and their time derivatives  $\frac{\partial \psi_1}{\partial t}, \frac{\partial S_1}{\partial t}$  as continuous functions of  $\alpha, \beta$*

with  $-\alpha_0 \leq \alpha \leq 0$  and  $\beta_L \leq \beta \leq \beta_{*L}$ , then one has

$$\left(\rho^2 \frac{\partial S_1}{\partial t}\right)(0, \beta) = -\frac{\rho_L^2 S'_{1,L}}{c_L^3} [\beta + c(0, \beta)] \cdot c^3(0, \beta), \quad (5.15)$$

$$\frac{\partial \psi_1}{\partial t}(0, \beta) = \frac{\rho_L^2 S'_{1,L}}{8c_L^3} [\psi_{1,L}(3c_L^2 - c^2) - 2\beta c^2](0, \beta) - \psi'_{1,L} \psi_1(0, \beta) - \frac{1}{2} W_x(0), \quad (5.16)$$

where

$$S'_{1,L} = \frac{1}{\rho_L^3} (p'_{11,L} - c_L^2 \rho'_L), \quad \psi'_{1,L} = u'_{1,L} + \frac{1}{\rho_L c_L} p'_{11,L} + \frac{\rho_L^2}{2c_L} S'_{1,L}, \quad (5.17)$$

obtained by (5.12) and (5.14).

*Proof.* (i) Computing  $(\rho^2 \frac{\partial S_1}{\partial t})(0, \beta)$ . Using (5.3) and (5.11) gives

$$\frac{\partial S_1}{\partial \beta} = \frac{\partial t}{\partial \beta} \left[ \frac{\partial S_1}{\partial t} + (u_1 + c) \frac{\partial S_1}{\partial x} \right] = \frac{\partial t}{\partial \beta} \cdot c \frac{\partial S_1}{\partial x}, \quad (5.18)$$

$$\frac{\partial S_1}{\partial \alpha} = \frac{\partial t}{\partial \alpha} \left[ \frac{\partial S_1}{\partial t} + (u_1 - c) \frac{\partial S_1}{\partial x} \right] = -\frac{\partial t}{\partial \alpha} \cdot c \frac{\partial S_1}{\partial x}. \quad (5.19)$$

Differentiating (5.18) with respect to  $\alpha$  and noting that  $\frac{\partial t}{\partial \beta}(0, \beta) = 0$ , one gets

$$\frac{\partial}{\partial \beta} \left( \frac{\partial S_1}{\partial \alpha}(0, \beta) \right) = \frac{1}{2} \frac{\partial t}{\partial \alpha}(0, \beta) \frac{\partial S_1}{\partial x}(0, \beta) = -\frac{1}{2c(0, \beta)} \frac{\partial S_1}{\partial \alpha}(0, \beta), \quad (5.20)$$

where (5.6) and (5.19) have been used in the first and second equality, respectively. Integrating (5.20) from  $\beta_L$  to  $\beta$  yields

$$\frac{\partial S_1}{\partial \alpha}(0, \beta) = \frac{\partial S_1}{\partial \alpha}(0, \beta_L) \cdot \exp \left( -\int_{\beta_L}^{\beta} \frac{1}{2c(0, \eta)} d\eta \right) = \frac{\partial S_1}{\partial \alpha}(0, \beta_L) \cdot \frac{c(0, \beta)}{c_L}. \quad (5.21)$$

Similarly, from (5.6), one has

$$\frac{\partial t}{\partial \alpha}(0, \beta) = \frac{\partial t}{\partial \alpha}(0, \beta_L) \cdot \frac{c_L}{c(0, \beta)}. \quad (5.22)$$

By (5.19), (5.21) and (5.22), one has

$$\begin{aligned} \frac{\partial S_1}{\partial x}(0, \beta) &= -\frac{\partial S_1}{\partial \alpha}(0, \beta) \cdot \left( c \frac{\partial t}{\partial \alpha} \right)^{-1}(0, \beta) \\ &= -\frac{\partial S_1}{\partial \alpha}(0, \beta_L) \cdot \frac{c(0, \beta)}{c_L} \frac{1}{c(0, \beta)} \left( \frac{\partial t}{\partial \alpha} \right)^{-1}(0, \beta_L) \cdot \frac{c(0, \beta)}{c_L} \\ &= -\frac{\partial S_1}{\partial \alpha}(0, \beta_L) \cdot \left( \frac{\partial t}{\partial \alpha} \right)^{-1}(0, \beta_L) \cdot \frac{c(0, \beta)}{c_L^2} \\ &= c_L \frac{\partial S_1}{\partial x}(0, \beta_L) \cdot \frac{c(0, \beta)}{c_L^2} = \frac{S'_{1,L}}{c_L} c(0, \beta), \end{aligned} \quad (5.23)$$

It follows that

$$\frac{\partial S_1}{\partial t}(0, \beta) = -u_1(0, \beta) \cdot \frac{\partial S_1}{\partial x}(0, \beta) = -\frac{S'_{1,L}}{c_L} [\beta + c(0, \beta)] \cdot c(0, \beta). \quad (5.24)$$

Because  $S_1 = p_{11}/\rho^3$  is a generalized Riemann invariant for the 1-rarefaction wave, it holds that

$$\frac{\rho^2(0, \beta)}{\rho_L^2} = \frac{(3p_{11}/\rho)(0, \beta)}{3p_{11,L}/\rho_L} = \frac{c^2(0, \beta)}{c_L^2}, \quad (5.25)$$

and then combining (5.24) and (5.25) gives (5.15).

(ii) Computing  $\frac{\partial \psi_1}{\partial t}(0, \beta)$ . Using (5.10) gives

$$\frac{\partial \psi_1}{\partial \beta} = \frac{\partial t}{\partial \beta} \Pi_1(\alpha, \beta), \quad (5.26)$$

$$\frac{\partial \psi_1}{\partial \alpha} = \frac{\partial t}{\partial \alpha} \left[ \frac{\partial \psi_1}{\partial t} + (u_1 - c) \frac{\partial \psi_1}{\partial x} \right] = \frac{\partial t}{\partial \alpha} \left[ \Pi_1(\alpha, \beta) - 2c \frac{\partial \psi_1}{\partial x} \right]. \quad (5.27)$$

Differentiating (5.26) with respect to  $\alpha$  and using (5.5), (5.6) gets

$$\frac{\partial}{\partial \beta} \left( \frac{\partial \psi_1}{\partial \alpha}(0, \beta) \right) = \frac{1}{2c(0, \beta)} \frac{\partial t}{\partial \alpha}(0, \beta) \cdot \Pi_1(0, \beta).$$

Integrating the above equation from  $\beta_L$  to  $\beta$  yields

$$\frac{\partial \psi_1}{\partial \alpha}(0, \beta) = \frac{\partial \psi_1}{\partial \alpha}(0, \beta_L) + \int_{\beta_L}^{\beta} \frac{1}{2c(0, \eta)} \frac{\partial t}{\partial \alpha}(0, \eta) \cdot \Pi_1(0, \eta) d\eta. \quad (5.28)$$

Due to (5.13) and (5.27), the initial value is computed as

$$\frac{\partial \psi_1}{\partial \alpha}(0, \beta_L) = \frac{\partial t}{\partial \alpha}(0, \beta_L) \cdot \left[ \frac{1}{2} \rho_L^2 S'_{1,L} - \frac{1}{2} W_x(0) - 2c_L \psi'_{1,L} \right]. \quad (5.29)$$

Moreover, by (5.8), (5.13), (5.23) and (5.25), one has

$$\Pi_1(0, \beta) = \frac{\rho_L^2 S'_{1,L}}{16c_L^3} (\psi_{1,L} - \beta)^3 - \frac{1}{2} W_x(0). \quad (5.30)$$

Thus the integral in (5.28) can be exactly obtained and

$$\int_{\beta_L}^{\beta} \frac{1}{2c(0, \eta)} \frac{\partial t}{\partial \alpha}(0, \eta) \cdot \Pi_1(0, \eta) d\eta = -\frac{\rho_L^2 S'_{1,L}}{8c_L^3} [c^2(0, \beta) - c_L^2] - \frac{1}{4} W_x(0) \left( \frac{1}{c(0, \beta)} - \frac{1}{c_L} \right), \quad (5.31)$$

where (5.9) has been used. Substituting (5.29) and (5.31) into (5.28) yields the expression of  $\frac{\partial \psi_1}{\partial \alpha}(0, \beta)$ . The second equality in (5.27) implies that

$$2c(0, \beta) \cdot \frac{\partial \psi_1}{\partial x}(0, \beta) = \Pi_1(0, \beta) - \left( \frac{\partial t}{\partial \alpha} \right)^{-1}(0, \beta) \cdot \frac{\partial \psi_1}{\partial \alpha}(0, \beta). \quad (5.32)$$

Combining (5.32) with the first equality in (5.27), one gets

$$\frac{\partial \psi_1}{\partial t}(0, \beta) = -\left( \frac{u_1 - c}{2c} \right)(0, \beta) \cdot \Pi_1(0, \beta) + \left( \frac{u_1 + c}{2c} \right)(0, \beta) \cdot \left( \frac{\partial t}{\partial \alpha} \right)^{-1}(0, \beta) \cdot \frac{\partial \psi_1}{\partial \alpha}(0, \beta). \quad (5.33)$$

Substituting the expression of  $\frac{\partial \psi_1}{\partial \alpha}(0, \beta)$  and (5.30) into (5.33) gives (5.16).  $\square$

**Lemma 5.2** (Resolution of the 1-rarefaction wave). *Assuming that the 1-rarefaction wave associated with  $u_1 - c$  moves to the left, the limiting values  $\frac{\mathcal{D}u_1}{\mathcal{D}t}(0, \beta)$  and  $\frac{\mathcal{D}p_{11}}{\mathcal{D}t}(0, \beta)$  satisfy*

$$\tilde{a}_1(0, \beta) \cdot \frac{\mathcal{D}u_1}{\mathcal{D}t}(0, \beta) + \tilde{b}_1(0, \beta) \cdot \frac{\mathcal{D}p_{11}}{\mathcal{D}t}(0, \beta) = \tilde{d}_1(0, \beta), \quad (5.34)$$

where

$$\begin{aligned} \tilde{a}_1(0, \beta) &= 1 + \frac{u_1(0, \beta)}{c(0, \beta)}, \quad \tilde{b}_1(0, \beta) = \left( \frac{u_1}{3p_{11}} + \frac{1}{\rho c} \right)(0, \beta), \\ \tilde{d}_1(0, \beta) &= \frac{\rho_L^2 S'_{1,L} \psi_{1,L}}{8c_L^3} [3c_L^2 + c^2(0, \beta)] - \psi'_{1,L} \psi_{1,L} - \frac{1}{2} \left( 1 + \frac{u_1(0, \beta)}{c(0, \beta)} \right) W_x(0). \end{aligned}$$

*Proof.* Using (5.14) gets

$$\frac{\partial u_1}{\partial t} + \frac{1}{\rho c} \frac{\partial p_{11}}{\partial t} = \frac{\partial \psi_1}{\partial t} - \frac{\rho^2}{2c} \frac{\partial S_1}{\partial t}. \quad (5.35)$$

Substituting (2.8) into above equation obtains

$$\left(1 + \frac{u_1}{c}\right) \frac{\mathcal{D}u_1}{\mathcal{D}t} + \left(\frac{u_1}{3p_{11}} + \frac{1}{\rho c}\right) \frac{\mathcal{D}p_{11}}{\mathcal{D}t} = \frac{\partial \psi_1}{\partial t} - \frac{\rho^2}{2c} \frac{\partial S_1}{\partial t} - \frac{u_1}{2c} W_x.$$

Combining it with (5.15) and (5.16) gives (5.34).  $\square$

Taking  $\beta = \beta_{*L}$  in (5.34) and using (2.8) obtains the first equation for  $\left(\frac{\mathcal{D}u_1}{\mathcal{D}t}\right)_*$  and  $\left(\frac{\mathcal{D}p_{11}}{\mathcal{D}t}\right)_*$  as follows

$$a_1 \left(\frac{\mathcal{D}u_1}{\mathcal{D}t}\right)_* + b_1 \left(\frac{\mathcal{D}p_{11}}{\mathcal{D}t}\right)_* = d_1, \quad (5.36)$$

where

$$\begin{cases} a_1 = \tilde{a}_1(0, \beta_{*L}) = 1 + \frac{u_{1,*}}{c_{*L}}, \\ b_1 = \tilde{b}_1(0, \beta_{*L}) = \frac{u_{1,*}}{3p_{11,*}} + \frac{1}{\rho_{*L}c_{*L}}, \\ d_1 = \tilde{d}_1(0, \beta_{*L}) = \left[\frac{\rho_L^2 S'_{1,L}}{8c_L^3} (3c_L^2 + c_{*L}^2) - \psi'_{1,L}\right] \psi_{1,L} - \frac{1}{2} \left(1 + \frac{u_{1,*}}{c_{*L}}\right) W_x(0). \end{cases} \quad (5.37)$$

**Remark 5.3.** It is necessary to prove that both the limiting values of  $\frac{\mathcal{D}u_1}{\mathcal{D}t}$  and  $\frac{\mathcal{D}p_{11}}{\mathcal{D}t}$  do not change in the whole domain between the 1-wave and the 6-wave, which are denoted by  $\left(\frac{\mathcal{D}u_1}{\mathcal{D}t}\right)_*$  and  $\left(\frac{\mathcal{D}p_{11}}{\mathcal{D}t}\right)_*$ , respectively.

To this end, we firstly prove that

$$\left(\frac{\mathcal{D}u_1}{\mathcal{D}t}\right)_{*K} = \left(\frac{\mathcal{D}u_1}{\mathcal{D}t}\right)_{**K}, \quad \left(\frac{\mathcal{D}p_{11}}{\mathcal{D}t}\right)_{*K} = \left(\frac{\mathcal{D}p_{11}}{\mathcal{D}t}\right)_{**K}, \quad K = L, R. \quad (5.38)$$

For  $K = L$ , because both  $u_1$  and  $p_{11}$  are the generalized Riemann invariants for the 2-shear wave, one has

$$\left(\frac{\mathcal{D}_2 u_1}{\mathcal{D}t}\right)_{*L} = \left(\frac{\mathcal{D}_2 u_1}{\mathcal{D}t}\right)_{**L}, \quad \left(\frac{\mathcal{D}_2 p_{11}}{\mathcal{D}t}\right)_{*L} = \left(\frac{\mathcal{D}_2 p_{11}}{\mathcal{D}t}\right)_{**L},$$

where  $\frac{\mathcal{D}_2}{\mathcal{D}t} := \frac{\partial}{\partial t} + \lambda_2 \frac{\partial}{\partial x}$  and  $\lambda_2 = u_{1,*} - \frac{c_{*L}}{\sqrt{3}}$ . By (2.6) and (2.7), it follows that

$$\begin{aligned} \left(\frac{\mathcal{D}u_1}{\mathcal{D}t}\right)_{*L} - \frac{\lambda_2 - u_{1,*}}{3p_{11,*}} \left(\frac{\mathcal{D}p_{11}}{\mathcal{D}t}\right)_{*L} &= \left(\frac{\mathcal{D}u_1}{\mathcal{D}t}\right)_{**L} - \frac{\lambda_2 - u_{1,*}}{3p_{11,*}} \left(\frac{\mathcal{D}p_{11}}{\mathcal{D}t}\right)_{**L}, \\ \left(\frac{\mathcal{D}p_{11}}{\mathcal{D}t}\right)_{*L} - \rho_{*L}(\lambda_2 - u_{1,*}) \left[\left(\frac{\mathcal{D}u_1}{\mathcal{D}t}\right)_{*L} + \frac{1}{2}W_x(0)\right] &= \left(\frac{\mathcal{D}p_{11}}{\mathcal{D}t}\right)_{**L} - \rho_{*L}(\lambda_2 - u_{1,*}) \left[\left(\frac{\mathcal{D}u_1}{\mathcal{D}t}\right)_{**L} + \frac{1}{2}W_x(0)\right]. \end{aligned}$$

The above two equations can imply (5.38) for  $K = L$ , and the proof for  $K = R$  is similar. Besides, both  $u_1$  and  $p_{11}$  are also the generalized Riemann invariants for the contact discontinuity, thus

$$\left(\frac{\mathcal{D}u_1}{\mathcal{D}t}\right)_{**L} = \left(\frac{\mathcal{D}u_1}{\mathcal{D}t}\right)_{**R}, \quad \left(\frac{\mathcal{D}p_{11}}{\mathcal{D}t}\right)_{**L} = \left(\frac{\mathcal{D}p_{11}}{\mathcal{D}t}\right)_{**R}. \quad (5.39)$$

In virtue of (5.38) and (5.39), one finds that both the limiting values of  $\frac{\mathcal{D}u_1}{\mathcal{D}t}$  and  $\frac{\mathcal{D}p_{11}}{\mathcal{D}t}$  do not change in the whole domain between the 1-wave and the 6-wave. Furthermore, combining (5.38) with (2.8), one obtains

$$\left(\frac{\partial u_1}{\partial t}\right)_{*K} = \left(\frac{\partial u_1}{\partial t}\right)_{**K}, \quad \left(\frac{\partial p_{11}}{\partial t}\right)_{*K} = \left(\frac{\partial p_{11}}{\partial t}\right)_{**K}, \quad K = L, R,$$

which means that both the limiting values of  $\frac{\partial u_1}{\partial t}$  and  $\frac{\partial p_{11}}{\partial t}$  do not change across the 2-shear wave and the 5-shear wave.

Up to now, we have established the first equation (5.36) that the limiting values  $\left(\frac{\mathcal{D}u_1}{\mathcal{D}t}\right)_*$  and  $\left(\frac{\mathcal{D}p_{11}}{\mathcal{D}t}\right)_*$  satisfy. To obtain their values, another equation is necessary by resolving the 6-shock wave. For the shock wavs, one



has

$$\sigma = \frac{\rho u_1 - \bar{\rho} \bar{u}_1}{\rho - \bar{\rho}}, \quad u_1 = \bar{u}_1 \pm \Phi(p_{11}; \bar{p}_{11}, \bar{\rho}), \quad \rho = H(p_{11}; \bar{p}_{11}, \bar{\rho}),$$

where  $(\rho, u_1, p_{11})$  and  $(\bar{\rho}, \bar{u}_1, \bar{p}_{11})$  are the states ahead and behind the shock wave with the speed  $\sigma$ , and in the second equality, the "+" is for 6-shock wave and "-" is for 1-shock wave. According to the discussion on the exact Riemann solver, one knows that

$$\begin{aligned} \Phi(p_{11}; \bar{p}_{11}, \bar{\rho}) &= (p_{11} - \bar{p}_{11}) \left[ \frac{1}{\bar{\rho}(2p_{11} + \bar{p}_{11})} \right]^{\frac{1}{2}}, \\ H(p_{11}; \bar{p}_{11}, \bar{\rho}) &= \frac{2p_{11} + \bar{p}_{11}}{p_{11} + 2\bar{p}_{11}} \bar{\rho}. \end{aligned}$$

Moreover, along the shock waves, there holds

$$\frac{\mathcal{D}_\sigma \Gamma}{\mathcal{D}t} = 0, \quad (5.40)$$

where  $\frac{\mathcal{D}_\sigma}{\mathcal{D}t} := \frac{\partial}{\partial t} + \sigma \frac{\partial}{\partial x}$  and  $\Gamma = u_1 - [\bar{u}_1 \pm \Phi(p_{11}; \bar{p}_{11}, \bar{\rho})]$  or  $\Gamma = \rho - H(p_{11}; \bar{p}_{11}, \bar{\rho})$ . Taking  $\Gamma = u_1 - [\bar{u}_1 \pm \Phi(p_{11}; \bar{p}_{11}, \bar{\rho})]$  in (5.40) and utilizing (2.5a), (2.5b), (2.5d), (2.6), (2.7) and (2.8) yields

$$\begin{aligned} & [1 \mp \rho(u_1 - \sigma)\Phi_1] \frac{\mathcal{D}u_1}{\mathcal{D}t} + \left[ \frac{u_1 - \sigma}{3p_{11}} \mp \Phi_1 \right] \frac{\mathcal{D}p_{11}}{\mathcal{D}t} \\ &= \pm \Phi_3(\sigma - \bar{u}_1)\bar{\rho}' + [\sigma - \bar{u}_1 \mp 3\bar{p}_{11}\Phi_2 \mp \bar{\rho}\Phi_3]\bar{u}_1' + \left[ -\frac{1}{\bar{\rho}} \pm (\sigma - \bar{u}_1)\Phi_2 \right] \bar{p}_{11}' - \frac{1}{2} [\mp \rho(u_1 - \sigma)\Phi_1 + 1] W_x, \end{aligned}$$

where

$$\begin{cases} \Phi_1 = \frac{\partial \Phi}{\partial p_{11}} = \frac{p_{11} + 2\bar{p}_{11}}{2p_{11} + \bar{p}_{11}} \left[ \frac{1}{\bar{\rho}(2p_{11} + \bar{p}_{11})} \right]^{\frac{1}{2}}, \\ \Phi_2 = \frac{\partial \Phi}{\partial \bar{p}_{11}} = -\frac{5p_{11} + \bar{p}_{11}}{4p_{11} + 2\bar{p}_{11}} \left[ \frac{1}{\bar{\rho}(2p_{11} + \bar{p}_{11})} \right]^{\frac{1}{2}}, \\ \Phi_3 = \frac{\partial \Phi}{\partial \bar{\rho}} = \frac{\bar{p}_{11} - p_{11}}{2\bar{\rho}} \left[ \frac{1}{\bar{\rho}(2p_{11} + \bar{p}_{11})} \right]^{\frac{1}{2}}. \end{cases} \quad (5.41)$$

Specifically, for the 6-shock wave, one has the following result.

**Lemma 5.4** (Resolution of the 6-shock wave). *Assume that the 6-shock wave associated with  $u_1 + c$  moves to the right. The limiting values  $(\frac{\mathcal{D}u_1}{\mathcal{D}t})_*$  and  $(\frac{\mathcal{D}p_{11}}{\mathcal{D}t})_*$  satisfy*

$$a_2 \left( \frac{\mathcal{D}u_1}{\mathcal{D}t} \right)_* + b_2 \left( \frac{\mathcal{D}p_{11}}{\mathcal{D}t} \right)_* = d_2, \quad (5.42)$$

where

$$\begin{cases} a_2 = 1 - \rho_{*R}(u_{1,*} - \sigma_R) \cdot \Phi_1^R, \\ b_2 = \frac{u_{1,*} - \sigma_R}{3p_{11,*}} - \Phi_1^R, \\ d_2 = L_\rho^R \cdot \rho'_R + L_{u_1}^R \cdot u'_{1,R} + L_{p_{11}}^R \cdot p'_{11,R} - \frac{1}{2} W_x(0) \cdot L_W^R, \end{cases} \quad (5.43)$$

and

$$\begin{aligned} L_\rho^R &= (\sigma_R - u_{1,R}) \cdot \Phi_3^R, \quad L_{u_1}^R = \sigma_R - u_{1,R} - 3p_{11,R} \cdot \Phi_2^R - \rho_R \cdot \Phi_3^R, \\ L_{p_{11}}^R &= -\frac{1}{\rho_R} + (\sigma_R - u_{1,R}) \cdot \Phi_2^R, \quad L_W^R = -\rho_{*R}(u_{1,*} - \sigma_R) \cdot \Phi_1^R + 1 \end{aligned}$$

with  $\Phi_i^R := \Phi_i(p_{11,*}; p_{11,R}, \rho_R)$  ( $i = 1, 2, 3$ ).

**Remark 5.5.** *We now prove that*

$$\left( \frac{\partial \rho}{\partial t} \right)_{*K} = \left( \frac{\partial \rho}{\partial t} \right)_{**K}, \quad K = L, R. \quad (5.44)$$

(i) If  $u_{1,*} = 0$ , then by (2.5a) and (2.6), one has  $\frac{\partial \rho}{\partial t} = \frac{\rho}{3p_{11}} \frac{\mathcal{D}p_{11}}{\mathcal{D}t}$ , and thus (5.44) may be concluded from

(5.38).

(ii) If  $u_{1,*} \neq 0$ , then since  $\rho$  is a generalized Riemann invariant for the 2-shear wave, one has

$$u_{1,*} \left( \frac{\mathcal{D}_2 \rho}{\mathcal{D}t} \right)_{*L} = u_{1,*} \left( \frac{\mathcal{D}_2 \rho}{\mathcal{D}t} \right)_{**L},$$

thus by using (2.5a), (2.6) and (5.38), one can have (5.44) for  $K = L$ . The proof for  $K = R$  is similar, because  $\rho$  is also a generalized Riemann invariant for the 5-shear wave.

In virtue of (5.44), henceforth, we will not distinguish  $\left( \frac{\partial \rho}{\partial t} \right)_{**K}$  from  $\left( \frac{\partial \rho}{\partial t} \right)_{*K}$  ( $K = L, R$ ) any more.

**Theorem 5.6** (Computing  $\left( \frac{\partial u_1}{\partial t} \right)_{*K}$ ,  $\left( \frac{\partial p_{11}}{\partial t} \right)_{*K}$  and  $\left( \frac{\partial \rho}{\partial t} \right)_{*K}$  ( $K = L, R$ )). *In the domain between the 1-rarefaction wave and the 6-shock wave, one has*

$$\left( \frac{\mathcal{D}u_1}{\mathcal{D}t} \right)_* = \frac{d_1 b_2 - d_2 b_1}{a_1 b_2 - a_2 b_1}, \quad \left( \frac{\mathcal{D}p_{11}}{\mathcal{D}t} \right)_* = \frac{d_1 a_2 - d_2 a_1}{a_2 b_1 - a_1 b_2}, \quad (5.45)$$

where  $a_1, b_1, d_1$  are given in (5.37) and  $a_2, b_2, d_2$  are given in (5.43). Then by (2.8), one gets

$$\begin{aligned} \left( \frac{\partial u_1}{\partial t} \right)_{*K} &= \frac{u_{1,*}}{3p_{11,*}} \left( \frac{\mathcal{D}p_{11}}{\mathcal{D}t} \right)_* + \left( \frac{\mathcal{D}u_1}{\mathcal{D}t} \right)_*, \\ \left( \frac{\partial p_{11}}{\partial t} \right)_{*K} &= \left( \frac{\mathcal{D}p_{11}}{\mathcal{D}t} \right)_* + \rho_{*K} u_{1,*} \left( \frac{\mathcal{D}u_1}{\mathcal{D}t} \right)_* + \frac{1}{2} \rho_{*K} u_{1,*} W_x(0) \end{aligned} \quad (5.46)$$

with  $K = L, R$ . Moreover,

$$\left( \frac{\partial \rho}{\partial t} \right)_{*L} = \frac{1}{c_{*L}^2} \left[ \left( \frac{\partial p_{11}}{\partial t} \right)_{*L} + \rho_L^2 S'_{1,L} \rho_{*L} u_{1,*} \frac{c_{*L}^3}{c_L^3} \right], \quad (5.47)$$

and  $\left( \frac{\partial \rho}{\partial t} \right)_{*R}$  satisfies

$$g_\rho^R \cdot \left( \frac{\partial \rho}{\partial t} \right)_{*R} + g_{u_1}^R \cdot \left( \frac{\mathcal{D}u_1}{\mathcal{D}t} \right)_* + g_{p_{11}}^R \cdot \left( \frac{\mathcal{D}p_{11}}{\mathcal{D}t} \right)_* = u_{1,*} \cdot f_R, \quad (5.48)$$

where

$$\begin{aligned} g_\rho^R &= u_{1,*} - \sigma_R, \quad g_{u_1}^R = \rho_{*R} u_{1,*} (\sigma_R - u_{1,*}) \cdot H_1^R, \quad g_{p_{11}}^R = \frac{\sigma_R}{c_{*R}^2} - u_{1,*} \cdot H_1^R, \\ f_R &= (\sigma_R - u_{1,R}) \cdot H_2^R \cdot p'_{11,R} + (\sigma_R - u_{1,R}) \cdot H_3^R \cdot \rho'_R - \rho_R (H_3^R + c_R^2 \cdot H_2^R) \cdot u'_{1,R} - \frac{1}{2} \rho_{*R} (\sigma_R - u_{1,*}) W_x(0) \cdot H_1^R \end{aligned}$$

with  $H_i^R = H_i(p_{11,*}; p_{11,R}, \rho_R)$  ( $i = 1, 2, 3$ ) and

$$H_1 = \frac{\partial H}{\partial p_{11}} = \frac{3\bar{\rho}\bar{p}_{11}}{(p_{11} + 2\bar{p}_{11})^2}, \quad H_2 = \frac{\partial H}{\partial \bar{p}_{11}} = -\frac{3\bar{\rho}\bar{p}_{11}}{(p_{11} + 2\bar{p}_{11})^2}, \quad H_3 = \frac{\partial H}{\partial \bar{\rho}} = \frac{2p_{11} + \bar{p}_{11}}{p_{11} + 2\bar{p}_{11}}. \quad (5.49)$$

*Proof.* In virtue of (5.36) and (5.42), the proofs of (5.45) and (5.46) are direct. At the 1-rarefaction side, due to (5.12), one has

$$\left( \frac{\partial p_{11}}{\partial t} \right)_{*L} = c_{*L}^2 \left( \frac{\partial \rho}{\partial t} \right)_{*L} + \rho_{*L}^3 \left( \frac{\partial S_1}{\partial t} \right)_{*L}.$$

Combing it with the result obtained by taking  $\beta = \beta_{*L}$  in (5.15) implies (5.47).

At the shock wave side, by taking  $\Gamma = \rho - H(p_{11}; \bar{p}_{11}, \bar{\rho})$  in (5.40), one gets

$$\frac{\partial \rho}{\partial t} + \sigma \frac{\partial \rho}{\partial x} = H_1 \cdot \left( \frac{\partial p_{11}}{\partial t} + \sigma \frac{\partial p_{11}}{\partial x} \right) + H_2 \cdot \left( \frac{\partial \bar{p}_{11}}{\partial t} + \sigma \frac{\partial \bar{p}_{11}}{\partial x} \right) + H_3 \cdot \left( \frac{\partial \bar{\rho}}{\partial t} + \sigma \frac{\partial \bar{\rho}}{\partial x} \right). \quad (5.50)$$

Then multiplying both sides of (5.50) by  $u_1$ , and utilizing (2.5a), (2.5d), (2.6) and (2.7), one obtains

$$\begin{aligned} & (u_1 - \sigma) \frac{\partial \rho}{\partial t} + \rho u_1 (\sigma - u_1) H_1 \frac{\mathcal{D}u_1}{\mathcal{D}t} + \left( \frac{\sigma}{c^2} - u_1 H_1 \right) \frac{\mathcal{D}p_{11}}{\mathcal{D}t} \\ & = u_1 \cdot \left[ (\sigma - \bar{u}_1) H_2 \cdot \bar{p}'_{11} + (\sigma - \bar{u}_1) H_3 \cdot \bar{p}' - \bar{\rho} (H_3 + \bar{c}^2 H_2) \cdot \bar{u}'_1 - \frac{1}{2} \rho (\sigma - u_1) W_x H_1 \right], \end{aligned} \quad (5.51)$$

where  $\bar{c} = \sqrt{\frac{3\bar{p}_{11}}{\bar{\rho}}}$ . Specifically, for the 6-shock wave, (5.51) implies (5.48).  $\square$

**Remark 5.7.** For other possible cases, computing  $(\frac{\partial u_1}{\partial t})_{*K}$ ,  $(\frac{\partial p_{11}}{\partial t})_{*K}$  and  $(\frac{\partial \rho}{\partial t})_{*K}$  ( $K = L, R$ ) is presented in Appendix B.

### 5.1.2. Computing $(\frac{\partial u_2}{\partial t})_{*L}$ , $(\frac{\partial p_{12}}{\partial t})_{*L}$ and $(\frac{\partial p_{22}}{\partial t})_{*L}$

This section gives the values of  $(\frac{\partial u_2}{\partial t})_{*L}$ ,  $(\frac{\partial p_{12}}{\partial t})_{*L}$  and  $(\frac{\partial p_{22}}{\partial t})_{*L}$  by utilizing the remaining three generalized Riemann invariants associated with the 1-rarefaction wave

$$\psi_2 := u_2 + \frac{\sqrt{3}p_{12}}{\sqrt{\rho p_{11}}}, \quad \psi_3 := \frac{p_{12}}{\rho^3}, \quad S_2 := \frac{\det(\mathbf{p})}{\rho^4}.$$

From those, one has the following three total differentials

$$d\psi_2 = du_2 + \frac{\sqrt{3}}{\sqrt{\rho p_{11}}} dp_{12} - \frac{\sqrt{3}p_{12}}{2\rho\sqrt{\rho p_{11}}} d\rho - \frac{\sqrt{3}p_{12}}{2p_{11}\sqrt{\rho p_{11}}} dp_{11}, \quad (5.52)$$

$$d\psi_3 = \frac{1}{\rho^3} dp_{12} - \frac{3p_{12}}{\rho^4} d\rho, \quad (5.53)$$

$$dS_2 = \frac{p_{11}}{\rho^4} dp_{22} + \frac{p_{22}}{\rho^4} dp_{11} - \frac{2p_{12}}{\rho^4} dp_{12} - \frac{4 \det(\mathbf{p})}{\rho^5} d\rho. \quad (5.54)$$

Combing them with (2.5a) and (2.5c)-(2.5f) gives

$$\frac{\partial \psi_2}{\partial t} + (u_1 + c) \frac{\partial \psi_2}{\partial x} = \Pi_2, \quad \frac{\partial \psi_3}{\partial t} + (u_1 + c) \frac{\partial \psi_3}{\partial x} = \Pi_3, \quad \frac{\partial S_2}{\partial t} + u_1 \frac{\partial S_2}{\partial x} = 0,$$

where

$$\Pi_2 := \frac{2}{\rho} \frac{\partial p_{12}}{\partial x} - \frac{3p_{12}}{2\rho^2} \frac{\partial \rho}{\partial x} - \frac{3p_{12}}{2\rho p_{11}} \frac{\partial p_{11}}{\partial x}, \quad (5.55)$$

$$\Pi_3 := \frac{c}{\rho^3} \frac{\partial p_{12}}{\partial x} + \frac{p_{12}}{\rho^3} \frac{\partial u_1}{\partial x} - \frac{p_{11}}{\rho^3} \frac{\partial u_2}{\partial x} - \frac{3p_{12}c}{\rho^4} \frac{\partial \rho}{\partial x}. \quad (5.56)$$

Similar to the derivation of (5.28), for  $\psi_2$ , one can also obtain

$$\frac{\partial \psi_2}{\partial \alpha}(0, \beta) = \frac{\partial \psi_2}{\partial \alpha}(0, \beta_L) + \int_{\beta_L}^{\beta} \frac{1}{2c(0, \eta)} \frac{\partial t}{\partial \alpha}(0, \eta) \cdot \Pi_2(0, \eta) d\eta, \quad (5.57)$$

where

$$\frac{\partial \psi_2}{\partial \alpha}(0, \beta_L) = \frac{\partial t}{\partial \alpha}(0, \beta_L) \cdot (\Pi_{2,L} - 2c_L \psi'_{2,L}),$$

with  $\Pi_{2,L}$  and  $\psi'_{2,L}$  being given by (5.55) and (5.52), respectively. Similar to (5.33), one has

$$\frac{\partial \psi_2}{\partial t}(0, \beta) = - \left( \frac{u_1 - c}{2c} \right) (0, \beta) \cdot \Pi_2(0, \beta) + \left( \frac{u_1 + c}{2c} \right) (0, \beta) \cdot \left( \frac{\partial t}{\partial \alpha} \right)^{-1} (0, \beta) \cdot \frac{\partial \psi_2}{\partial \alpha}(0, \beta). \quad (5.58)$$

Note that if one wants to get the explicit expression of  $\frac{\partial \psi_2}{\partial t}(0, \beta)$  in a way similar to the derivation of (5.16) in Lemma 5.1, one has to first obtain the explicit expression of  $\Pi_2(0, \beta)$  so as to exactly obtain the integral in (5.57). Such task seems to be difficultly completed since it is hard to explicitly represent the spatial derivatives of the primitive variables with the characteristic coordinate  $(\alpha, \beta)$ . In practice, it may not be necessary to exactly

get the integral in (5.57) and a second-order numerical approximation to the integral is enough. Specifically, applying the trapezoidal rule in (5.57) obtains

$$\frac{\partial \psi_2}{\partial \alpha}(0, \beta) = \frac{\partial \psi_2}{\partial \alpha}(0, \beta_L) + \frac{\beta - \beta_L}{2} \left[ \frac{1}{4c(0, \beta)} \Pi_2(0, \beta) + \frac{1}{4c_L} \Pi_{2,L} \right].$$

Substituting it into (5.58) gets

$$\frac{\partial \psi_2}{\partial t}(0, \beta) = \left[ \frac{\partial \psi_2}{\partial \alpha}(0, \beta_L) + \frac{\Pi_{2,L}}{8c_L} (\beta - \beta_L) \right] \psi_{1,L} + \frac{1}{2c(0, \beta)} \left( \frac{\beta - \beta_L}{4} \psi_{1,L} - \beta \right) \cdot \Pi_2(0, \beta). \quad (5.59)$$

Moreover, by using (5.12), (5.55) is rewritten into

$$\Pi_2 = \frac{2}{\rho} \frac{\partial p_{12}}{\partial x} - \frac{2p_{12}}{\rho p_{11}} \frac{\partial p_{11}}{\partial x} + \frac{\rho^2 p_{12}}{2p_{11}} \frac{\partial S_1}{\partial x}.$$

Substituting (2.7) and (2.10) into above expression yields

$$\Pi_2 = -2 \frac{\mathcal{D}u_2}{\mathcal{D}t} + \frac{2p_{12}}{p_{11}} \left( \frac{\mathcal{D}u_1}{\mathcal{D}t} + \frac{1}{2} W_x \right) + \frac{\rho^2 p_{12}}{2p_{11}} \frac{\partial S_1}{\partial x}. \quad (5.60)$$

**Lemma 5.8** (Resolution of the 1-rarefaction wave). *Assume that the 1-rarefaction wave associated with  $u_1 - c$  moves to the left. Then  $\frac{\mathcal{D}u_2}{\mathcal{D}t}(0, \beta)$  and  $\frac{\mathcal{D}p_{12}}{\mathcal{D}t}(0, \beta)$  satisfy*

$$\tilde{a}_{3,L}(0, \beta) \cdot \frac{\mathcal{D}u_2}{\mathcal{D}t}(0, \beta) + \tilde{b}_{3,L}(0, \beta) \cdot \frac{\mathcal{D}p_{12}}{\mathcal{D}t}(0, \beta) = \tilde{d}_{3,L}(0, \beta), \quad (5.61)$$

where

$$\begin{aligned} \tilde{a}_{3,L}(0, \beta) &= 1 + \left( \frac{\sqrt{3}\rho u_1}{\sqrt{\rho p_{11}}} \right) (0, \beta) + \frac{1}{c(0, \beta)} \left( \frac{\beta - \beta_L}{4} \psi_{1,L} - \beta \right), \\ \tilde{b}_{3,L}(0, \beta) &= \left( \frac{u_1}{p_{11}} + \frac{\sqrt{3}}{\sqrt{\rho p_{11}}} \right) (0, \beta), \\ \tilde{d}_{3,L}(0, \beta) &= \left[ \frac{\partial \psi_2}{\partial \alpha}(0, \beta_L) + \frac{\Pi_{2,L}}{8c_L} (\beta - \beta_L) \right] \psi_{1,L} + \frac{1}{2c(0, \beta)} \left( \frac{\beta - \beta_L}{4} \psi_{1,L} - \beta \right) \left\{ \left( \frac{2p_{12}}{p_{11}} \right) (0, \beta) \right. \\ &\quad \cdot \left[ \left( \frac{\mathcal{D}u_1}{\mathcal{D}t} \right) (0, \beta) + \frac{1}{2} W_x(0) \right] + \frac{S'_{1,L}}{c_L} \left( \frac{c\rho^2 p_{12}}{2p_{11}} \right) (0, \beta) \left. \right\} + \left( \frac{\sqrt{3}p_{12}}{2\rho\sqrt{\rho p_{11}}} \frac{\partial \rho}{\partial t} \right) (0, \beta) \\ &\quad + \left( \frac{\sqrt{3}p_{12}}{2p_{11}\sqrt{\rho p_{11}}} \frac{\partial p_{11}}{\partial t} \right) (0, \beta) + \left( \frac{2u_1 p_{12}}{3p_{11}^2} \frac{\mathcal{D}p_{11}}{\mathcal{D}t} \right) (0, \beta). \end{aligned}$$

*Proof.* Due to (5.52), one has

$$\frac{\partial u_2}{\partial t} + \frac{\sqrt{3}}{\sqrt{\rho p_{11}}} \frac{\partial p_{12}}{\partial t} = \frac{\partial \psi_2}{\partial t} + \frac{\sqrt{3}p_{12}}{2\rho\sqrt{\rho p_{11}}} \frac{\partial \rho}{\partial t} + \frac{\sqrt{3}p_{12}}{2p_{11}\sqrt{\rho p_{11}}} \frac{\partial p_{11}}{\partial t}.$$

Substituting (2.11) into the above expression gives

$$\left( 1 + \frac{\sqrt{3}\rho u_1}{\sqrt{\rho p_{11}}} \right) \frac{\mathcal{D}u_2}{\mathcal{D}t} + \left( \frac{u_1}{p_{11}} + \frac{\sqrt{3}}{\sqrt{\rho p_{11}}} \right) \frac{\mathcal{D}p_{12}}{\mathcal{D}t} - \frac{2u_1 p_{12}}{3p_{11}^2} \frac{\mathcal{D}p_{11}}{\mathcal{D}t} = \frac{\partial \psi_2}{\partial t} + \frac{\sqrt{3}p_{12}}{2\rho\sqrt{\rho p_{11}}} \frac{\partial \rho}{\partial t} + \frac{\sqrt{3}p_{12}}{2p_{11}\sqrt{\rho p_{11}}} \frac{\partial p_{11}}{\partial t}. \quad (5.62)$$

Taking the limiting value at  $(0, \beta)$  in (5.62), and combining it with (5.59) and (5.60), one obtains (5.61). Note that in the expression of  $\tilde{d}_{3,L}(0, \beta)$ , (5.23) has been used.  $\square$

Taking  $\beta = \beta_{*L}$  in (5.61), one obtains the first equation that  $\left(\frac{\mathcal{D}u_2}{\mathcal{D}t}\right)_{*L}$  and  $\left(\frac{\mathcal{D}p_{12}}{\mathcal{D}t}\right)_{*L}$  satisfy

$$a_{3,L} \left(\frac{\mathcal{D}u_2}{\mathcal{D}t}\right)_{*L} + b_{3,L} \left(\frac{\mathcal{D}p_{12}}{\mathcal{D}t}\right)_{*L} = d_{3,L}, \quad (5.63)$$

with  $a_{3,L} = \tilde{a}_{3,L}(0, \beta_{*L})$ ,  $b_{3,L} = \tilde{b}_{3,L}(0, \beta_{*L})$  and  $d_{3,L} = \tilde{d}_{3,L}(0, \beta_{*L})$ .

For  $\psi_3$ , similar to  $\psi_2$ , one can get the following results

$$\frac{\partial\psi_3}{\partial\alpha}(0, \beta) = \frac{\partial\psi_3}{\partial\alpha}(0, \beta_L) + \int_{\beta_L}^{\beta} \frac{1}{2c(0, \eta)} \frac{\partial t}{\partial\alpha}(0, \eta) \cdot \Pi_3(0, \eta) d\eta, \quad (5.64)$$

$$\frac{\partial\psi_3}{\partial t}(0, \beta) = - \left(\frac{u_1 - c}{2c}\right)(0, \beta) \cdot \Pi_3(0, \beta) + \left(\frac{u_1 + c}{2c}\right)(0, \beta) \cdot \left(\frac{\partial t}{\partial\alpha}\right)^{-1}(0, \beta) \cdot \frac{\partial\psi_3}{\partial\alpha}(0, \beta), \quad (5.65)$$

where

$$\frac{\partial\psi_3}{\partial\alpha}(0, \beta_L) = \frac{\partial t}{\partial\alpha}(0, \beta_L) \cdot (\Pi_{3,L} - 2c_L\psi'_{3,L}),$$

with  $\Pi_{3,L}$  and  $\psi'_{3,L}$  being given by (5.56) and (5.53), respectively. Applying the trapezoidal rule in (5.64) obtains

$$\frac{\partial\psi_3}{\partial\alpha}(0, \beta) = \frac{\partial\psi_3}{\partial\alpha}(0, \beta_L) + \frac{\beta - \beta_L}{2} \left[ \frac{1}{4c(0, \beta)} \Pi_3(0, \beta) + \frac{1}{4c_L} \Pi_{3,L} \right].$$

Substituting it into (5.65) gets

$$\frac{\partial\psi_3}{\partial t}(0, \beta) = \left[ \frac{\partial\psi_3}{\partial\alpha}(0, \beta_L) + \frac{\Pi_{3,L}(\beta - \beta_L)}{8c_L} \right] \psi_{1,L} + \frac{1}{2c(0, \beta)} \left( \frac{\beta - \beta_L}{4} \psi_{1,L} - \beta \right) \cdot \Pi_3(0, \beta). \quad (5.66)$$

Besides, by using (5.12), (2.10), (2.6), (2.9) and (2.7), one can rewrite (5.56) into

$$\Pi_3 = \frac{1}{\rho^3} \left[ -\rho c \frac{\mathcal{D}u_2}{\mathcal{D}t} - \frac{p_{12}}{p_{11}} \frac{\mathcal{D}p_{11}}{\mathcal{D}t} + \frac{\mathcal{D}p_{12}}{\mathcal{D}t} + \frac{3p_{12}}{c} \left( \frac{\mathcal{D}u_1}{\mathcal{D}t} + \frac{1}{2} W_x \right) \right] + \frac{3p_{12}}{\rho c} \frac{\partial S_1}{\partial x}. \quad (5.67)$$

**Lemma 5.9** (Resolution of the 1-rarefaction wave). *Assume that the 1-rarefaction wave associated with  $u_1 - c$  moves to the left. Then  $\frac{\mathcal{D}u_2}{\mathcal{D}t}(0, \beta)$  and  $\frac{\mathcal{D}p_{12}}{\mathcal{D}t}(0, \beta)$  satisfy*

$$\tilde{a}_{4,L}(0, \beta) \cdot \frac{\mathcal{D}u_2}{\mathcal{D}t}(0, \beta) + \tilde{b}_{4,L}(0, \beta) \cdot \frac{\mathcal{D}p_{12}}{\mathcal{D}t}(0, \beta) = \tilde{d}_{4,L}(0, \beta), \quad (5.68)$$

where

$$\begin{aligned} \tilde{a}_{4,L}(0, \beta) &= \frac{1}{\rho^2(0, \beta)} \left[ u_1(0, \beta) + \frac{1}{2} \left( \frac{\beta - \beta_L}{4} \psi_{1,L} - \beta \right) \right], \\ \tilde{b}_{4,L}(0, \beta) &= \frac{1}{\rho^3(0, \beta)} \left[ 1 - \frac{1}{2c(0, \beta)} \left( \frac{\beta - \beta_L}{4} \psi_{1,L} - \beta \right) \right], \\ \tilde{d}_{4,L}(0, \beta) &= \left[ \frac{\partial\psi_3}{\partial\alpha}(0, \beta_L) + \frac{\Pi_{3,L}(\beta - \beta_L)}{8c_L} \right] \psi_{1,L} + \left( \frac{3p_{12}}{\rho^4} \frac{\partial\rho}{\partial t} \right)(0, \beta) + \frac{1}{2c(0, \beta)} \left( \frac{\beta - \beta_L}{4} \psi_{1,L} - \beta \right) \\ &\quad \cdot \left\{ \frac{1}{\rho^3(0, \beta)} \left[ -\frac{p_{12}}{p_{11}} \frac{\mathcal{D}p_{11}}{\mathcal{D}t} + \frac{3p_{12}}{c} \left( \frac{\mathcal{D}u_1}{\mathcal{D}t} + \frac{1}{2} W_x(0) \right) \right] (0, \beta) + \frac{S'_{1,L}}{c_L} \left( \frac{3p_{12}}{\rho} \right) (0, \beta) \right\}. \end{aligned}$$

*Proof.* By (5.53) and (2.11), one has

$$\frac{\partial\psi_3}{\partial t} = \frac{1}{\rho^3} \left( \frac{\mathcal{D}p_{12}}{\mathcal{D}t} + \rho u_1 \frac{\mathcal{D}u_2}{\mathcal{D}t} \right) - \frac{3p_{12}}{\rho^4} \frac{\partial\rho}{\partial t}.$$

Combining it with (5.67) and (5.66) gives (5.68). Similarly, in the expression of  $\tilde{d}_{4,L}(0, \beta)$ , (5.23) has been used.  $\square$

Taking  $\beta = \beta_{*L}$  in (5.68), one obtains the second equation that  $\left(\frac{\mathcal{D}u_2}{\mathcal{D}t}\right)_{*L}$  and  $\left(\frac{\mathcal{D}p_{12}}{\mathcal{D}t}\right)_{*L}$  satisfy

$$a_{4,L} \left(\frac{\mathcal{D}u_2}{\mathcal{D}t}\right)_{*L} + b_{4,L} \left(\frac{\mathcal{D}p_{12}}{\mathcal{D}t}\right)_{*L} = d_{4,L}, \quad (5.69)$$

with  $a_{4,L} = \tilde{a}_{4,L}(0, \beta_{*L})$ ,  $b_{4,L} = \tilde{b}_{4,L}(0, \beta_{*L})$  and  $d_{4,L} = \tilde{d}_{4,L}(0, \beta_{*L})$ .

For  $S_2$ , with the similar derivation of (5.24), one can obtain

$$\frac{\partial S_2}{\partial t}(0, \beta) = -\frac{S'_{2,L}}{c_L}(cu_1)(0, \beta), \quad (5.70)$$

with  $S'_{2,L}$  being given by (5.54). Moreover, by (5.54), one has

$$\left(\frac{p_{11}}{\rho^4} \frac{\partial p_{22}}{\partial t}\right)(0, \beta) = \frac{\partial S_2}{\partial t}(0, \beta) - \left(\frac{p_{22}}{\rho^4} \frac{\partial p_{11}}{\partial t}\right)(0, \beta) + \left(\frac{2p_{12}}{\rho^4} \frac{\partial p_{12}}{\partial t}\right)(0, \beta) + \left(\frac{4 \det(\mathbf{p})}{\rho^5} \frac{\partial \rho}{\partial t}\right)(0, \beta). \quad (5.71)$$

**Theorem 5.10** (Computing  $\left(\frac{\partial u_2}{\partial t}\right)_{*L}$ ,  $\left(\frac{\partial p_{12}}{\partial t}\right)_{*L}$  and  $\left(\frac{\partial p_{22}}{\partial t}\right)_{*L}$ ). *Assume that the 1-rarefaction wave associated with  $u_1 - c$  move to the left. Then one has*

$$\left(\frac{\mathcal{D}u_2}{\mathcal{D}t}\right)_{*L} = \frac{d_{3,L}b_{4,L} - d_{4,L}b_{3,L}}{a_{3,L}b_{4,L} - a_{4,L}b_{3,L}}, \quad \left(\frac{\mathcal{D}p_{12}}{\mathcal{D}t}\right)_{*L} = \frac{d_{3,L}a_{4,L} - d_{4,L}a_{3,L}}{b_{3,L}a_{4,L} - b_{4,L}a_{3,L}}, \quad (5.72)$$

and

$$\begin{aligned} \left(\frac{\partial u_2}{\partial t}\right)_{*L} &= \left(\frac{\mathcal{D}u_2}{\mathcal{D}t}\right)_{*L} + \frac{u_{1,*}}{p_{11,*}} \left[ \left(\frac{\mathcal{D}p_{12}}{\mathcal{D}t}\right)_{*L} - \frac{2p_{12,*L}}{3p_{11,*}} \left(\frac{\mathcal{D}p_{11}}{\mathcal{D}t}\right)_* \right], \\ \left(\frac{\partial p_{12}}{\partial t}\right)_{*L} &= \left(\frac{\mathcal{D}p_{12}}{\mathcal{D}t}\right)_{*L} + \rho_{*L} u_{1,*} \left(\frac{\mathcal{D}u_2}{\mathcal{D}t}\right)_{*L}. \end{aligned} \quad (5.73)$$

The limiting value  $\left(\frac{\partial p_{22}}{\partial t}\right)_{*L}$  can be obtained by

$$\left(\frac{p_{11}}{\rho^4} \frac{\partial p_{22}}{\partial t}\right)_{*L} = -\frac{S'_{2,L}}{c_L} c_{*L} u_{1,*} - \left(\frac{p_{22}}{\rho^4} \frac{\partial p_{11}}{\partial t}\right)_{*L} + \left(\frac{2p_{12}}{\rho^4} \frac{\partial p_{12}}{\partial t}\right)_{*L} + \left(\frac{4 \det(\mathbf{p})}{\rho^5} \frac{\partial \rho}{\partial t}\right)_{*L}. \quad (5.74)$$

*Proof.* Combining (5.63) and (5.69) yields (5.72), and then can get (5.73) by (2.11). Substituting (5.70) into (5.71) and taking  $\beta = \beta_{*L}$  obtain (5.74).  $\square$

**Remark 5.11.** *For the 1-shock wave, computing  $\left(\frac{\partial u_2}{\partial t}\right)_{*L}$ ,  $\left(\frac{\partial p_{12}}{\partial t}\right)_{*L}$  and  $\left(\frac{\partial p_{22}}{\partial t}\right)_{*L}$  is presented in Appendix C.*

### 5.1.3. Computing $\left(\frac{\partial u_2}{\partial t}\right)_{*R}$ , $\left(\frac{\partial p_{12}}{\partial t}\right)_{*R}$ and $\left(\frac{\partial p_{22}}{\partial t}\right)_{*R}$

At the 6-shock wave side, the Rankine-Hugoniot jump conditions will be used to derive the limiting values  $\left(\frac{\partial u_2}{\partial t}\right)_{*R}$ ,  $\left(\frac{\partial p_{12}}{\partial t}\right)_{*R}$  and  $\left(\frac{\partial p_{22}}{\partial t}\right)_{*R}$ .

Across the shock wave with speed  $\sigma$ , the Rankine-Hugoniot jump condition for  $m_2$  implies

$$\rho u_2(u_1 - \sigma) + p_{12} = \bar{\rho} \bar{u}_2(\bar{u}_1 - \sigma) + \bar{p}_{12}.$$

If denoting  $\Gamma_{m_2} := \rho u_2(u_1 - \sigma) + p_{12}$ , one has  $\Gamma_{m_2} = \Gamma_{\bar{m}_2}$  and

$$d\Gamma_{m_2} = u_2(u_1 - \sigma)d\rho + \rho u_2 du_1 + \rho(u_1 - \sigma)du_2 + dp_{12} - \rho u_2 d\sigma.$$

It follows that

$$\frac{\mathcal{D}_\sigma \Gamma_{m_2}}{\mathcal{D}t} = u_2(u_1 - \sigma) \frac{\mathcal{D}_\sigma \rho}{\mathcal{D}t} + \rho u_2 \frac{\mathcal{D}_\sigma u_1}{\mathcal{D}t} + \rho(u_1 - \sigma) \frac{\mathcal{D}_\sigma u_2}{\mathcal{D}t} + \frac{\mathcal{D}_\sigma p_{12}}{\mathcal{D}t} - \rho u_2 \frac{\mathcal{D}_\sigma \sigma}{\mathcal{D}t},$$

and then one can utilize the relation along the shock wave, i.e.,  $\frac{\mathcal{D}_\sigma \Gamma_{m_2}}{\mathcal{D}t} = \frac{\mathcal{D}_\sigma \Gamma_{\bar{m}_2}}{\mathcal{D}t}$ , to get the first equation that the limiting values  $\left(\frac{\mathcal{D}u_2}{\mathcal{D}t}\right)_{*K}$  and  $\left(\frac{\mathcal{D}p_{12}}{\mathcal{D}t}\right)_{*K}$  ( $K = L, R$ ) satisfy.

Specifically, for the 6-shock wave, one has

$$\frac{\mathcal{D}_{\sigma_R} \Gamma_{m_{2,*R}}}{\mathcal{D}t} = \frac{\mathcal{D}_{\sigma_R} \Gamma_{m_{2,R}}}{\mathcal{D}t}, \quad (5.75)$$

where

$$\sigma_R = u_{1,R} + \left(\frac{2p_{11,*} + p_{11,R}}{\rho_R}\right)^{\frac{1}{2}}, \quad (5.76)$$

$$\begin{aligned} \frac{\mathcal{D}_{\sigma_R} \Gamma_{m_{2,*R}}}{\mathcal{D}t} &= u_{2,*R}(u_{1,*} - \sigma_R) \left(\frac{\mathcal{D}_{\sigma_R} \rho}{\mathcal{D}t}\right)_{*R} + \rho_{*R} u_{2,*R} \left(\frac{\mathcal{D}_{\sigma_R} u_1}{\mathcal{D}t}\right)_{*R} \\ &\quad + \rho_{*R}(u_{1,*} - \sigma_R) \left(\frac{\mathcal{D}_{\sigma_R} u_2}{\mathcal{D}t}\right)_{*R} + \left(\frac{\mathcal{D}_{\sigma_R} p_{12}}{\mathcal{D}t}\right)_{*R} - \rho_{*R} u_{2,*R} \frac{\mathcal{D}_{\sigma_R} \sigma_R}{\mathcal{D}t}, \end{aligned} \quad (5.77)$$

$$\begin{aligned} \frac{\mathcal{D}_{\sigma_R} \Gamma_{m_{2,R}}}{\mathcal{D}t} &= u_{2,R}(u_{1,R} - \sigma_R) \frac{\mathcal{D}_{\sigma_R} \rho_R}{\mathcal{D}t} + \rho_R u_{2,R} \frac{\mathcal{D}_{\sigma_R} u_{1,R}}{\mathcal{D}t} \\ &\quad + \rho_R (u_{1,R} - \sigma_R) \frac{\mathcal{D}_{\sigma_R} u_{2,R}}{\mathcal{D}t} + \frac{\mathcal{D}_{\sigma_R} p_{12,R}}{\mathcal{D}t} - \rho_R u_{2,R} \frac{\mathcal{D}_{\sigma_R} \sigma_R}{\mathcal{D}t}. \end{aligned} \quad (5.78)$$

By (2.6), one has

$$\left(\frac{\mathcal{D}_{\sigma_R} u_1}{\mathcal{D}t}\right)_{*R} = \left(\frac{\partial u_1}{\partial t}\right)_{*R} - \frac{\sigma_R}{3p_{11,*}} \left(\frac{\mathcal{D}p_{11}}{\mathcal{D}t}\right)_*. \quad (5.79)$$

By (2.9), one gets

$$\left(\frac{\mathcal{D}_{\sigma_R} u_2}{\mathcal{D}t}\right)_{*R} = \left(\frac{\mathcal{D}u_2}{\mathcal{D}t}\right)_{*R} - \frac{\sigma_R - u_{1,*}}{p_{11,*}} \left[ \left(\frac{\mathcal{D}p_{12}}{\mathcal{D}t}\right)_{*R} - \frac{2p_{12,*R}}{3p_{11,*}} \left(\frac{\mathcal{D}p_{11}}{\mathcal{D}t}\right)_* \right]. \quad (5.80)$$

By (2.10), one obtains

$$\left(\frac{\mathcal{D}_{\sigma_R} p_{12}}{\mathcal{D}t}\right)_{*R} = \left(\frac{\mathcal{D}p_{12}}{\mathcal{D}t}\right)_{*R} - \rho_{*R}(\sigma_R - u_{1,*}) \left(\frac{\mathcal{D}u_2}{\mathcal{D}t}\right)_{*R}. \quad (5.81)$$

By (2.5) and (5.76), one has

$$\frac{\mathcal{D}_{\sigma_R} \rho_R}{\mathcal{D}t} = (\sigma_R - u_{1,R}) \rho'_R - \rho_R u'_{1,R}, \quad (5.82a)$$

$$\frac{\mathcal{D}_{\sigma_R} u_{1,R}}{\mathcal{D}t} = (\sigma_R - u_{1,R}) u'_{1,R} - \frac{1}{\rho_R} p'_{11,R} - \frac{1}{2} W_x(0), \quad (5.82b)$$

$$\frac{\mathcal{D}_{\sigma_R} u_{2,R}}{\mathcal{D}t} = (\sigma_R - u_{1,R}) u'_{2,R} - \frac{1}{\rho_R} p'_{12,R}, \quad (5.82c)$$

$$\frac{\mathcal{D}_{\sigma_R} p_{11,R}}{\mathcal{D}t} = (\sigma_R - u_{1,R}) p'_{11,R} - 3p_{11,R} u'_{1,R}, \quad (5.82d)$$

$$\frac{\mathcal{D}_{\sigma_R} p_{12,R}}{\mathcal{D}t} = (\sigma_R - u_{1,R}) p'_{12,R} - 2p_{12,R} u'_{1,R} - p_{11,R} u'_{2,R}, \quad (5.82e)$$

$$\frac{\mathcal{D}_{\sigma_R} \sigma_R}{\mathcal{D}t} = \frac{\mathcal{D}_{\sigma_R} u_{1,R}}{\mathcal{D}t} - \frac{\sqrt{2p_{11,*} + p_{11,R}}}{2\rho_R \sqrt{\rho_R}} \frac{\mathcal{D}_{\sigma_R} \rho_R}{\mathcal{D}t} + \frac{1}{2\sqrt{\rho_R(2p_{11,*} + p_{11,R})}} \frac{\mathcal{D}_{\sigma_R} p_{11,R}}{\mathcal{D}t} + \frac{1}{\sqrt{\rho_R(2p_{11,*} + p_{11,R})}} \frac{\mathcal{D}_{\sigma_R} p_{11,*}}{\mathcal{D}t}. \quad (5.82f)$$

By (2.7), one obtains

$$\frac{\mathcal{D}_{\sigma_R} p_{11,*}}{\mathcal{D}t} = \left(\frac{\mathcal{D}p_{11}}{\mathcal{D}t}\right)_* - \rho_{*R}(\sigma_R - u_{1,*}) \left[ \left(\frac{\mathcal{D}u_1}{\mathcal{D}t}\right)_* + \frac{1}{2} W_x(0) \right]. \quad (5.83)$$

Substituting (5.82a), (5.82b), (5.82d) and (5.83) into (5.82f) can obtain the value of  $\frac{\mathcal{D}_{\sigma_R} \sigma_R}{\mathcal{D}t}$ . Similarly, substituting (5.82a), (5.82b), (5.82c), (5.82e) and (5.82f) into (5.78) may get the value of  $\frac{\mathcal{D}_{\sigma_R} \Gamma_{m_{2,R}}}{\mathcal{D}t}$ . As for the

computation of  $\left(\frac{\mathcal{D}_{\sigma_R}\rho}{\mathcal{D}t}\right)_{*R}$ , one uses the relation across the shock wave, i.e.,  $\rho = H(p_{11}; \bar{p}_{11}, \bar{\rho})$ , to obtain

$$\frac{\mathcal{D}\sigma\rho}{\mathcal{D}t} = H_1 \cdot \frac{\mathcal{D}\sigma p_{11}}{\mathcal{D}t} + H_2 \cdot \frac{\mathcal{D}\sigma \bar{p}_{11}}{\mathcal{D}t} + H_3 \cdot \frac{\mathcal{D}\sigma \bar{\rho}}{\mathcal{D}t}.$$

Applying it to the 6-shock wave gets

$$\left(\frac{\mathcal{D}_{\sigma_R}\rho}{\mathcal{D}t}\right)_{*R} = H_1^R \cdot \frac{\mathcal{D}_{\sigma_R} p_{11,*}}{\mathcal{D}t} + H_2^R \cdot \frac{\mathcal{D}_{\sigma_R} p_{11,R}}{\mathcal{D}t} + H_3^R \cdot \frac{\mathcal{D}_{\sigma_R} \rho_R}{\mathcal{D}t}. \quad (5.84)$$

**Lemma 5.12** (Resolution of the 6-shock wave). *Assume that the 6-shock wave associated with  $u_1 + c$  moves to the right. Then the limiting values  $\left(\frac{\mathcal{D}u_2}{\mathcal{D}t}\right)_{*R}$  and  $\left(\frac{\mathcal{D}p_{12}}{\mathcal{D}t}\right)_{*R}$  satisfy*

$$a_{3,R} \left(\frac{\mathcal{D}u_2}{\mathcal{D}t}\right)_{*R} + b_{3,R} \left(\frac{\mathcal{D}p_{12}}{\mathcal{D}t}\right)_{*R} = d_{3,R}, \quad (5.85)$$

where

$$\begin{aligned} a_{3,R} &= 2\rho_{*R}(u_{1,*} - \sigma_R), \quad b_{3,R} = 1 + \frac{\rho_{*R}(u_{1,*} - \sigma_R)^2}{p_{11,*}}, \\ d_{3,R} &= \frac{\mathcal{D}_{\sigma_R}\Gamma_{m_{2,R}}}{\mathcal{D}t} + \rho_{*R}u_{2,*R} \frac{\mathcal{D}_{\sigma_R}\sigma_R}{\mathcal{D}t} - u_{2,*R}(u_{1,*} - \sigma_R) \left(\frac{\mathcal{D}_{\sigma_R}\rho}{\mathcal{D}t}\right)_{*R} \\ &\quad - \rho_{*R}u_{2,*R} \left(\frac{\mathcal{D}_{\sigma_R}u_1}{\mathcal{D}t}\right)_{*R} + \frac{2\rho_{*R}p_{12,*R}(u_{1,*} - \sigma_R)^2}{3p_{11,*}^2} \left(\frac{\mathcal{D}p_{11}}{\mathcal{D}t}\right)_*. \end{aligned}$$

Here the values of  $\frac{\mathcal{D}_{\sigma_R}\Gamma_{m_{2,R}}}{\mathcal{D}t}$ ,  $\frac{\mathcal{D}_{\sigma_R}\sigma_R}{\mathcal{D}t}$ ,  $\left(\frac{\mathcal{D}_{\sigma_R}\rho}{\mathcal{D}t}\right)_{*R}$ ,  $\left(\frac{\mathcal{D}_{\sigma_R}u_1}{\mathcal{D}t}\right)_{*R}$  and  $\left(\frac{\mathcal{D}p_{11}}{\mathcal{D}t}\right)_*$  are given by (5.78), (5.82f), (5.84), (5.79) and (5.45), respectively.

*Proof.* One can first substitute (5.80) and (5.81) into (5.77), and then combine (5.77) with (5.75) to yield (5.85).  $\square$

Across the shock wave with speed  $\sigma$ , the Rankine-Hugoniot jump condition for  $E_{12}$  implies that  $\Gamma_{E_{12}} = \Gamma_{\bar{E}_{12}}$  with

$$\Gamma_{E_{12}} := \frac{1}{2}(\rho u_1 u_2 + p_{12})(u_1 - \sigma) + \frac{1}{2}(p_{11} u_2 + p_{12} u_1).$$

It follows that

$$\begin{aligned} \frac{\mathcal{D}_{\sigma}\Gamma_{E_{12}}}{\mathcal{D}t} &= \frac{1}{2}u_1 u_2 (u_1 - \sigma) \frac{\mathcal{D}\sigma\rho}{\mathcal{D}t} + \left(2E_{12} - \frac{1}{2}\rho u_2 \sigma\right) \frac{\mathcal{D}_{\sigma}u_1}{\mathcal{D}t} + \left(E_{11} - \frac{1}{2}\rho u_1 \sigma\right) \frac{\mathcal{D}_{\sigma}u_2}{\mathcal{D}t} \\ &\quad + \frac{1}{2}u_2 \frac{\mathcal{D}_{\sigma}p_{11}}{\mathcal{D}t} + \left(u_1 - \frac{1}{2}\sigma\right) \frac{\mathcal{D}_{\sigma}p_{12}}{\mathcal{D}t} - E_{12} \frac{\mathcal{D}_{\sigma}\sigma}{\mathcal{D}t}. \end{aligned}$$

Then one can use the relation along the shock wave, i.e.,  $\frac{\mathcal{D}_{\sigma}\Gamma_{E_{12}}}{\mathcal{D}t} = \frac{\mathcal{D}_{\sigma}\Gamma_{\bar{E}_{12}}}{\mathcal{D}t}$ , to build the second equation that the limiting values  $\left(\frac{\mathcal{D}u_2}{\mathcal{D}t}\right)_{*K}$  and  $\left(\frac{\mathcal{D}p_{12}}{\mathcal{D}t}\right)_{*K}$  ( $K = L, R$ ) satisfy.

Specifically, for the 6-shock wave, one has

$$\frac{\mathcal{D}_{\sigma_R}\Gamma_{E_{12,*R}}}{\mathcal{D}t} = \frac{\mathcal{D}_{\sigma_R}\Gamma_{E_{12,R}}}{\mathcal{D}t}, \quad (5.86)$$

where

$$\begin{aligned} \frac{\mathcal{D}_{\sigma_R}\Gamma_{E_{12,*R}}}{\mathcal{D}t} &= \frac{1}{2}u_{1,*}u_{2,*R}(u_{1,*} - \sigma_R) \left(\frac{\mathcal{D}_{\sigma_R}\rho}{\mathcal{D}t}\right)_{*R} + \left(2E_{12,*R} - \frac{1}{2}\rho_{*R}u_{2,*R}\sigma_R\right) \left(\frac{\mathcal{D}_{\sigma_R}u_1}{\mathcal{D}t}\right)_{*R} \\ &\quad + \left(E_{11,*R} - \frac{1}{2}\rho_{*R}u_{1,*}\sigma_R\right) \left(\frac{\mathcal{D}_{\sigma_R}u_2}{\mathcal{D}t}\right)_{*R} + \frac{1}{2}u_{2,*R} \frac{\mathcal{D}_{\sigma_R}p_{11,*}}{\mathcal{D}t} \\ &\quad + \left(u_{1,*} - \frac{1}{2}\sigma_R\right) \left(\frac{\mathcal{D}_{\sigma_R}p_{12}}{\mathcal{D}t}\right)_{*R} - E_{12,*R} \frac{\mathcal{D}_{\sigma_R}\sigma_R}{\mathcal{D}t}, \end{aligned} \quad (5.87)$$



$$\begin{aligned} \frac{\mathcal{D}_{\sigma_R} \Gamma_{E_{12,R}}}{\mathcal{D}t} &= \frac{1}{2} u_{1,R} u_{2,R} (u_{1,R} - \sigma_R) \frac{\mathcal{D}_{\sigma_R} \rho_R}{\mathcal{D}t} + \left( 2E_{12,R} - \frac{1}{2} \rho_R u_{2,R} \sigma_R \right) \frac{\mathcal{D}_{\sigma_R} u_{1,R}}{\mathcal{D}t} \\ &+ \left( E_{11,R} - \frac{1}{2} \rho_R u_{1,R} \sigma_R \right) \frac{\mathcal{D}_{\sigma_R} u_{2,R}}{\mathcal{D}t} + \frac{1}{2} u_{2,R} \frac{\mathcal{D}_{\sigma_R} p_{11,R}}{\mathcal{D}t} + \left( u_{1,R} - \frac{1}{2} \sigma_R \right) \frac{\mathcal{D}_{\sigma_R} p_{12,R}}{\mathcal{D}t} - E_{12,R} \frac{\mathcal{D}_{\sigma_R} \sigma_R}{\mathcal{D}t}. \end{aligned} \quad (5.88)$$

Substituting (5.82) into (5.88) can obtain the value of  $\frac{\mathcal{D}_{\sigma_R} \Gamma_{E_{12,R}}}{\mathcal{D}t}$ .

**Lemma 5.13** (Resolution of the 6-shock wave). *Assume that the 6-shock wave associated with  $u_1 + c$  moves to the right. Then the limiting values  $\left(\frac{\mathcal{D}u_2}{\mathcal{D}t}\right)_{*R}$  and  $\left(\frac{\mathcal{D}p_{12}}{\mathcal{D}t}\right)_{*R}$  satisfy*

$$a_{4,R} \left( \frac{\mathcal{D}u_2}{\mathcal{D}t} \right)_{*R} + b_{4,R} \left( \frac{\mathcal{D}p_{12}}{\mathcal{D}t} \right)_{*R} = d_{4,R}, \quad (5.89)$$

where

$$\begin{aligned} a_{4,R} &= E_{11,*R} + \rho_{*R} (u_{1,*} - \sigma_R)^2 - \frac{1}{2} \rho_{*R} \sigma_R^2, \quad b_{4,R} = \left( E_{11,*R} - \frac{1}{2} \rho_{*R} u_{1,*} \sigma_R \right) \frac{u_{1,*} - \sigma_R}{p_{11,*}} + u_{1,*} - \frac{1}{2} \sigma_R, \\ d_{4,R} &= \frac{\mathcal{D}_{\sigma_R} \Gamma_{E_{12,R}}}{\mathcal{D}t} + E_{12,*R} \frac{\mathcal{D}_{\sigma_R} \sigma_R}{\mathcal{D}t} - \frac{1}{2} u_{1,*} u_{2,*R} (u_{1,*} - \sigma_R) \left( \frac{\mathcal{D}_{\sigma_R} \rho}{\mathcal{D}t} \right)_{*R} - \frac{1}{2} u_{2,*R} \frac{\mathcal{D}_{\sigma_R} p_{11,*}}{\mathcal{D}t} \\ &- \left( 2E_{12,*R} - \frac{1}{2} \rho_{*R} u_{2,*R} \sigma_R \right) \left( \frac{\mathcal{D}_{\sigma_R} u_1}{\mathcal{D}t} \right)_{*R} + \left( E_{11,*R} - \frac{1}{2} \rho_{*R} u_{1,*} \sigma_R \right) \frac{2p_{12,*R} (u_{1,*} - \sigma_R)}{3p_{11,*}^2} \left( \frac{\mathcal{D}p_{11}}{\mathcal{D}t} \right)_*. \end{aligned}$$

Here the value of  $d_{4,R}$  can be obtained by (5.88), (5.82f), (5.84), (5.83), (5.79) and (5.45).

*Proof.* The proof is easily completed by combining (5.80), (5.81), (5.87) and (5.86).  $\square$

Across the shock wave with speed  $\sigma$ , the Rankine-Hugoniot jump condition for  $E_{22}$  implies that  $\Gamma_{E_{22}} = \Gamma_{\bar{E}_{22}}$  with

$$\Gamma_{E_{22}} := \frac{1}{2} (p_{22} + \rho u_2^2) (u_1 - \sigma) + p_{12} u_2.$$

It follows that

$$\begin{aligned} \frac{\mathcal{D}_{\sigma} \Gamma_{E_{22}}}{\mathcal{D}t} &= \frac{1}{2} u_2^2 (u_1 - \sigma) \frac{\mathcal{D}_{\sigma} \rho}{\mathcal{D}t} + E_{22} \frac{\mathcal{D}_{\sigma} u_1}{\mathcal{D}t} + (2E_{12} - \rho u_2 \sigma) \frac{\mathcal{D}_{\sigma} u_2}{\mathcal{D}t} \\ &+ u_2 \frac{\mathcal{D}_{\sigma} p_{12}}{\mathcal{D}t} + \frac{1}{2} (u_1 - \sigma) \frac{\mathcal{D}_{\sigma} p_{22}}{\mathcal{D}t} - E_{22} \frac{\mathcal{D}_{\sigma} \sigma}{\mathcal{D}t}. \end{aligned}$$

Then one can utilize the relation along the shock wave, i.e.,  $\frac{\mathcal{D}_{\sigma} \Gamma_{E_{22}}}{\mathcal{D}t} = \frac{\mathcal{D}_{\sigma} \Gamma_{\bar{E}_{22}}}{\mathcal{D}t}$ , to compute the limiting value  $\left(\frac{\partial p_{22}}{\partial t}\right)_{*K}$ ,  $K = L, R$ .

Specifically, for the 6-shock wave, one has

$$\frac{\mathcal{D}_{\sigma_R} \Gamma_{E_{22,*R}}}{\mathcal{D}t} = \frac{\mathcal{D}_{\sigma_R} \Gamma_{E_{22,R}}}{\mathcal{D}t}, \quad (5.90)$$

where

$$\begin{aligned} \frac{\mathcal{D}_{\sigma_R} \Gamma_{E_{22,*R}}}{\mathcal{D}t} &= \frac{1}{2} u_{2,*R}^2 (u_{1,*} - \sigma_R) \left( \frac{\mathcal{D}_{\sigma_R} \rho}{\mathcal{D}t} \right)_{*R} + E_{22,*R} \left( \frac{\mathcal{D}_{\sigma_R} u_1}{\mathcal{D}t} \right)_{*R} + (2E_{12,*R} - \rho_{*R} u_{2,*R} \sigma_R) \left( \frac{\mathcal{D}_{\sigma_R} u_2}{\mathcal{D}t} \right)_{*R} \\ &+ u_{2,*R} \left( \frac{\mathcal{D}_{\sigma_R} p_{12}}{\mathcal{D}t} \right)_{*R} + \frac{1}{2} (u_{1,*} - \sigma_R) \left( \frac{\mathcal{D}_{\sigma_R} p_{22}}{\mathcal{D}t} \right)_{*R} - E_{22,*R} \frac{\mathcal{D}_{\sigma_R} \sigma_R}{\mathcal{D}t}, \end{aligned} \quad (5.91)$$

$$\begin{aligned} \frac{\mathcal{D}_{\sigma_R} \Gamma_{E_{22,R}}}{\mathcal{D}t} &= \frac{1}{2} u_{2,R}^2 (u_{1,R} - \sigma_R) \frac{\mathcal{D}_{\sigma_R} \rho_R}{\mathcal{D}t} + E_{22,R} \frac{\mathcal{D}_{\sigma_R} u_{1,R}}{\mathcal{D}t} + (2E_{12,R} - \rho_R u_{2,R} \sigma_R) \frac{\mathcal{D}_{\sigma_R} u_{2,R}}{\mathcal{D}t} \\ &+ u_{2,R} \frac{\mathcal{D}_{\sigma_R} p_{12,R}}{\mathcal{D}t} + \frac{1}{2} (u_{1,R} - \sigma_R) \frac{\mathcal{D}_{\sigma_R} p_{22,R}}{\mathcal{D}t} - E_{22,R} \frac{\mathcal{D}_{\sigma_R} \sigma_R}{\mathcal{D}t}. \end{aligned} \quad (5.92)$$

By (2.5f), one has

$$\frac{\mathcal{D}_{\sigma_R} p_{22,R}}{\mathcal{D}t} = (\sigma_R - u_{1,R}) p'_{22,R} - p_{22,R} u'_{1,R} - 2p_{12,R} u'_{2,R}. \quad (5.93)$$

Substituting (5.82a), (5.82b), (5.82c), (5.82e) and (5.93) into (5.92) may obtain the value of  $\frac{\mathcal{D}_{\sigma_R} \Gamma_{E_{22,R}}}{\mathcal{D}t}$ .

**Theorem 5.14** (Computing  $(\frac{\partial u_2}{\partial t})_{*R}$ ,  $(\frac{\partial p_{12}}{\partial t})_{*R}$  and  $(\frac{\partial p_{22}}{\partial t})_{*R}$ ). *Assume that the 6-shock wave associated with  $u_1 + c$  moves to the right. Then the limiting values  $(\frac{\mathcal{D}u_2}{\mathcal{D}t})_{*R}$  and  $(\frac{\mathcal{D}p_{12}}{\mathcal{D}t})_{*R}$  are*

$$\left(\frac{\mathcal{D}u_2}{\mathcal{D}t}\right)_{*R} = \frac{d_{3,R}b_{4,R} - d_{4,R}b_{3,R}}{a_{3,R}b_{4,R} - a_{4,R}b_{3,R}}, \quad \left(\frac{\mathcal{D}p_{12}}{\mathcal{D}t}\right)_{*R} = \frac{d_{3,R}a_{4,R} - d_{4,R}a_{3,R}}{b_{3,R}a_{4,R} - b_{4,R}a_{3,R}}. \quad (5.94)$$

It follows that

$$\begin{aligned} \left(\frac{\partial u_2}{\partial t}\right)_{*R} &= \left(\frac{\mathcal{D}u_2}{\mathcal{D}t}\right)_{*R} + \frac{u_{1,*}}{p_{11,*}} \left[ \left(\frac{\mathcal{D}p_{12}}{\mathcal{D}t}\right)_{*R} - \frac{2p_{12,*R}}{3p_{11,*}} \left(\frac{\mathcal{D}p_{11}}{\mathcal{D}t}\right)_{*} \right], \\ \left(\frac{\partial p_{12}}{\partial t}\right)_{*R} &= \left(\frac{\mathcal{D}p_{12}}{\mathcal{D}t}\right)_{*R} + \rho_{*R} u_{1,*} \left(\frac{\mathcal{D}u_2}{\mathcal{D}t}\right)_{*R}. \end{aligned} \quad (5.95)$$

Moreover, the limiting value  $(\frac{\partial p_{22}}{\partial t})_{*R}$  is computed by

$$g_{p_{22}}^{*R} \left(\frac{\partial p_{22}}{\partial t}\right)_{*R} = f_{p_{22}}^{*R}, \quad (5.96)$$

where

$$\begin{aligned} g_{p_{22}}^{*R} &= \frac{1}{2}(u_{1,*} - \sigma_R)^2, \\ f_{p_{22}}^{*R} &= u_{1,*} \cdot \tilde{f}_{p_{22}}^{*R} - \frac{(p_{11,*} p_{22,*R} - 4p_{12,*R}^2)(u_{1,*} - \sigma_R)\sigma_R}{6p_{11,*}^2} \left(\frac{\mathcal{D}p_{11}}{\mathcal{D}t}\right)_{*} - \frac{p_{12,*R}\sigma_R(u_{1,*} - \sigma_R)}{p_{11,*}} \left(\frac{\mathcal{D}p_{12}}{\mathcal{D}t}\right)_{*R}, \end{aligned}$$

with

$$\begin{aligned} \tilde{f}_{p_{22}}^{*R} &= \frac{\mathcal{D}_{\sigma_R} \Gamma_{E_{22,R}}}{\mathcal{D}t} + E_{22,*R} \frac{\mathcal{D}_{\sigma_R} \sigma_R}{\mathcal{D}t} - \frac{1}{2} u_{2,*R} (u_{1,*} - \sigma_R) \left(\frac{\mathcal{D}_{\sigma_R} \rho}{\mathcal{D}t}\right)_{*R} \\ &\quad - E_{22,*R} \left(\frac{\mathcal{D}_{\sigma_R} u_1}{\mathcal{D}t}\right)_{*R} - (2E_{12,*R} - \rho_{*R} u_{2,*R} \sigma_R) \left(\frac{\mathcal{D}_{\sigma_R} u_2}{\mathcal{D}t}\right)_{*R} - u_{2,*R} \left(\frac{\mathcal{D}_{\sigma_R} p_{12}}{\mathcal{D}t}\right)_{*R}. \end{aligned}$$

*Proof.* One can deduce (5.94) from (5.85) and (5.89), and then by (2.11), get (5.95). To derive (5.96), one can first utilize (2.5f), (2.6) and (2.9) to obtain

$$u_{1,*} \left(\frac{\mathcal{D}_{\sigma_R} p_{22}}{\mathcal{D}t}\right)_{*R} = (u_{1,*} - \sigma_R) \left(\frac{\partial p_{22}}{\partial t}\right)_{*R} + \frac{(p_{11,*} p_{22,*R} - 4p_{12,*R}^2)\sigma_R}{3p_{11,*}^2} \left(\frac{\mathcal{D}p_{11}}{\mathcal{D}t}\right)_{*} + \frac{2p_{12,*R}\sigma_R}{p_{11,*}} \left(\frac{\mathcal{D}p_{12}}{\mathcal{D}t}\right)_{*R}. \quad (5.97)$$

Multiplying both sides of (5.90) by  $u_{1,*}$  yields

$$u_{1,*} \frac{\mathcal{D}_{\sigma_R} \Gamma_{E_{22,*R}}}{\mathcal{D}t} = u_{1,*} \frac{\mathcal{D}_{\sigma_R} \Gamma_{E_{22,R}}}{\mathcal{D}t}. \quad (5.98)$$

Then substituting (5.91) and (5.92) into (5.98) and applying (5.97) gets (5.96).  $\square$

**Remark 5.15.** For the 6-rarefaction wave, computing  $(\frac{\partial u_2}{\partial t})_{*R}$ ,  $(\frac{\partial p_{12}}{\partial t})_{*R}$  and  $(\frac{\partial p_{22}}{\partial t})_{*R}$  is in [Appendix D](#).

#### 5.1.4. Computing $(\frac{\partial u_2}{\partial t})_{**K}$ , $(\frac{\partial p_{12}}{\partial t})_{**K}$ and $(\frac{\partial p_{22}}{\partial t})_{**K}$ ( $K = L, R$ )

In this subsection, the generalized Riemann invariants associated with the 2- and 5-shear waves are used to derive the limiting values  $(\frac{\partial u_2}{\partial t})_{**K}$ ,  $(\frac{\partial p_{12}}{\partial t})_{**K}$  and  $(\frac{\partial p_{22}}{\partial t})_{**K}$  ( $K = L, R$ ).

If denoting  $\Theta_2 := u_2 + \frac{p_{12}}{\sqrt{\rho p_{11}}}$  and recalling that  $\frac{\mathcal{D}_2}{\mathcal{D}t} := \frac{\partial}{\partial t} + \lambda_2 \frac{\partial}{\partial x}$  with  $\lambda_2 = u_{1,*} - \frac{c_{*L}}{\sqrt{3}}$ , then

$$\frac{\mathcal{D}_2 \Theta_2}{\mathcal{D}t} = -\frac{p_{12}}{2\rho\sqrt{\rho p_{11}}} \frac{\mathcal{D}_2 \rho}{\mathcal{D}t} + \frac{\mathcal{D}_2 u_2}{\mathcal{D}t} - \frac{p_{12}}{2p_{11}\sqrt{\rho p_{11}}} \frac{\mathcal{D}_2 p_{11}}{\mathcal{D}t} + \frac{1}{\sqrt{\rho p_{11}}} \frac{\mathcal{D}_2 p_{12}}{\mathcal{D}t}.$$

Because  $\Theta_2$  is a generalized Riemann invariant associated with the 2-shear wave, one has

$$\frac{\mathcal{D}_2\Theta_{2,**L}}{\mathcal{D}t} = \frac{\mathcal{D}_2\Theta_{2,*L}}{\mathcal{D}t}, \quad (5.99)$$

where

$$\frac{\mathcal{D}_2\Theta_{2,**L}}{\mathcal{D}t} = -\frac{p_{12,**}}{2\rho_{*L}\sqrt{\rho_{*L}p_{11,*}}} \left(\frac{\mathcal{D}_2\rho}{\mathcal{D}t}\right)_{**L} + \left(\frac{\mathcal{D}_2u_2}{\mathcal{D}t}\right)_{**L} - \frac{p_{12,**}}{2p_{11,*}\sqrt{\rho_{*L}p_{11,*}}} \left(\frac{\mathcal{D}_2p_{11}}{\mathcal{D}t}\right)_{**L} + \frac{1}{\sqrt{\rho_{*L}p_{11,*}}} \left(\frac{\mathcal{D}_2p_{12}}{\mathcal{D}t}\right)_{**L}, \quad (5.100)$$

$$\frac{\mathcal{D}_2\Theta_{2,*L}}{\mathcal{D}t} = -\frac{p_{12,*L}}{2\rho_{*L}\sqrt{\rho_{*L}p_{11,*}}} \left(\frac{\mathcal{D}_2\rho}{\mathcal{D}t}\right)_{*L} + \left(\frac{\mathcal{D}_2u_2}{\mathcal{D}t}\right)_{*L} - \frac{p_{12,*L}}{2p_{11,*}\sqrt{\rho_{*L}p_{11,*}}} \left(\frac{\mathcal{D}_2p_{11}}{\mathcal{D}t}\right)_{*L} + \frac{1}{\sqrt{\rho_{*L}p_{11,*}}} \left(\frac{\mathcal{D}_2p_{12}}{\mathcal{D}t}\right)_{*L}. \quad (5.101)$$

Because both  $\rho$  and  $p_{11}$  are the generalized Riemann invariants associated with the 2-shear wave, one actually has  $\left(\frac{\mathcal{D}_2\rho}{\mathcal{D}t}\right)_{**L} = \left(\frac{\mathcal{D}_2\rho}{\mathcal{D}t}\right)_{*L}$  and  $\left(\frac{\mathcal{D}_2p_{11}}{\mathcal{D}t}\right)_{**L} = \left(\frac{\mathcal{D}_2p_{11}}{\mathcal{D}t}\right)_{*L}$ . By (2.7), one gets

$$\left(\frac{\mathcal{D}_2p_{11}}{\mathcal{D}t}\right)_{**L} = \left(\frac{\mathcal{D}_2p_{11}}{\mathcal{D}t}\right)_{*L} = \left(\frac{\mathcal{D}p_{11}}{\mathcal{D}t}\right)_* - \rho_{*L}(\lambda_2 - u_{1,*}) \left[ \left(\frac{\mathcal{D}u_1}{\mathcal{D}t}\right)_* + \frac{1}{2}W_x(0) \right].$$

As for the value of  $\left(\frac{\mathcal{D}_2\rho}{\mathcal{D}t}\right)_{*L}$ , recalling the equation (5.12), that is  $dp_{11} = c^2d\rho + \rho^3dS_1$ , one has

$$\left(\frac{\partial\rho}{\partial x}\right)_{*L} = \frac{1}{c_{*L}^2} \left(\frac{\partial p_{11}}{\partial x}\right)_{*L} - \frac{\rho_{*L}^3}{c_{*L}^2} \left(\frac{\partial S_1}{\partial x}\right)_{*L} = -\frac{\rho_{*L}}{c_{*L}^2} \left[ \left(\frac{\mathcal{D}u_1}{\mathcal{D}t}\right)_* + \frac{1}{2}W_x(0) \right] - \frac{\rho_{*L}^3 S'_{1,L}}{c_{*L}c_L},$$

where (2.7) and (5.23) have been used in the second equality, and  $S'_{1,L}$  is given in (5.17), then  $\left(\frac{\mathcal{D}_2\rho}{\mathcal{D}t}\right)_{*L} = \left(\frac{\partial\rho}{\partial t}\right)_{*L} + \lambda_2 \left(\frac{\partial\rho}{\partial x}\right)_{*L}$  can be obtained.

**Remark 5.16.** For the 1-shock wave, one can get the value of  $\left(\frac{\mathcal{D}_{\sigma_L}\rho}{\mathcal{D}t}\right)_{*L}$  in a similar way to compute  $\left(\frac{\mathcal{D}_{\sigma_R}\rho}{\mathcal{D}t}\right)_{*R}$  in Subsection 5.1.3, see (5.84). Thus

$$\left(\frac{\mathcal{D}_2\rho}{\mathcal{D}t}\right)_{*L} = \left(1 - \frac{\lambda_2}{\sigma_L}\right) \left(\frac{\partial\rho}{\partial t}\right)_{*L} + \frac{\lambda_2}{\sigma_L} \left(\frac{\mathcal{D}_{\sigma_L}\rho}{\mathcal{D}t}\right)_{*L}.$$

By (2.9), one has

$$\begin{aligned} \left(\frac{\mathcal{D}_2u_2}{\mathcal{D}t}\right)_{**L} &= \left(\frac{\mathcal{D}u_2}{\mathcal{D}t}\right)_{**} - \frac{\lambda_2 - u_{1,*}}{p_{11,*}} \left[ \left(\frac{\mathcal{D}p_{12}}{\mathcal{D}t}\right)_{**} - \frac{2p_{12,**}}{3p_{11,*}} \left(\frac{\mathcal{D}p_{11}}{\mathcal{D}t}\right)_* \right], \\ \left(\frac{\mathcal{D}_2u_2}{\mathcal{D}t}\right)_{*L} &= \left(\frac{\mathcal{D}u_2}{\mathcal{D}t}\right)_{*L} - \frac{\lambda_2 - u_{1,*}}{p_{11,*}} \left[ \left(\frac{\mathcal{D}p_{12}}{\mathcal{D}t}\right)_{*L} - \frac{2p_{12,*L}}{3p_{11,*}} \left(\frac{\mathcal{D}p_{11}}{\mathcal{D}t}\right)_* \right], \end{aligned} \quad (5.102)$$

where the notations  $\left(\frac{\mathcal{D}u_2}{\mathcal{D}t}\right)_{**} := \left(\frac{\mathcal{D}u_2}{\mathcal{D}t}\right)_{**L} = \left(\frac{\mathcal{D}u_2}{\mathcal{D}t}\right)_{**R}$  and  $\left(\frac{\mathcal{D}p_{12}}{\mathcal{D}t}\right)_{**} := \left(\frac{\mathcal{D}p_{12}}{\mathcal{D}t}\right)_{**L} = \left(\frac{\mathcal{D}p_{12}}{\mathcal{D}t}\right)_{**R}$  have been used because both  $u_2$  and  $p_{12}$  are generalized Riemann invariants associated with the contact discontinuity. By (2.10), one has

$$\begin{aligned} \left(\frac{\mathcal{D}_2p_{12}}{\mathcal{D}t}\right)_{**L} &= \left(\frac{\mathcal{D}p_{12}}{\mathcal{D}t}\right)_{**} - \rho_{*L}(\lambda_2 - u_{1,*}) \left(\frac{\mathcal{D}u_2}{\mathcal{D}t}\right)_{**}, \\ \left(\frac{\mathcal{D}_2p_{12}}{\mathcal{D}t}\right)_{*L} &= \left(\frac{\mathcal{D}p_{12}}{\mathcal{D}t}\right)_{*L} - \rho_{*L}(\lambda_2 - u_{1,*}) \left(\frac{\mathcal{D}u_2}{\mathcal{D}t}\right)_{*L}. \end{aligned} \quad (5.103)$$

Note that the limiting values  $\left(\frac{\mathcal{D}u_2}{\mathcal{D}t}\right)_{*L}$  and  $\left(\frac{\mathcal{D}p_{12}}{\mathcal{D}t}\right)_{*L}$  have been obtained in Subsection 5.1.2, see Theorem 5.10.

**Lemma 5.17.** Assume that the 2-shear wave associated with  $u_1 - \frac{c}{\sqrt{3}}$  moves to the left. Then the limiting

values  $\left(\frac{\mathcal{D}u_2}{\mathcal{D}t}\right)_{**}$  and  $\left(\frac{\mathcal{D}p_{12}}{\mathcal{D}t}\right)_{**}$  satisfy

$$a_{5,L} \left(\frac{\mathcal{D}u_2}{\mathcal{D}t}\right)_{**} + b_{5,L} \left(\frac{\mathcal{D}p_{12}}{\mathcal{D}t}\right)_{**} = d_{5,L}, \quad (5.104)$$

where

$$\begin{aligned} a_{5,L} &= 2, \quad b_{5,L} = \frac{2}{\sqrt{\rho_{*L} p_{11,*}}}, \\ d_{5,L} &= \frac{p_{12,**} - p_{12,*L}}{2\rho_{*L} \sqrt{\rho_{*L} p_{11,*}}} \left(\frac{\mathcal{D}_2 \rho}{\mathcal{D}t}\right)_{*L} + \left(\frac{\mathcal{D}_2 u_2}{\mathcal{D}t}\right)_{*L} + \frac{p_{12,**} - p_{12,*L}}{2p_{11,*} \sqrt{\rho_{*L} p_{11,*}}} \left(\frac{\mathcal{D}_2 p_{11}}{\mathcal{D}t}\right)_{*L} \\ &\quad + \frac{1}{\sqrt{\rho_{*L} p_{11,*}}} \left(\frac{\mathcal{D}_2 p_{12}}{\mathcal{D}t}\right)_{*L} - \frac{2p_{12,**}(\lambda_2 - u_{1,*})}{3p_{11,*}^2} \left(\frac{\mathcal{D}p_{11}}{\mathcal{D}t}\right)_*. \end{aligned}$$

*Proof.* Substituting (5.100) and (5.101) into (5.99) and utilizing (5.102) and (5.103) may obtain (5.104).  $\square$

If denoting  $\Theta_5 := u_2 - \frac{p_{12}}{\sqrt{\rho p_{11}}}$  and  $\frac{\mathcal{D}_5}{\mathcal{D}t} := \frac{\partial}{\partial t} + \lambda_5 \frac{\partial}{\partial x}$  with  $\lambda_5 = u_{1,*} + \frac{c_{*R}}{\sqrt{3}}$ , then

$$d\Theta_5 = \frac{p_{12}}{2\rho\sqrt{\rho p_{11}}} d\rho + du_2 + \frac{p_{12}}{2p_{11}\sqrt{\rho p_{11}}} dp_{11} - \frac{1}{\sqrt{\rho p_{11}}} dp_{12}.$$

Because  $\Theta_5$  is a generalized Riemann invariant associated with the 5-shear wave, one has

$$\frac{\mathcal{D}_5 \Theta_{5,**R}}{\mathcal{D}t} = \frac{\mathcal{D}_5 \Theta_{5,*R}}{\mathcal{D}t}.$$

With similar derivation to build (5.104), one can obtain the following result.

**Lemma 5.18.** *Assume that the 5-shear wave associated with  $u_1 + \frac{c}{\sqrt{3}}$  moves to the right. Then the limiting values  $\left(\frac{\mathcal{D}u_2}{\mathcal{D}t}\right)_{**}$  and  $\left(\frac{\mathcal{D}p_{12}}{\mathcal{D}t}\right)_{**}$  satisfy*

$$a_{5,R} \left(\frac{\mathcal{D}u_2}{\mathcal{D}t}\right)_{**} + b_{5,R} \left(\frac{\mathcal{D}p_{12}}{\mathcal{D}t}\right)_{**} = d_{5,R}, \quad (5.105)$$

where

$$\begin{aligned} a_{5,R} &= 2, \quad b_{5,R} = -\frac{2}{\sqrt{\rho_{*R} p_{11,*}}}, \\ d_{5,R} &= \frac{p_{12,*R} - p_{12,**}}{2\rho_{*R} \sqrt{\rho_{*R} p_{11,*}}} \left(\frac{\mathcal{D}_5 \rho}{\mathcal{D}t}\right)_{*R} + \left(\frac{\mathcal{D}_5 u_2}{\mathcal{D}t}\right)_{*R} + \frac{p_{12,*R} - p_{12,**}}{2p_{11,*} \sqrt{\rho_{*R} p_{11,*}}} \left(\frac{\mathcal{D}_5 p_{11}}{\mathcal{D}t}\right)_{*R} \\ &\quad - \frac{1}{\sqrt{\rho_{*R} p_{11,*}}} \left(\frac{\mathcal{D}_5 p_{12}}{\mathcal{D}t}\right)_{*R} - \frac{2p_{12,**}(\lambda_5 - u_{1,*})}{3p_{11,*}^2} \left(\frac{\mathcal{D}p_{11}}{\mathcal{D}t}\right)_*. \end{aligned}$$

with the computation of  $\left(\frac{\mathcal{D}_5 \rho}{\mathcal{D}t}\right)_{*R}$  being similar to  $\left(\frac{\mathcal{D}_2 \rho}{\mathcal{D}t}\right)_{*L}$  for the 1-shock wave case, see Remark 5.16, and

$$\begin{aligned} \left(\frac{\mathcal{D}_5 p_{11}}{\mathcal{D}t}\right)_{*R} &= \left(\frac{\mathcal{D}p_{11}}{\mathcal{D}t}\right)_* - \rho_{*R}(\lambda_5 - u_{1,*}) \left[ \left(\frac{\mathcal{D}u_1}{\mathcal{D}t}\right)_* + \frac{1}{2} W_x(0) \right], \\ \left(\frac{\mathcal{D}_5 u_2}{\mathcal{D}t}\right)_{*R} &= \left(\frac{\mathcal{D}u_2}{\mathcal{D}t}\right)_{*R} - \frac{\lambda_5 - u_{1,*}}{p_{11,*}} \left[ \left(\frac{\mathcal{D}p_{12}}{\mathcal{D}t}\right)_{*R} - \frac{2p_{12,*R}}{3p_{11,*}} \left(\frac{\mathcal{D}p_{11}}{\mathcal{D}t}\right)_* \right], \\ \left(\frac{\mathcal{D}_5 p_{12}}{\mathcal{D}t}\right)_{*R} &= \left(\frac{\mathcal{D}p_{12}}{\mathcal{D}t}\right)_{*R} - \rho_{*R}(\lambda_5 - u_{1,*}) \left(\frac{\mathcal{D}u_2}{\mathcal{D}t}\right)_{*R}. \end{aligned}$$

**Remark 5.19.** *For the 6-rarefaction wave case, similar to the 1-rarefaction wave case, one has*

$$\left(\frac{\partial \rho}{\partial x}\right)_{*R} = -\frac{\rho_{*R}}{c_{*R}^2} \left[ \left(\frac{\mathcal{D}u_1}{\mathcal{D}t}\right)_* + \frac{1}{2} W_x(0) \right] - \frac{\rho_{*R}^3 S'_{1,R}}{c_{*R} c_{*R}},$$

where  $S'_{1,R} = \frac{1}{\rho_R^2}(p'_{11,R} - c_R^2 \rho'_R)$ . Thus the value of  $\left(\frac{\mathcal{D}_5 \rho}{\mathcal{D}t}\right)_{*R} = \left(\frac{\partial \rho}{\partial t}\right)_{*R} + \lambda_5 \left(\frac{\partial \rho}{\partial x}\right)_{*R}$  can be obtained.

**Theorem 5.20** (Computing  $\left(\frac{\partial u_2}{\partial t}\right)_{**K}$  and  $\left(\frac{\partial p_{12}}{\partial t}\right)_{**K}$  with  $K = L, R$ ). Assume that the 2-shear wave associated with  $u_1 - \frac{c}{\sqrt{3}}$  moves to the left and the 5-shear wave associated with  $u_1 + \frac{c}{\sqrt{3}}$  moves to the right. Then one has

$$\begin{aligned} \left(\frac{\mathcal{D}u_2}{\mathcal{D}t}\right)_{**} &= \frac{d_{5,L}b_{5,R} - d_{5,R}b_{5,L}}{a_{5,L}b_{5,R} - a_{5,R}b_{5,L}}, \\ \left(\frac{\mathcal{D}p_{12}}{\mathcal{D}t}\right)_{**} &= \frac{d_{5,L}a_{5,R} - d_{5,R}a_{5,L}}{a_{5,R}b_{5,L} - a_{5,L}b_{5,R}}. \end{aligned} \quad (5.106)$$

It follows that

$$\begin{aligned} \left(\frac{\partial u_2}{\partial t}\right)_{**K} &= \left(\frac{\mathcal{D}u_2}{\mathcal{D}t}\right)_{**} + \frac{u_{1,*}}{p_{11,*}} \left[ \left(\frac{\mathcal{D}p_{12}}{\mathcal{D}t}\right)_{**} - \frac{2p_{12,**}}{3p_{11,*}} \left(\frac{\mathcal{D}p_{11}}{\mathcal{D}t}\right)_* \right], \\ \left(\frac{\partial p_{12}}{\partial t}\right)_{**K} &= \left(\frac{\mathcal{D}p_{12}}{\mathcal{D}t}\right)_{**} + \rho_{*K} u_{1,*} \left(\frac{\mathcal{D}u_2}{\mathcal{D}t}\right)_{**}, \end{aligned} \quad (5.107)$$

with  $K = L, R$ .

*Proof.* (5.106) is the direct result from (5.104) and (5.105). Applying (2.11) may obtain (5.107).  $\square$

Because  $\det(\mathbf{p})$  is a generalized Riemann invariant for the 2-shear wave, one has

$$\frac{\mathcal{D}_2 \det(\mathbf{p}_{**L})}{\mathcal{D}t} = \frac{\mathcal{D}_2 \det(\mathbf{p}_{*L})}{\mathcal{D}t}. \quad (5.108)$$

Due to  $d(\det(\mathbf{p})) = p_{22}dp_{11} - 2p_{12}dp_{12} + p_{11}dp_{22}$ , one has

$$\begin{aligned} \frac{\mathcal{D}_2 \det(\mathbf{p}_{**L})}{\mathcal{D}t} &= p_{22,**L} \left(\frac{\mathcal{D}_2 p_{11}}{\mathcal{D}t}\right)_{**L} - 2p_{12,**} \left(\frac{\mathcal{D}_2 p_{12}}{\mathcal{D}t}\right)_{**L} + p_{11,*} \left(\frac{\mathcal{D}_2 p_{22}}{\mathcal{D}t}\right)_{**L}, \\ \frac{\mathcal{D}_2 \det(\mathbf{p}_{*L})}{\mathcal{D}t} &= p_{22,*L} \left(\frac{\mathcal{D}_2 p_{11}}{\mathcal{D}t}\right)_{*L} - 2p_{12,*L} \left(\frac{\mathcal{D}_2 p_{12}}{\mathcal{D}t}\right)_{*L} + p_{11,*} \left(\frac{\mathcal{D}_2 p_{22}}{\mathcal{D}t}\right)_{*L}. \end{aligned} \quad (5.109)$$

Using (2.5f), (2.6) and (2.9) yields

$$\begin{aligned} u_{1,*} \left(\frac{\mathcal{D}_2 p_{22}}{\mathcal{D}t}\right)_{**L} &= (u_{1,*} - \lambda_2) \left(\frac{\partial p_{22}}{\partial t}\right)_{**L} + \frac{\lambda_2(p_{11,*}p_{22,**L} - 4p_{12,**}^2)}{3p_{11,*}^2} \left(\frac{\mathcal{D}p_{11}}{\mathcal{D}t}\right)_* + \frac{2\lambda_2 p_{12,**}}{p_{11,*}} \left(\frac{\mathcal{D}p_{12}}{\mathcal{D}t}\right)_{**}, \\ u_{1,*} \left(\frac{\mathcal{D}_2 p_{22}}{\mathcal{D}t}\right)_{*L} &= (u_{1,*} - \lambda_2) \left(\frac{\partial p_{22}}{\partial t}\right)_{*L} + \frac{\lambda_2(p_{11,*}p_{22,*L} - 4p_{12,*L}^2)}{3p_{11,*}^2} \left(\frac{\mathcal{D}p_{11}}{\mathcal{D}t}\right)_* + \frac{2\lambda_2 p_{12,*L}}{p_{11,*}} \left(\frac{\mathcal{D}p_{12}}{\mathcal{D}t}\right)_{*L}. \end{aligned} \quad (5.110)$$

Similarly, one has

$$\begin{aligned} u_{1,*} \left(\frac{\mathcal{D}_5 p_{22}}{\mathcal{D}t}\right)_{**R} &= (u_{1,*} - \lambda_5) \left(\frac{\partial p_{22}}{\partial t}\right)_{**R} + \frac{\lambda_5(p_{11,*}p_{22,**R} - 4p_{12,**}^2)}{3p_{11,*}^2} \left(\frac{\mathcal{D}p_{11}}{\mathcal{D}t}\right)_* + \frac{2\lambda_5 p_{12,**}}{p_{11,*}} \left(\frac{\mathcal{D}p_{12}}{\mathcal{D}t}\right)_{**}, \\ u_{1,*} \left(\frac{\mathcal{D}_5 p_{22}}{\mathcal{D}t}\right)_{*R} &= (u_{1,*} - \lambda_5) \left(\frac{\partial p_{22}}{\partial t}\right)_{*R} + \frac{\lambda_5(p_{11,*}p_{22,*R} - 4p_{12,*R}^2)}{3p_{11,*}^2} \left(\frac{\mathcal{D}p_{11}}{\mathcal{D}t}\right)_* + \frac{2\lambda_5 p_{12,*R}}{p_{11,*}} \left(\frac{\mathcal{D}p_{12}}{\mathcal{D}t}\right)_{*R}. \end{aligned}$$

**Theorem 5.21** (Computing  $\left(\frac{\partial p_{22}}{\partial t}\right)_{**K}$  ( $K = L, R$ )). Assume that the 2-shear wave associated with  $u_1 - \frac{c}{\sqrt{3}}$  moves to the left and the 5-shear wave associated with  $u_1 + \frac{c}{\sqrt{3}}$  moves to the right. Then  $\left(\frac{\partial p_{22}}{\partial t}\right)_{**K}$  satisfies

$$g_{p_{22}}^{**K} \left(\frac{\partial p_{22}}{\partial t}\right)_{**K} = f_{p_{22}}^{**K}, \quad K = L, R, \quad (5.111)$$

where

$$\begin{aligned} g_{p_{22}}^{**L} &= p_{11,*}(u_{1,*} - \lambda_2), & g_{p_{22}}^{**R} &= p_{11,*}(u_{1,*} - \lambda_5), \\ \hat{f}_{p_{22}}^{**K} &= u_{1,*} \cdot \tilde{f}_{p_{22}}^{**K} + p_{11,*} \cdot \hat{f}_{p_{22}}^{**K}, & K &= L, R, \end{aligned}$$

and

$$\begin{aligned} \tilde{f}_{p_{22}}^{**L} &= (p_{22,*L} - p_{22,**L}) \left( \frac{\mathcal{D}_2 p_{11}}{\mathcal{D}t} \right)_{*L} - 2p_{12,*L} \left( \frac{\mathcal{D}_2 p_{12}}{\mathcal{D}t} \right)_{*L} + 2p_{12,**} \left( \frac{\mathcal{D}_2 p_{12}}{\mathcal{D}t} \right)_{**L}, \\ \tilde{f}_{p_{22}}^{**R} &= (p_{22,*R} - p_{22,**R}) \left( \frac{\mathcal{D}_5 p_{11}}{\mathcal{D}t} \right)_{*R} - 2p_{12,*R} \left( \frac{\mathcal{D}_5 p_{12}}{\mathcal{D}t} \right)_{*R} + 2p_{12,**} \left( \frac{\mathcal{D}_5 p_{12}}{\mathcal{D}t} \right)_{**R}, \\ \hat{f}_{p_{22}}^{**L} &= (u_{1,*} - \lambda_2) \left( \frac{\partial p_{22}}{\partial t} \right)_{*L} + \frac{\lambda_2}{3p_{11,*}^2} (p_{11,*} p_{22,*L} - 4p_{12,*L}^2 - p_{11,*} p_{22,**L} + 4p_{12,**}^2) \left( \frac{\mathcal{D} p_{11}}{\mathcal{D}t} \right)_{*} \\ &\quad + \frac{2\lambda_2}{p_{11,*}} \left[ p_{12,*L} \left( \frac{\mathcal{D} p_{12}}{\mathcal{D}t} \right)_{*L} - p_{12,**} \left( \frac{\mathcal{D} p_{12}}{\mathcal{D}t} \right)_{**} \right], \\ \hat{f}_{p_{22}}^{**R} &= (u_{1,*} - \lambda_5) \left( \frac{\partial p_{22}}{\partial t} \right)_{*R} + \frac{\lambda_5}{3p_{11,*}^2} (p_{11,*} p_{22,*R} - 4p_{12,*R}^2 - p_{11,*} p_{22,**R} + 4p_{12,**}^2) \left( \frac{\mathcal{D} p_{11}}{\mathcal{D}t} \right)_{*} \\ &\quad + \frac{2\lambda_5}{p_{11,*}} \left[ p_{12,*R} \left( \frac{\mathcal{D} p_{12}}{\mathcal{D}t} \right)_{*R} - p_{12,**} \left( \frac{\mathcal{D} p_{12}}{\mathcal{D}t} \right)_{**} \right], \end{aligned}$$

with

$$\left( \frac{\mathcal{D}_5 p_{12}}{\mathcal{D}t} \right)_{**R} = \left( \frac{\mathcal{D} p_{12}}{\mathcal{D}t} \right)_{**} - \rho_{*R} (\lambda_5 - u_{1,*}) \left( \frac{\mathcal{D} u_2}{\mathcal{D}t} \right)_{**}.$$

*Proof.* Multiplying both sides of (5.108) by  $u_{1,*}$  gets

$$u_{1,*} \frac{\mathcal{D}_2 \det(\mathbf{p}_{**L})}{\mathcal{D}t} = u_{1,*} \frac{\mathcal{D}_2 \det(\mathbf{p}_{*L})}{\mathcal{D}t}. \quad (5.112)$$

Then substituting (5.109) into (5.112), and utilizing (5.110) yields (5.111) for  $K = L$ . Because  $\det(\mathbf{p})$  is also a generalized Riemann invariant for the 5-shear wave, one can also complete the proof for  $K = R$  with similar derivation.  $\square$

## 5.2. Sonic case

When the  $t$ -axis is located inside a rarefaction fan, the sonic case happens, and the results for the nonsonic case can not be applied directly. Without loss of generality, consider the local wave configuration where  $t$ -axis is within the 1-rarefaction wave. The local characteristic coordinates  $(\alpha, \beta)$  within the 1-rarefaction wave are also introduced similar to those in Subsection 5.1.1.

Denote  $\phi := u_1 - c$ , then

$$d\phi = du_1 + \frac{c}{2\rho} d\rho - \frac{3}{2\rho c} dp_{11} = du_1 - \frac{1}{\rho c} dp_{11} - \frac{\rho^2}{2c} dS_1, \quad (5.113)$$

where (5.12) has been used. By (2.5a), (2.5b) and (2.5d), one has

$$\frac{\partial \phi}{\partial t} + (u_1 - c) \frac{\partial \phi}{\partial x} = \Pi_1,$$

where  $\Pi_1 = \frac{\rho^2}{2} \frac{\partial S_1}{\partial x} - \frac{1}{2} W_x$ . Denote  $\mathbf{V}_0$  is the limiting value of  $\mathbf{V}$  when  $t \rightarrow 0+$  along the  $t$ -axis. Then along this characteristic curve which is tangential to  $t$ -axis, one has  $\beta_0 = u_{1,0} - c_0 = 0$ . It follows that

$$\left( \frac{\partial \phi}{\partial t} \right)_0 = \left( \frac{\partial \phi}{\partial t} \right)_0 + (u_{1,0} - c_0) \left( \frac{\partial \phi}{\partial x} \right)_0 = \left( \frac{\rho^2}{2} \frac{\partial S_1}{\partial x} \right)_0 - \frac{1}{2} W_x(0).$$

Hence, by (5.113), one has

$$\left( \frac{\partial u_1}{\partial t} \right)_0 - \frac{1}{\rho_0 c_0} \left( \frac{\partial p_{11}}{\partial t} \right)_0 = -\frac{1}{2} W_x(0), \quad (5.114)$$

where the equality  $\left(\frac{\partial S_1}{\partial t}\right)_0 = -u_{1,0} \left(\frac{\partial S_1}{\partial x}\right)_0 = -c_0 \left(\frac{\partial S_1}{\partial x}\right)_0$  has been used. Taking the limit as  $t \rightarrow 0$  in (5.35), and let  $\beta = \beta_0 = 0$  in (5.15) and (5.16) obtains

$$\left(\frac{\partial u_1}{\partial t}\right)_0 + \frac{1}{\rho_0 c_0} \left(\frac{\partial p_{11}}{\partial t}\right)_0 = \tilde{d}_{L,0}, \quad (5.115)$$

where

$$\tilde{d}_{L,0} = \frac{\rho_L^2 S'_{1,L}}{4c_L^3} u_{1,0} (3c_L^2 + u_{1,0}^2) - 2\psi'_{1,L} u_{1,0} - \frac{1}{2} W_x(0),$$

with the values of  $S'_{1,L}$  and  $\psi'_{1,L}$  being given in (5.17).

**Theorem 5.22** (Computing  $\left(\frac{\partial u_1}{\partial t}\right)_0$ ,  $\left(\frac{\partial p_{11}}{\partial t}\right)_0$  and  $\left(\frac{\partial \rho}{\partial t}\right)_0$ ). *Assume that the  $t$ -axis is located inside the 1-rarefaction wave associated with the  $u_1 - c$  characteristic family. Then*

$$\left(\frac{\partial u_1}{\partial t}\right)_0 = \frac{1}{2} \left[ \tilde{d}_{L,0} - \frac{1}{2} W_x(0) \right], \quad (5.116)$$

$$\left(\frac{\partial p_{11}}{\partial t}\right)_0 = \frac{\rho_0 c_0}{2} \left[ \tilde{d}_{L,0} + \frac{1}{2} W_x(0) \right],$$

$$\left(\frac{\partial \rho}{\partial t}\right)_0 = \frac{1}{c_0^2} \left[ \left(\frac{\partial p_{11}}{\partial t}\right)_0 + \frac{S'_{1,L}}{c_L} \rho_0^3 u_{1,0}^2 \right]. \quad (5.117)$$

*Proof.* By (5.114) and (5.115), (5.116) may be obtained. One takes  $\beta = \beta_0 = 0$  in (5.24) to get

$$\left(\frac{\partial S_1}{\partial t}\right)_0 = -\frac{S'_{1,L}}{c_L} u_{1,0}^2.$$

Substituting it into

$$\left(\frac{\partial \rho}{\partial t}\right)_0 = \frac{1}{c_0^2} \left[ \left(\frac{\partial p_{11}}{\partial t}\right)_0 - \rho_0^3 \left(\frac{\partial S_1}{\partial t}\right)_0 \right]$$

which is derived from (5.12), one obtains (5.117).  $\square$

It is noted that for the sonic case, one has the relation  $p_{11,0} = \frac{1}{3}(\rho u_1^2)_0$  which is derived from  $u_{1,0} - c_0 = 0$ ; and (2.11) induces that if  $p_{11} \neq \rho u_1^2$ , one has

$$\begin{aligned} \frac{Du_2}{Dt} &= \frac{p_{11}}{p_{11} - \rho u_1^2} \left( \frac{\partial u_2}{\partial t} + \frac{2u_1 p_{12}}{3p_{11}^2} \frac{Dp_{11}}{Dt} - \frac{u_1}{p_{11}} \frac{\partial p_{12}}{\partial t} \right), \\ \frac{Dp_{12}}{Dt} &= \frac{-p_{11}}{p_{11} - \rho u_1^2} \left[ \rho u_1 \left( \frac{\partial u_2}{\partial t} + \frac{2u_1 p_{12}}{3p_{11}^2} \frac{Dp_{11}}{Dt} \right) - \frac{\partial p_{12}}{\partial t} \right]. \end{aligned} \quad (5.118)$$

Hence, substituting (5.118) into (5.61) and (5.68), one can acquire the two equations which  $\frac{\partial u_2}{\partial t}(0, \beta)$  and  $\frac{\partial p_{12}}{\partial t}(0, \beta)$  satisfy inside the 1-rarefaction wave, and taking  $\beta = \beta_0 = 0$  yields the following system

$$\begin{cases} \tilde{a}_{3,L,0} \left(\frac{\partial u_2}{\partial t}\right)_0 + \tilde{b}_{3,L,0} \left(\frac{\partial p_{12}}{\partial t}\right)_0 = \tilde{d}_{3,L,0}, \\ \tilde{a}_{4,L,0} \left(\frac{\partial u_2}{\partial t}\right)_0 + \tilde{b}_{4,L,0} \left(\frac{\partial p_{12}}{\partial t}\right)_0 = \tilde{d}_{4,L,0}, \end{cases} \quad (5.119)$$

where

$$\begin{aligned} \tilde{a}_{3,L,0} &= 1 + \frac{\beta_L}{4}, \quad \tilde{a}_{4,L,0} = \frac{\beta_L c_0}{4\rho_0^2}, \quad \tilde{b}_{3,L,0} = \frac{u_{1,0}}{p_{11,0}} \left(1 - \frac{\beta_L}{4}\right), \quad \tilde{b}_{4,L,0} = \frac{1}{\rho_0^3} \left(1 - \frac{\beta_L}{2}\right), \\ \tilde{d}_{3,L,0} &= \left[ \frac{\partial \psi_2}{\partial \alpha}(0, \beta_L) - \frac{\Pi_{2,L} \beta_L}{8c_L} \right] \psi_{1,L} - \frac{\beta_L}{4} \cdot \left\{ \left(\frac{2p_{12}}{p_{11}}\right)_0 \cdot \left[ \left(\frac{\partial u_1}{\partial t}\right)_0 + \frac{1}{2} W_x(0) \right] + \frac{S'_{1,L}}{c_L} \left(\frac{c\rho^2 p_{12}}{2p_{11}}\right)_0 \right\} \\ &\quad + \left( \frac{\sqrt{3}p_{12}}{2\rho\sqrt{\rho p_{11}}} \frac{\partial \rho}{\partial t} \right)_0 + \left( \frac{\sqrt{3}p_{12}}{2p_{11}\sqrt{\rho p_{11}}} \frac{\partial p_{11}}{\partial t} \right)_0, \\ \tilde{d}_{4,L,0} &= \left[ \frac{\partial \psi_3}{\partial \alpha}(0, \beta_L) - \frac{\Pi_{3,L} \beta_L}{8c_L} \right] \psi_{1,L} - \frac{\beta_L}{4} \cdot \left\{ \left(\frac{3p_{12}}{c\rho^3}\right)_0 \left[ \left(\frac{\partial u_1}{\partial t}\right)_0 + \frac{1}{2} W_x(0) \right] + \frac{S'_{1,L}}{c_L} \left(\frac{3p_{12}}{\rho}\right)_0 \right\} + \left(\frac{3p_{12}}{\rho^4} \frac{\partial \rho}{\partial t}\right)_0. \end{aligned}$$

It is noted that (2.8) has been used during deriving the above coefficients.

**Theorem 5.23** (Computing  $\left(\frac{\partial u_2}{\partial t}\right)_0$ ,  $\left(\frac{\partial p_{12}}{\partial t}\right)_0$  and  $\left(\frac{\partial p_{22}}{\partial t}\right)_0$ ). Assume that the  $t$ -axis is located inside the 1-rarefaction wave associated with the  $u_1 - c$  characteristic family. Then

$$\left(\frac{\partial u_2}{\partial t}\right)_0 = \frac{\tilde{d}_{3,L,0}\tilde{b}_{4,L,0} - \tilde{d}_{4,L,0}\tilde{b}_{3,L,0}}{\tilde{a}_{3,L,0}\tilde{b}_{4,L,0} - \tilde{a}_{4,L,0}\tilde{b}_{3,L,0}}, \quad \left(\frac{\partial p_{12}}{\partial t}\right)_0 = \frac{\tilde{d}_{3,L,0}\tilde{a}_{4,L,0} - \tilde{d}_{4,L,0}\tilde{a}_{3,L,0}}{\tilde{a}_{4,L,0}\tilde{b}_{3,L,0} - \tilde{a}_{3,L,0}\tilde{b}_{4,L,0}}. \quad (5.120)$$

The limiting value  $\left(\frac{\partial p_{22}}{\partial t}\right)_0$  is computed by

$$\left(\frac{p_{11}}{\rho^4} \frac{\partial p_{22}}{\partial t}\right)_0 = -\frac{S'_{2,L}}{c_L} u_{1,0}^2 - \left(\frac{p_{22}}{\rho^4} \frac{\partial p_{11}}{\partial t}\right)_0 + \left(\frac{2p_{12}}{\rho^4} \frac{\partial p_{12}}{\partial t}\right)_0 + \left(\frac{4 \det(\mathbf{p})}{\rho^5} \frac{\partial \rho}{\partial t}\right)_0. \quad (5.121)$$

*Proof.* (5.120) is directly obtained by solving the system (5.119). Taking  $\beta = \beta_0 = 0$  in (5.71) and using (5.70) yields (5.121).  $\square$

**Remark 5.24.** For the case that the  $t$ -axis is located inside the 6-rarefaction wave, computing  $\left(\frac{\partial \mathbf{V}}{\partial t}\right)_0$  is presented in Appendix E.

### 5.3. Acoustic case

When  $\mathbf{U}_L = \mathbf{U}_* = \mathbf{U}_R$  but  $\mathbf{U}'_L \neq \mathbf{U}'_R$ , the acoustic case happens. Only the linear waves emanate from the origin  $(x, t) = (0, 0)$ . This case will be simpler than the general case discussed before.

#### 5.3.1. Computing $\left(\frac{\partial u_1}{\partial t}\right)_*$ , $\left(\frac{\partial p_{11}}{\partial t}\right)_*$ and $\left(\frac{\partial \rho}{\partial t}\right)_*$ ( $K = L, R$ )

For the 1-acoustic wave in the left associated with  $u_1 - c$ , since the solution is continuous across the 1-acoustic wave, taking the differentiation along it, one has

$$\left(\frac{\partial u_1}{\partial t}\right)_* + (u_{1,*} - c_*) \left(\frac{\partial u_1}{\partial x}\right)_* = \frac{\partial u_{1,L}}{\partial t} + (u_{1,*} - c_*) \frac{\partial u_{1,L}}{\partial x}.$$

By (2.6) and (2.7), it follows that

$$\left(\frac{\partial u_1}{\partial t}\right)_* - \frac{u_{1,*} - c_*}{3p_{11,*}} \left(\frac{\mathcal{D}p_{11}}{\mathcal{D}t}\right)_* = -\frac{p'_{11,L}}{\rho_*} - c_* u'_{1,L} - \frac{1}{2} W_x(0). \quad (5.122)$$

By resolving the 6-acoustic wave in the right associated with  $u_1 + c$ , one has

$$\left(\frac{\partial u_1}{\partial t}\right)_* - \frac{u_{1,*} + c_*}{3p_{11,*}} \left(\frac{\mathcal{D}p_{11}}{\mathcal{D}t}\right)_* = -\frac{p'_{11,R}}{\rho_*} + c_* u'_{1,R} - \frac{1}{2} W_x(0). \quad (5.123)$$

**Theorem 5.25** (Computing  $\left(\frac{\partial u_1}{\partial t}\right)_*$ ,  $\left(\frac{\partial p_{11}}{\partial t}\right)_*$  and  $\left(\frac{\partial \rho}{\partial t}\right)_*$  ( $K = L, R$ )). For the acoustic case, one has

$$\left(\frac{\partial u_1}{\partial t}\right)_* = \frac{1}{2c_*} \left[ \left( -\frac{p'_{11,L}}{\rho_*} - c_* u'_{1,L} - \frac{1}{2} W_x(0) \right) (u_{1,*} + c_*) + \left( \frac{p'_{11,R}}{\rho_*} - c_* u'_{1,R} + \frac{1}{2} W_x(0) \right) (u_{1,*} - c_*) \right], \quad (5.124)$$

$$\left(\frac{\partial p_{11}}{\partial t}\right)_* = -\frac{\rho_* c_*}{2} \left[ \left( u'_{1,L} + \frac{p'_{11,L}}{\rho_* c_*} \right) (u_{1,*} + c_*) - \left( u'_{1,R} - \frac{p'_{11,R}}{\rho_* c_*} \right) (u_{1,*} - c_*) \right], \quad (5.125)$$

and

$$\left(\frac{\partial \rho}{\partial t}\right)_* = \frac{1}{c_*^2} \left[ \left(\frac{\partial p_{11}}{\partial t}\right)_* + u_{1,*} (p'_{11,K} - c_*^2 \rho'_K) \right], \quad K = L, R. \quad (5.126)$$



*Proof.* Combining (5.122) with (5.123) yields (5.124) and

$$\left(\frac{\mathcal{D}p_{11}}{\mathcal{D}t}\right)_* = \frac{3p_{11,*}}{2c_*} \left[ \frac{1}{\rho_*} (p'_{11,R} - p'_{11,L}) - c_* (u'_{1,L} + u'_{1,R}) \right]. \quad (5.127)$$

By utilizing (2.8) and

$$\left(\frac{\mathcal{D}u_1}{\mathcal{D}t}\right)_* = \left(\frac{\partial u_1}{\partial t}\right)_* - \frac{u_{1,*}}{3p_{11,*}} \left(\frac{\mathcal{D}p_{11}}{\mathcal{D}t}\right)_*,$$

where (2.6) has been used, one obtains (5.125). Applying (5.12) and (5.24) gives (5.126).  $\square$

5.3.2. Computing  $\left(\frac{\partial u_2}{\partial t}\right)_{*K}$ ,  $\left(\frac{\partial p_{12}}{\partial t}\right)_{*K}$  and  $\left(\frac{\partial p_{22}}{\partial t}\right)_{*K}$  ( $K = L, R$ )

Taking the differentiation along the 1-acoustic wave for  $u_2$  and  $p_{12}$  gives

$$\begin{aligned} \left(\frac{\partial u_2}{\partial t}\right)_{*L} + (u_{1,*} - c_*) \left(\frac{\partial u_2}{\partial x}\right)_{*L} &= \frac{\partial u_{2,L}}{\partial t} + (u_{1,*} - c_*) u'_{2,L}, \\ \left(\frac{\partial p_{12}}{\partial t}\right)_{*L} + (u_{1,*} - c_*) \left(\frac{\partial p_{12}}{\partial x}\right)_{*L} &= \frac{\partial p_{12,L}}{\partial t} + (u_{1,*} - c_*) p'_{12,L}. \end{aligned}$$

Applying (2.5c), (2.5e), (2.9) and (2.10) to above two equations obtains

$$\begin{aligned} \left(\frac{\mathcal{D}u_2}{\mathcal{D}t}\right)_{*L} + \frac{c_*}{p_{11,*}} \left(\frac{\mathcal{D}p_{12}}{\mathcal{D}t}\right)_{*L} &= \frac{2p_{12,*}c_*}{3p_{11,*}^2} \left(\frac{\mathcal{D}p_{11}}{\mathcal{D}t}\right)_* - \frac{p'_{12,L}}{\rho_L} - c_* u'_{2,L}, \\ \rho_* c_* \left(\frac{\mathcal{D}u_2}{\mathcal{D}t}\right)_{*L} + \left(\frac{\mathcal{D}p_{12}}{\mathcal{D}t}\right)_{*L} &= -c_* p'_{12,L} - 2p_{12,L} u'_{1,L} - p_{11,L} u'_{2,L}. \end{aligned}$$

It follows that

$$\begin{aligned} \left(\frac{\mathcal{D}u_2}{\mathcal{D}t}\right)_{*L} &= -\frac{p'_{12,L}}{\rho_L} - \frac{c_* p_{12,L}}{p_{11,*}} u'_{1,L} - \frac{p_{12,*}c_*}{3p_{11,*}^2} \left(\frac{\mathcal{D}p_{11}}{\mathcal{D}t}\right)_*, \\ \left(\frac{\mathcal{D}p_{12}}{\mathcal{D}t}\right)_{*L} &= \frac{p_{12,*}}{p_{11,*}} \left(\frac{\mathcal{D}p_{11}}{\mathcal{D}t}\right)_* + p_{12,L} u'_{1,L} - p_{11,L} u'_{2,L}. \end{aligned} \quad (5.128)$$

Taking the differentiation along the 1-acoustic wave for  $p_{22}$  yields

$$\left(\frac{\partial p_{22}}{\partial x}\right)_{*L} = \frac{1}{c_*} \left[ \left(\frac{\mathcal{D}p_{22}}{\mathcal{D}t}\right)_{*L} + p_{22,L} u'_{1,L} + 2p_{12,L} u'_{2,L} + c_* p'_{22,L} \right], \quad (5.129)$$

where (2.5f) has been used. Moreover, resolving the 6-acoustic wave has

$$\begin{cases} \left(\frac{\mathcal{D}u_2}{\mathcal{D}t}\right)_{*R} = -\frac{p'_{12,R}}{\rho_R} + \frac{c_* p_{12,R}}{p_{11,*}} u'_{1,R} + \frac{p_{12,*}c_*}{3p_{11,*}^2} \left(\frac{\mathcal{D}p_{11}}{\mathcal{D}t}\right)_*, \\ \left(\frac{\mathcal{D}p_{12}}{\mathcal{D}t}\right)_{*R} = \frac{p_{12,*}}{p_{11,*}} \left(\frac{\mathcal{D}p_{11}}{\mathcal{D}t}\right)_* + p_{12,R} u'_{1,R} - p_{11,R} u'_{2,R}, \\ \left(\frac{\partial p_{22}}{\partial x}\right)_{*R} = \frac{1}{c_*} \left[ -p_{22,R} u'_{1,R} - 2p_{12,R} u'_{2,R} + c_* p'_{22,R} - \left(\frac{\mathcal{D}p_{22}}{\mathcal{D}t}\right)_{*R} \right]. \end{cases} \quad (5.130)$$

**Theorem 5.26** (Computing  $\left(\frac{\partial u_2}{\partial t}\right)_{*K}$ ,  $\left(\frac{\partial p_{12}}{\partial t}\right)_{*K}$  and  $\left(\frac{\partial p_{22}}{\partial t}\right)_{*K}$   $K = L, R$ ). *For the acoustic case, one has*

$$\begin{aligned} \left(\frac{\partial u_2}{\partial t}\right)_{*K} &= \left(\frac{\mathcal{D}u_2}{\mathcal{D}t}\right)_{*K} + \frac{u_{1,*}}{p_{11,*}} \left[ \left(\frac{\mathcal{D}p_{12}}{\mathcal{D}t}\right)_{*K} - \frac{2p_{12,*}}{3p_{11,*}} \left(\frac{\mathcal{D}p_{11}}{\mathcal{D}t}\right)_* \right], \\ \left(\frac{\partial p_{12}}{\partial t}\right)_{*K} &= \left(\frac{\mathcal{D}p_{12}}{\mathcal{D}t}\right)_{*K} + \rho_* u_{1,*} \left(\frac{\mathcal{D}u_2}{\mathcal{D}t}\right)_{*K}, \end{aligned} \quad (5.131)$$

and

$$\left(\frac{\partial p_{22}}{\partial t}\right)_{*K} = \left(\frac{\mathcal{D}p_{22}}{\mathcal{D}t}\right)_{*K} - u_{1,*} \left(\frac{\partial p_{22}}{\partial x}\right)_{*K}, \quad (5.132)$$

where

$$\left(\frac{\mathcal{D}p_{22}}{\mathcal{D}t}\right)_{*K} = \left(\frac{p_{11}p_{22} - 4p_{12}^2}{3p_{11}^2} \frac{\mathcal{D}p_{11}}{\mathcal{D}t}\right)_* + \frac{2p_{12,*}}{p_{11,*}} \left(\frac{\mathcal{D}p_{12}}{\mathcal{D}t}\right)_{*K}, \quad (5.133)$$

and  $\left(\frac{\mathcal{D}p_{11}}{\mathcal{D}t}\right)_*$ ,  $\left(\frac{\mathcal{D}u_2}{\mathcal{D}t}\right)_{*K}$ ,  $\left(\frac{\mathcal{D}p_{12}}{\mathcal{D}t}\right)_{*K}$  and  $\left(\frac{\partial p_{22}}{\partial x}\right)_{*K}$  are given by (5.127)-(5.130),  $K = L, R$ .

*Proof.* Utilizing (2.11) yields (5.131). (5.132) is direct, and applying (2.12) gives (5.133).  $\square$

5.3.3. Computing  $\left(\frac{\partial u_2}{\partial t}\right)_{**}$ ,  $\left(\frac{\partial p_{12}}{\partial t}\right)_{**}$  and  $\left(\frac{\partial p_{22}}{\partial t}\right)_{**K}$  ( $K = L, R$ )

Since the solution is continuous across the 2-acoustic wave, taking the differentiation along the 2-acoustic wave for  $u_2$ , one has

$$\left(\frac{\partial u_2}{\partial t}\right)_{**} + (u_{1,*} - \frac{c_*}{\sqrt{3}}) \left(\frac{\partial u_2}{\partial x}\right)_{**} = \left(\frac{\partial u_2}{\partial t}\right)_{*L} + (u_{1,*} - \frac{c_*}{\sqrt{3}}) \left(\frac{\partial u_2}{\partial x}\right)_{*L}.$$

Applying (2.9) to the above formula gives

$$\left(\frac{\mathcal{D}u_2}{\mathcal{D}t}\right)_{**} + \frac{c_*}{\sqrt{3}p_{11,*}} \left(\frac{\mathcal{D}p_{12}}{\mathcal{D}t}\right)_{**} = \left(\frac{\mathcal{D}u_2}{\mathcal{D}t}\right)_{*L} + \frac{c_*}{\sqrt{3}p_{11,*}} \left(\frac{\mathcal{D}p_{12}}{\mathcal{D}t}\right)_{*L}.$$

Resolving the 5-acoustic wave yields

$$\left(\frac{\mathcal{D}u_2}{\mathcal{D}t}\right)_{**} - \frac{c_*}{\sqrt{3}p_{11,*}} \left(\frac{\mathcal{D}p_{12}}{\mathcal{D}t}\right)_{**} = \left(\frac{\mathcal{D}u_2}{\mathcal{D}t}\right)_{*R} - \frac{c_*}{\sqrt{3}p_{11,*}} \left(\frac{\mathcal{D}p_{12}}{\mathcal{D}t}\right)_{*R}.$$

Then it follows from the above two equations that

$$\begin{aligned} \left(\frac{\mathcal{D}u_2}{\mathcal{D}t}\right)_{**} &= \frac{1}{2} \left[ \left(\frac{\mathcal{D}u_2}{\mathcal{D}t}\right)_{*L} + \left(\frac{\mathcal{D}u_2}{\mathcal{D}t}\right)_{*R} + \frac{c_*}{\sqrt{3}p_{11,*}} \left( \left(\frac{\mathcal{D}p_{12}}{\mathcal{D}t}\right)_{*L} - \left(\frac{\mathcal{D}p_{12}}{\mathcal{D}t}\right)_{*R} \right) \right], \\ \left(\frac{\mathcal{D}p_{12}}{\mathcal{D}t}\right)_{**} &= \frac{\sqrt{3}p_{11,*}}{2c_*} \left[ \left(\frac{\mathcal{D}u_2}{\mathcal{D}t}\right)_{*L} - \left(\frac{\mathcal{D}u_2}{\mathcal{D}t}\right)_{*R} + \frac{c_*}{\sqrt{3}p_{11,*}} \left( \left(\frac{\mathcal{D}p_{12}}{\mathcal{D}t}\right)_{*L} + \left(\frac{\mathcal{D}p_{12}}{\mathcal{D}t}\right)_{*R} \right) \right]. \end{aligned} \quad (5.134)$$

Taking the differentiation along the 2-acoustic wave or the 5-acoustic wave for  $p_{22}$ , one has

$$\begin{aligned} \left(\frac{\partial p_{22}}{\partial x}\right)_{**L} &= \frac{\sqrt{3}}{c_*} \left[ \left(\frac{\mathcal{D}p_{22}}{\mathcal{D}t}\right)_{**} - \left(\frac{\mathcal{D}p_{22}}{\mathcal{D}t}\right)_{*L} \right] - \left(\frac{\partial p_{22}}{\partial x}\right)_{*L}, \\ \left(\frac{\partial p_{22}}{\partial x}\right)_{**R} &= \left(\frac{\partial p_{22}}{\partial x}\right)_{*R} + \frac{\sqrt{3}}{c_*} \left[ \left(\frac{\mathcal{D}p_{22}}{\mathcal{D}t}\right)_{*R} - \left(\frac{\mathcal{D}p_{22}}{\mathcal{D}t}\right)_{**} \right], \end{aligned} \quad (5.135)$$

where  $\left(\frac{\partial p_{22}}{\partial x}\right)_{*L}$  and  $\left(\frac{\partial p_{22}}{\partial x}\right)_{*R}$  are given in (5.129) and (5.130), respectively, and  $\left(\frac{\mathcal{D}p_{22}}{\mathcal{D}t}\right)_{*K}$  ( $K = L, R$ ) are given by (5.133).

**Theorem 5.27** (Computing  $\left(\frac{\partial u_2}{\partial t}\right)_{**}$ ,  $\left(\frac{\partial p_{12}}{\partial t}\right)_{**}$  and  $\left(\frac{\partial p_{22}}{\partial t}\right)_{**K}$  ( $K = L, R$ )). *For the acoustic case, one has*

$$\begin{aligned} \left(\frac{\partial u_2}{\partial t}\right)_{**} &= \left(\frac{\mathcal{D}u_2}{\mathcal{D}t}\right)_{**} + \frac{u_{1,*}}{p_{11,*}} \left[ \left(\frac{\mathcal{D}p_{12}}{\mathcal{D}t}\right)_{**} - \frac{2p_{12,*}}{3p_{11,*}} \left(\frac{\mathcal{D}p_{11}}{\mathcal{D}t}\right)_* \right], \\ \left(\frac{\partial p_{12}}{\partial t}\right)_{**} &= \left(\frac{\mathcal{D}p_{12}}{\mathcal{D}t}\right)_{**} + \rho_* u_{1,*} \left(\frac{\mathcal{D}u_2}{\mathcal{D}t}\right)_{**}, \end{aligned} \quad (5.136)$$

and

$$\left(\frac{\partial p_{22}}{\partial t}\right)_{**K} = \left(\frac{\mathcal{D}p_{22}}{\mathcal{D}t}\right)_{**} - u_{1,*} \left(\frac{\partial p_{22}}{\partial x}\right)_{**K}, \quad (5.137)$$

where

$$\left(\frac{\mathcal{D}p_{22}}{\mathcal{D}t}\right)_{**} = \left(\frac{p_{11}p_{22} - 4p_{12}^2}{3p_{11}^2} \frac{\mathcal{D}p_{11}}{\mathcal{D}t}\right)_* + \frac{2p_{12,*}}{p_{11,*}} \left(\frac{\mathcal{D}p_{12}}{\mathcal{D}t}\right)_{**}, \quad (5.138)$$

and  $\left(\frac{\mathcal{D}p_{11}}{\mathcal{D}t}\right)_*$ ,  $\left(\frac{\mathcal{D}u_2}{\mathcal{D}t}\right)_{**}$ ,  $\left(\frac{\mathcal{D}p_{12}}{\mathcal{D}t}\right)_{**}$  and  $\left(\frac{\partial p_{22}}{\partial x}\right)_{**K}$  are given by (5.127), (5.134) and (5.135),  $K = L, R$ .

*Proof.* Utilizing (2.11) yields (5.136). (5.137) is direct, and applying (2.12) gives (5.138).  $\square$

## 6. Numerical experiments

In this section, some initial value and initial-boundary-value problems of the 1D and 2D ten-moment equations will be solved to verify the accuracy and performance of the proposed GRP schemes. It should be emphasized that several examples of 2D Riemann problems are constructed for the first time. For the 1D case, the time step size is computed by

$$\Delta t = C_{\text{cff}} \frac{\Delta x}{\max_j \{\lambda_{\text{max}}^x(\mathbf{V}_j)\}},$$

where  $\lambda_{\text{max}}^x(\mathbf{V}_j) := |u_{1,j}| + \sqrt{\frac{3p_{11,j}}{\rho_j}}$ ,  $j = 1, \dots, N_x$  with  $N_x$  denoting the number of cells in the  $x$ -direction. For the 2D case, the time step size is computed by

$$\Delta t = \frac{C_{\text{cff}}}{\frac{\max_{j,k} \{\lambda_{\text{max}}^x(\mathbf{V}_{j,k})\}}{\Delta x} + \frac{\max_{j,k} \{\lambda_{\text{max}}^y(\mathbf{V}_{j,k})\}}{\Delta y}},$$

where  $\lambda_{\text{max}}^x(\mathbf{V}_{j,k}) := |u_{1,j,k}| + \sqrt{\frac{3p_{11,j,k}}{\rho_{j,k}}}$  and  $\lambda_{\text{max}}^y(\mathbf{V}_{j,k}) := |u_{2,j,k}| + \sqrt{\frac{3p_{22,j,k}}{\rho_{j,k}}}$ ,  $j = 1, \dots, N_x$ ,  $k = 1, \dots, N_y$  with  $N_x, N_y$  denoting respectively the numbers of cells in the  $x$ - and  $y$ -directions. The CFL number  $C_{\text{cff}}$  is taken as 0.45. Without special station, the van Leer slope limiter (3.7) with characteristic decomposition is utilized.

### Example 6.1. Accuracy test 1 without source term

The first example is a smooth problem within the interval  $[-0.5, 0.5]$  without source term, and the exact solution is

$$\rho = 2 + \sin(2\pi(x - t)), \quad u_1 = 1, \quad u_2 = 0, \quad p_{11} = 1, \quad p_{12} = 0, \quad p_{22} = 1.$$

The periodic boundary conditions are imposed. The proposed GRP scheme is applied to solve this problem up to the final time  $t = 0.5$ . Table 1 shows the errors and corresponding orders of the density  $\rho$ . One can see that almost second-order convergence rates are obtained for the  $l^1$  and  $l^2$  errors, but the  $l^\infty$  convergence rate is lower than 1.5, which is coincided with those convergent results in [19].

Table 1: Example 6.1: The convergent results of  $\rho$  at  $t = 0.5$  for the accuracy test 1.

	$N_x$	$l^1$ error	order	$l^2$ error	order	$l^\infty$ error	order
$\rho$	10	8.8236e-02	–	1.1507e-01	–	2.1657e-01	–
	20	3.4526e-02	1.35	4.1664e-02	1.47	7.8594e-02	1.46
	40	9.6788e-03	1.83	1.2793e-02	1.70	3.1038e-02	1.34
	80	2.4275e-03	2.00	3.8036e-03	1.75	1.1914e-02	1.38
	160	5.7060e-04	2.09	1.1138e-03	1.77	4.4951e-03	1.41
	320	1.3677e-04	2.06	3.2356e-04	1.78	1.6742e-03	1.42
	640	3.2039e-05	2.09	9.3616e-05	1.79	6.1817e-04	1.44

### Example 6.2. Accuracy test 2 with nontrivial source term

This example examines a smooth problem within the interval  $[-0.25, 0.25]$  with the nontrivial potential  $W(x) = x$ , and the exact solution is

$$\rho = \epsilon + \sin^2(2\pi(x - t)), \quad u_1 = 1, \quad u_2 = 0, \quad p_{11} = 1 + (t - x) \left( \frac{\epsilon}{2} + \frac{1}{4} \right) + \frac{\sin(4\pi(x - t))}{16\pi}, \quad p_{12} = 0, \quad p_{22} = 1.$$

The parameter  $\epsilon$  is taken as  $10^{-2}$ . For the density  $\rho$ , the periodic boundary conditions are imposed, and for the pressure component  $p_{11}$ , the exact boundary conditions are imposed. The proposed GRP scheme is applied to solve this problem up to the final time  $t = 0.1$ . Table 2 shows the errors and corresponding orders of the

density  $\rho$  and the pressure component  $p_{11}$ . One can see that for the density  $\rho$ , there are similar convergent rates with those in accuracy test 1, and for the pressure component  $p_{11}$ , almost second-order convergent rates are obtained on the fine meshes, which may be due to the  $p_{11}$  being close to a linear function.

Table 2: Example 6.2: The convergent results of  $\rho$  and  $p_{11}$  at  $t = 0.1$  for the accuracy test 2 with  $\epsilon = 10^{-2}$ .

	$N_x$	$l^1$ error	order	$l^2$ error	order	$l^\infty$ error	order
$\rho$	10	2.6529e-02	–	3.2438e-02	–	5.5835e-02	–
	20	1.0243e-02	1.37	1.1660e-02	1.48	2.3462e-02	1.25
	40	2.6514e-03	1.95	3.6216e-03	1.69	9.4498e-03	1.31
	80	6.6426e-04	2.00	1.0997e-03	1.72	3.6870e-03	1.36
	160	1.6390e-04	2.02	3.2991e-04	1.74	1.4114e-03	1.39
	320	4.0720e-05	2.01	9.7789e-05	1.75	5.3239e-04	1.41
	640	1.0855e-05	1.91	2.9285e-05	1.74	1.9890e-04	1.42
$p_{11}$	10	3.9221e-03	–	4.8356e-03	–	8.5007e-03	–
	20	2.3719e-03	0.73	3.5839e-03	0.43	1.2636e-02	-0.57
	40	9.8731e-04	1.26	1.6739e-03	1.10	8.0796e-03	0.65
	80	2.9479e-04	1.74	5.3125e-04	1.66	2.3384e-03	1.79
	160	8.1947e-05	1.85	1.6025e-04	1.73	1.0013e-03	1.22
	320	2.2038e-05	1.89	4.1142e-05	1.96	1.7405e-04	2.52
	640	6.5996e-06	1.74	1.0550e-05	1.96	3.9586e-05	2.14

### Example 6.3. 1D Riemann problems

Three 1D Riemann problems are considered here to test the wave-capturing ability of the proposed GRP scheme. Their initial conditions and setups are as follows:

(i) 1D Riemann problem 1:

$$(\rho, u_1, u_2, p_{11}, p_{12}, p_{22}) = \begin{cases} (1, 0, 0, 2, 0.05, 0.6), & x \leq 0.5, \\ (0.125, 0, 0, 0.2, 0.1, 0.2), & x > 0.5. \end{cases} \quad (6.1)$$

The discontinuity is located at  $x = 0.5$  in the interval  $[0, 1]$ . The final time is  $t = 0.125$ . This is the Sod shock-tube problem, and the solutions at the final time contains five waves: the left rarefaction wave, the left shear wave, the middle contact discontinuity, the right shear wave, and the right shock wave, see Figure 5.

(ii) 1D Riemann problem 2:

$$(\rho, u_1, u_2, p_{11}, p_{12}, p_{22}) = \begin{cases} (1, 1, 1, 1, 0, 1), & x \leq 0, \\ (1, -1, -1, 1, 0, 1), & x > 0. \end{cases} \quad (6.2)$$

The discontinuity is located at  $x = 0$  in the interval  $[-0.5, 0.5]$ . The final time is  $t = 0.125$ . The solutions at the final time contains four waves: the left shock wave, the left shear wave, the right shear wave, and the right shock wave, see Figure 6.

(iii) 1D Riemann problem 3:

$$(\rho, u_1, u_2, p_{11}, p_{12}, p_{22}) = \begin{cases} (2, -0.5, -0.5, 1.5, 0.5, 1.5), & x \leq 0, \\ (1, 1, 1, 1, 0, 1), & x > 0. \end{cases} \quad (6.3)$$

The discontinuity is located at  $x = 0$  in the interval  $[-0.5, 0.5]$ . The final time is  $t = 0.15$ . The solutions at the final time contains five waves: the left rarefaction wave, the left shear wave, the middle contact discontinuity, the right shear wave, and the right rarefaction wave, see Figure 7.

For the above three problems, the outflow boundary conditions are imposed. They are simulated by the GRP scheme on a mesh consisting of 400 cells. The numerical results are respectively presented in Figures 5-7. One can find that the GRP scheme captures all possible waves well and has high resolution for the shock waves.

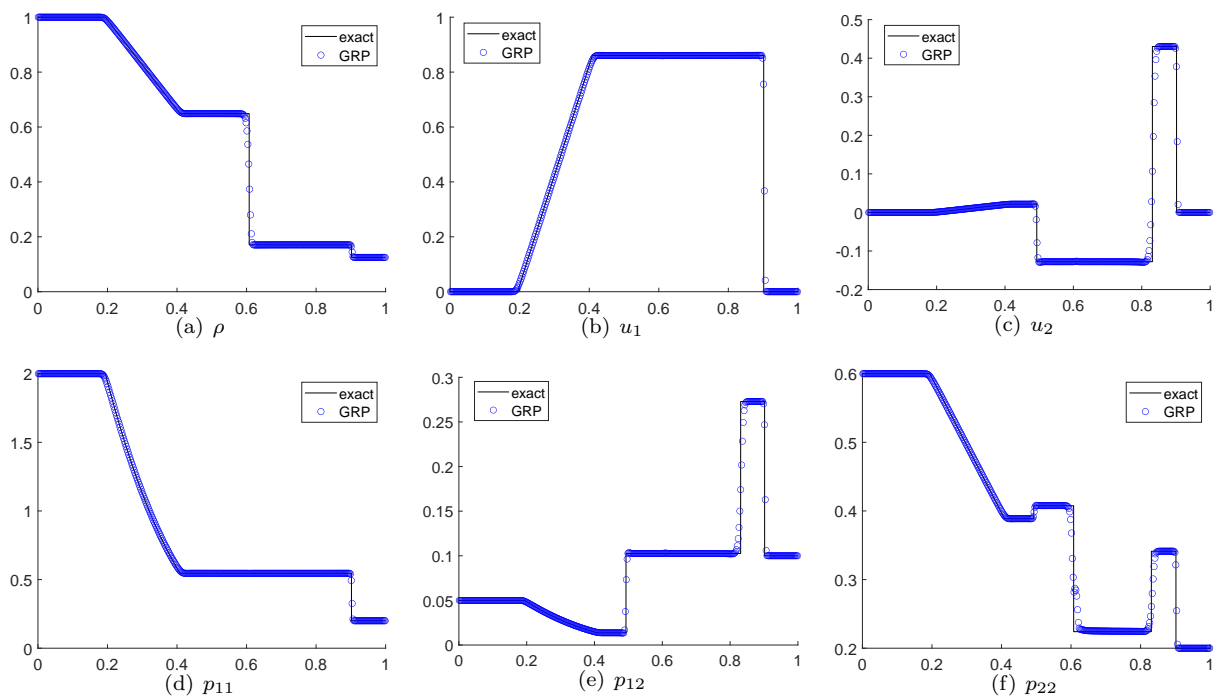


Figure 5: Example 6.3: The numerical solutions of the GRP scheme on 400 uniform cells for the 1D Riemann problem (6.1).

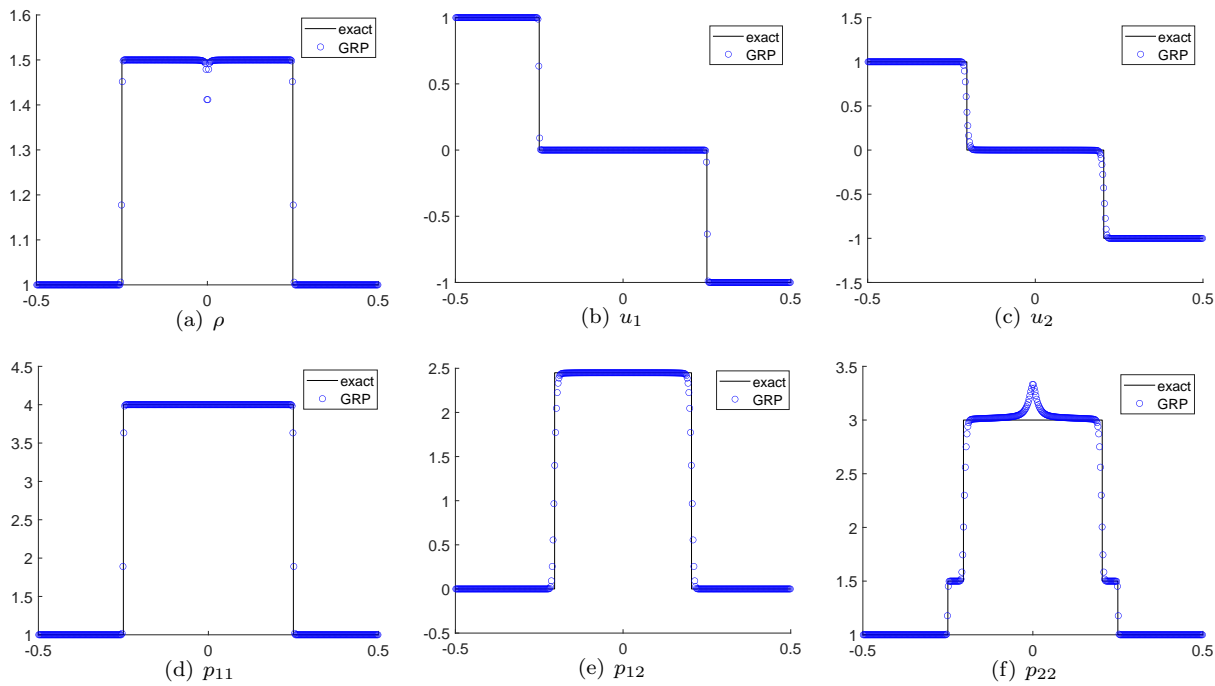


Figure 6: Example 6.3: The numerical solutions of the GRP scheme on 400 uniform cells for the 1D Riemann problem (6.2).

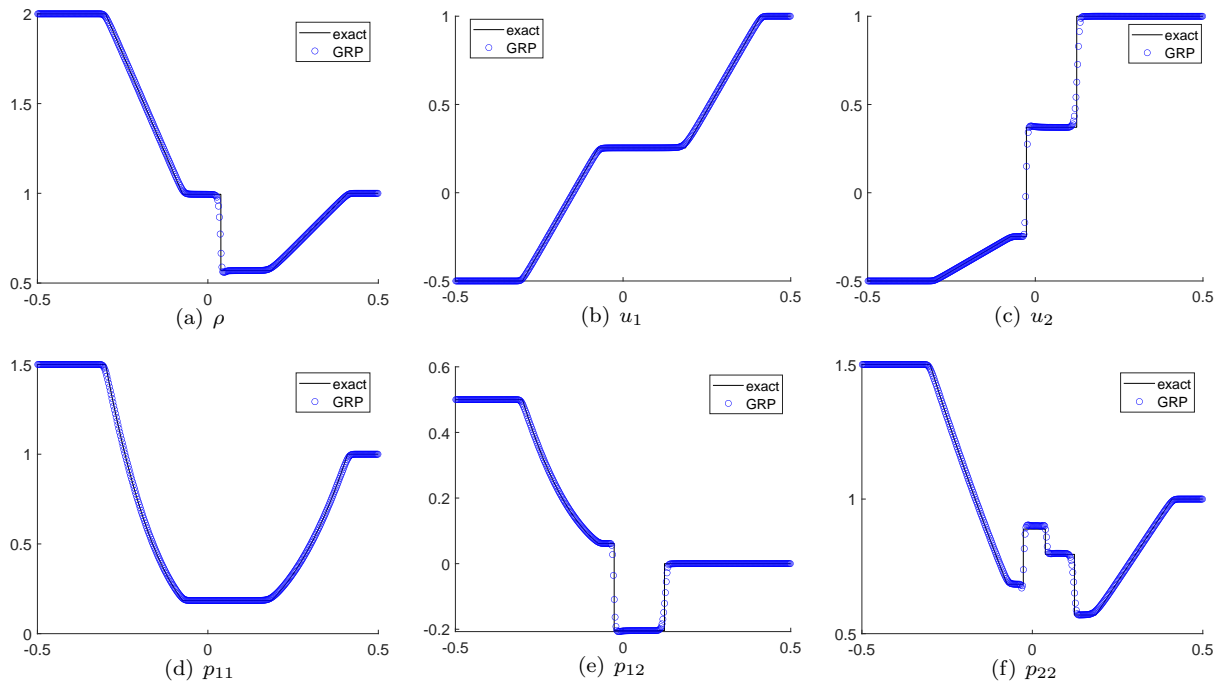


Figure 7: Example 6.3: The numerical solutions of the GRP scheme on 400 uniform cells for the 1D Riemann problem (6.3).

**Example 6.4. Leblanc problem**

The Leblanc problem is considered in this test, which is an extension of the Leblanc problem of the Euler equations. The initial solution is given by

$$(\rho, u_1, u_2, p_{11}, p_{12}, p_{22}) = \begin{cases} (2, 0, 0, 10^9, 0, 10^9), & x \leq 5, \\ (0.001, 0, 0, 1, 0, 1), & x > 5. \end{cases}$$

This problem is highly challenging due to the presence of the strong jumps in the initial density and pressure. The computational domain is taken as  $[0, 10]$  with the outflow boundary conditions. This problem is simulated until the time  $t = 0.00004$ . Figure 8 displays the numerical solutions obtained on a mesh with 800 cells. For this problem, the minmod slope limiter (3.6) with  $\theta = 1.8$  is utilized. One can see that the proposed GRP scheme is able to capture the strong discontinuities with high resolution.

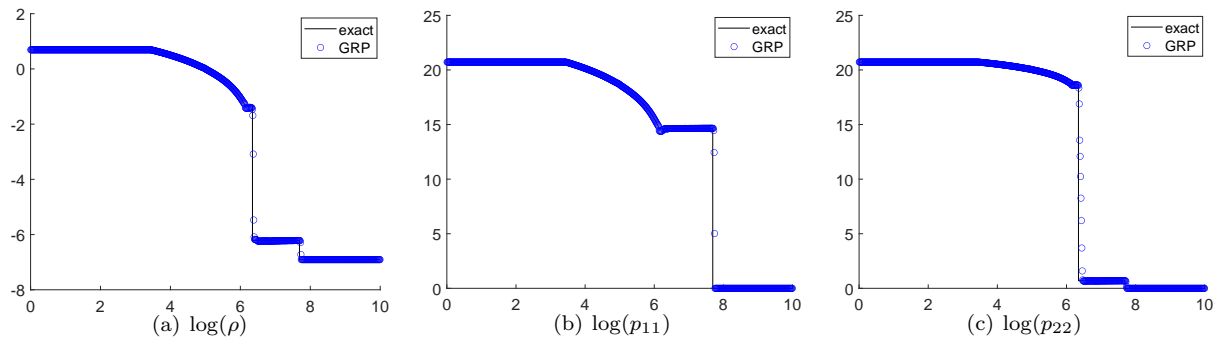


Figure 8: Example 6.4: The log plots of density  $\rho$  (left), the pressure components  $p_{11}$  (middle) and  $p_{22}$  (right) for the Leblanc problem obtained by the GRP scheme with the minmod slope limiter and  $\theta = 1.8$  on 800 uniform cells.

**Example 6.5. Shu-Osher problem**

The Shu-Osher problem of the ten-moment equations is considered, and it is an extension of the Shu-Osher

problem of the Euler equations [41]. The initial solution is given by

$$(\rho, u_1, u_2, p_{11}, p_{12}, p_{22}) = \begin{cases} (3.857143, 2.629369, 0, 10.33333, 0, 10.33333), & x \leq -4, \\ (1 + 0.2 \sin(5x), 0, 0, 1, 0, 1), & x > -4. \end{cases}$$

The computational interval is taken as  $[-5, 5]$ . The outflow boundary conditions are imposed. This problem is simulated until the time  $t = 1.4$  on a mesh with 800 cells. Figure 9 displays the numerical solutions. The reference solutions are obtained by the GRP scheme with 10000 cells.

To observe all the waves clearly, the plots of the reference solutions  $\rho$ ,  $u_1$ ,  $p_{11}$  and  $p_{22}$  are presented together in Figure 10, where the plots of  $p_{11}$  and  $p_{22}$  translate downward by 10 and 8 units, respectively. One can observe that there are three right-going shock waves near  $x = -4.68$ ,  $x = -3.61$  and  $x = 3.40$ , respectively, and a contact discontinuity near  $x = -0.69$ . In the regions between these locations, the solutions are smooth. From Figure 9, one can see that the GRP scheme captures these waves well and resolves the shock waves with high resolution on the mesh with 800 cells.

Moreover, one can find that the pressure component  $p_{11}$  is continuous across the contact discontinuity, but its slope changes. This phenomenon is reasonable. At this moment, the material derivative  $\frac{Du_1}{Dt}$  is non-trivial near the contact discontinuity, and the density has a jump across the contact discontinuity, so by (2.7), one knows that  $\frac{\partial p_{11}}{\partial x}$  takes different values at the left and right side of the contact discontinuity.

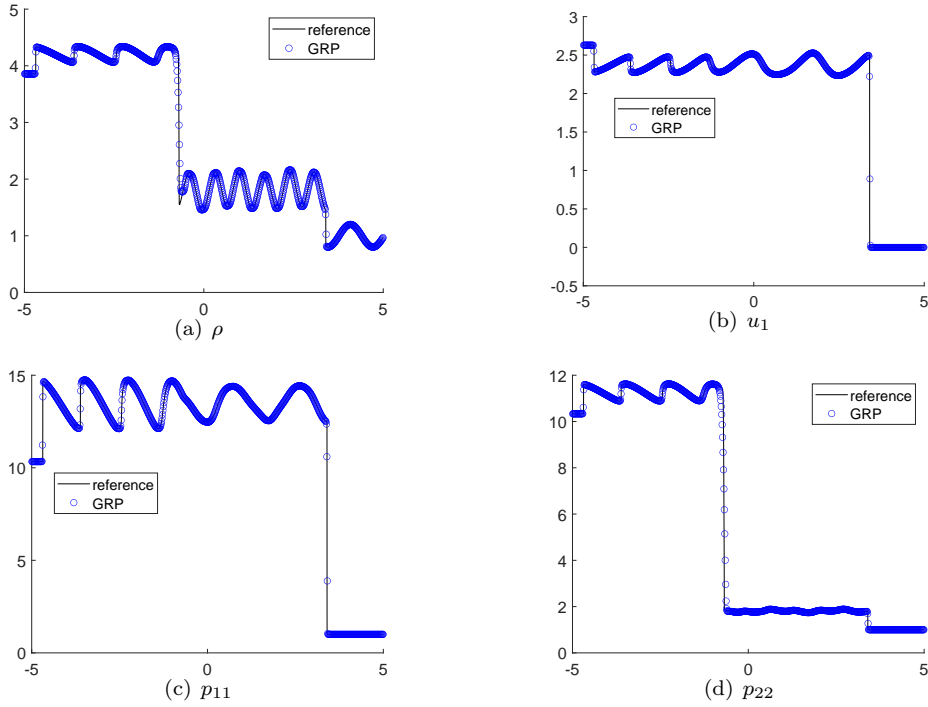


Figure 9: Example 6.5: The numerical solutions of the GRP scheme on 800 uniform cells for Shu-Osher problem.

### Example 6.6. 2D Riemann problems

In this example, four 2D Riemann problems are constructed for the first time to verify the performance of the proposed GRP schemes. The domain is taken as  $[0, 1]^2$  with the outflow boundary conditions. The initial discontinuities are located on the line  $x = 0.5$  for the  $x$ -direction and on the line  $y = 0.5$  for the  $y$ -direction. Hence, the domain is divided into four subdomains, which are counterclockwise denoted by I, II, III and IV as depicted in Figure 11. The proposed GRP scheme will be applied to simulate these four problems on a mesh of  $200 \times 200$  cells up to different final time.

(i) 2D Riemann problem 1:

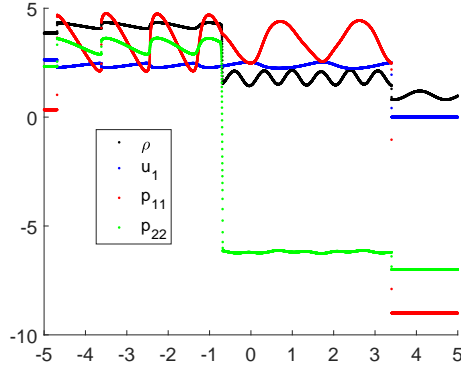


Figure 10: Example 6.5: The comparison of the reference solutions  $\rho$ ,  $u_1$ ,  $p_{11}$  and  $p_{22}$  for Shu-Osher problem.

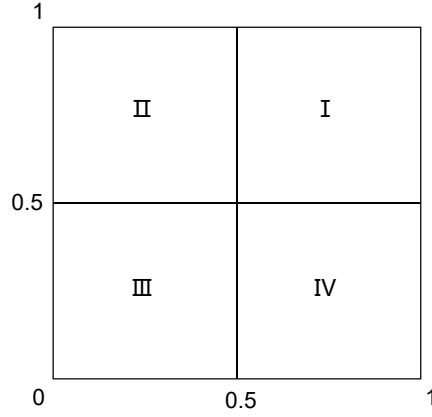


Figure 11: The partition of the domain for the 2D Riemann problems in Example 6.6.

$$(\rho, u_1, u_2, p_{11}, p_{12}, p_{22}) = \begin{cases} (1, 0.8939, 0.8939, 1.0541337, 0, 1.0541337), & 0.5 < x < 1, 0.5 < y < 1, \\ (1.0541337, 0.8939, 0.8, 1.0541337, 0, 1.1716956), & 0 < x < 0.5, 0.5 < y < 1, \\ (1, 0.8939, 0.8939, 1, 0, 1), & 0 < x < 0.5, 0 < y < 0.5, \\ (1.0541337, 0.8, 0.8939, 1.1716956, 0, 1.0541337), & 0.5 < x < 1, 0 < y < 0.5. \end{cases} \quad (6.4)$$

For this problem, all the possible local wave patterns are elaborated as follows:

- Between II and I: The wave shown by  $\rho$  is a right-going contact discontinuity.  $u_1$  and  $p_{11}$  keep constant. The waves shown by  $u_2$  and  $p_{12}$  both contain a left-going shock wave and a right-going shock wave. The waves shown by  $p_{22}$  include a left-going shock wave, a right-going contact discontinuity and a right-going shock wave. However, the two shock waves jumps observed in  $p_{22}$  are both small and approximately equal to 0.0022628.
- Between III and II:  $u_1$  and  $p_{12}$  are constants. The waves shown by  $\rho$ ,  $u_2$ ,  $p_{11}$  and  $p_{22}$  are all down-going shock waves.
- Between III and IV:  $u_2$  and  $p_{12}$  are constants. The waves shown by  $\rho$ ,  $u_1$ ,  $p_{11}$  and  $p_{22}$  are all left-going shock waves.
- Between IV and I: The wave shown by  $\rho$  is an up-going contact discontinuity.  $u_2$  and  $p_{22}$  keep constant. The waves shown by  $u_1$  and  $p_{12}$  both contain a down-going shock wave and an up-going shock wave. The waves shown by  $p_{11}$  include a down-going shock wave, an up-going contact discontinuity and an up-going shock wave. However, the jumps across the two shock waves shown by  $p_{11}$  are both small and approximately equal to 0.0022628.



This problem is simulated up to  $t = 0.15$ . The plots with 40 equally spaced contour lines of the primitive variables are presented in Figure 12. From Figures 12(d) and 12(f), it seems that the shock waves shown by  $p_{11}$  and  $p_{22}$  are lost. It is due to their small shock jumps and only 40 contour lines being displayed. Actually, if setting many more equally spaced contour lines, the shock waves in  $p_{11}$  and  $p_{22}$  can be viewed, see Figure 13.

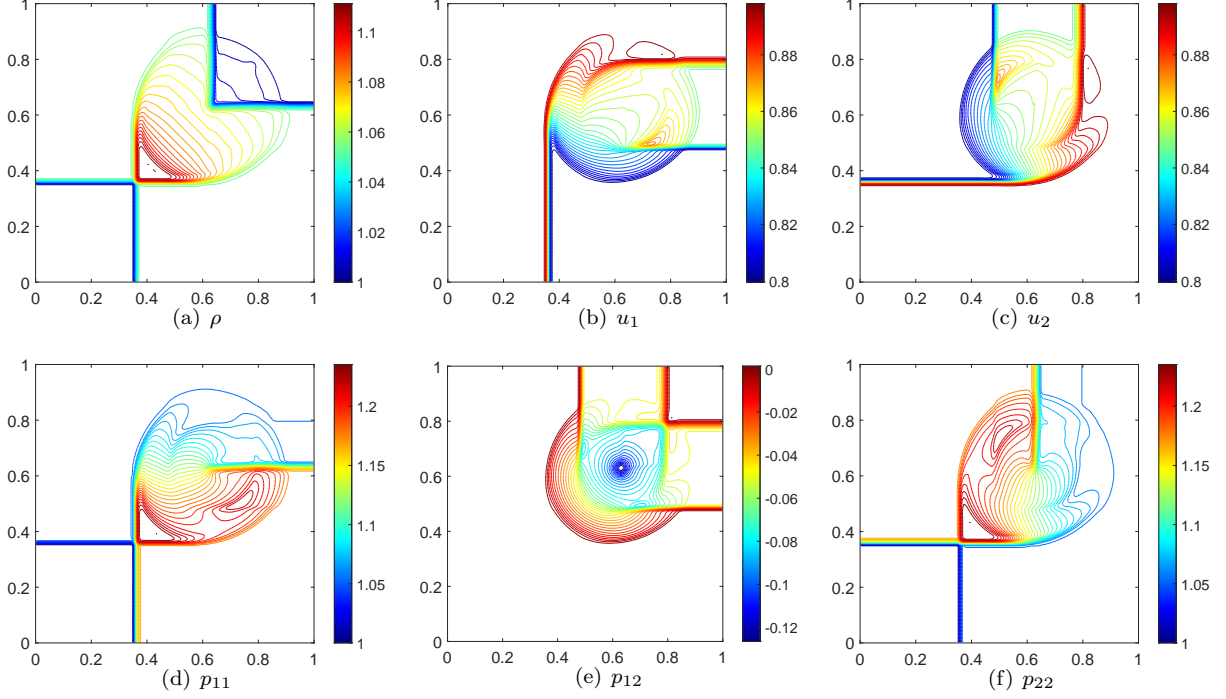


Figure 12: Example 6.6: The contour plots of solutions obtained by the GRP scheme for the 2D Riemann problem (6.4) on a mesh of  $200 \times 200$  cells. 40 equally spaced contour lines are displayed.

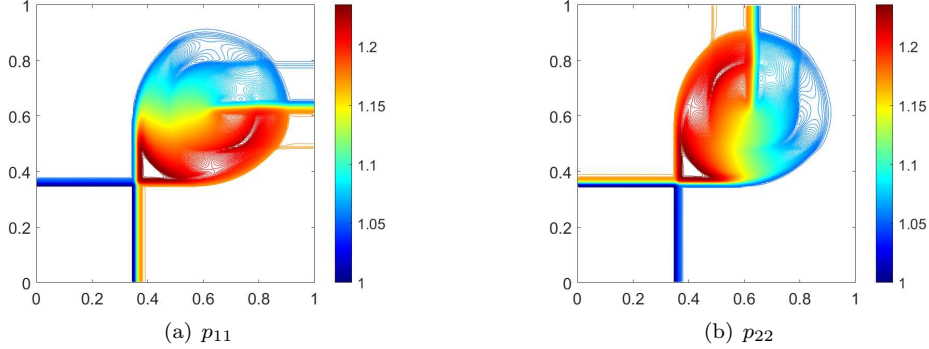


Figure 13: Example 6.6: The contour plots of  $p_{11}$  and  $p_{22}$  obtained by the GRP scheme for the 2D Riemann problem (6.4) on a mesh of  $200 \times 200$  cells. 400 equally spaced contour lines are displayed.

(ii) 2D Riemann problem 2:

$$(\rho, u_1, u_2, p_{11}, p_{12}, p_{22}) = \begin{cases} (1, 0.75, -0.5, 1, 0.5, 1), & 0.5 < x < 1, 0.5 < y < 1, \\ (1, 0.75, 0.5, 1, -0.5, 1), & 0 < x < 0.5, 0.5 < y < 1, \\ (1, -0.25, 0.5, 1, 0.5, 1), & 0 < x < 0.5, 0 < y < 0.5, \\ (1, -0.25, -0.5, 1, -0.5, 1), & 0.5 < x < 1, 0 < y < 0.5. \end{cases} \quad (6.5)$$

For this problem, the local wave patterns are demonstrated as follows:

- Between II and I:  $\rho$ ,  $u_1$ ,  $p_{11}$  and  $p_{22}$  are all constants. Two waves in  $u_2$  and  $p_{12}$  are the left-going shear waves.

- Between III and II:  $\rho$ ,  $u_2$ ,  $p_{11}$  and  $p_{22}$  are all constants. Two waves in  $u_1$  and  $p_{12}$  are the down-going shear waves.
- Between III and IV:  $\rho$ ,  $u_1$ ,  $p_{11}$  and  $p_{22}$  are all constants. Two waves in  $u_2$  and  $p_{12}$  are the right-going shear waves.
- Between IV and I:  $\rho$ ,  $u_2$ ,  $p_{11}$  and  $p_{22}$  are all constants. Two waves in  $u_1$  and  $p_{12}$  are the up-going shear waves.

The final time is  $t = 0.15$ . The contour plots with 40 equally spaced contour lines are illustrated in Figure 14.

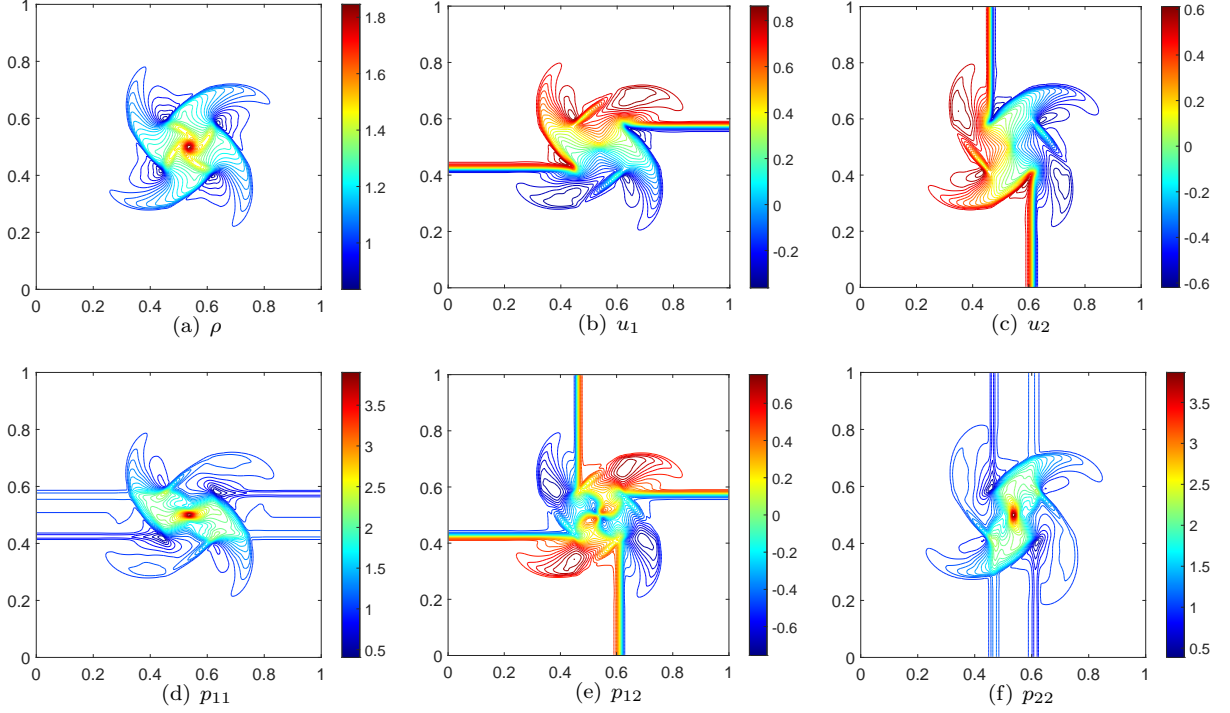


Figure 14: Example 6.6: The contour plots of solutions obtained by the GRP scheme for the 2D Riemann problem (6.5) on a mesh of  $200 \times 200$  cells. 40 equally spaced contour lines are displayed.

(iii) 2D Riemann problem 3:

$$(\rho, u_1, u_2, p_{11}, p_{12}, p_{22}) = \begin{cases} (1, -0.5, -0.5, 1, 0, 1), & 0.5 < x < 1, 0.5 < y < 1, \\ (0.9422650, -0.6, -0.5, 0.8366024, 0, 0.9422650), & 0 < x < 0.5, 0.5 < y < 1, \\ (1, -0.5, -0.5, 0.9422650, 0, 0.9422650), & 0 < x < 0.5, 0 < y < 0.5, \\ (0.9422650, -0.5, -0.6, 0.9422650, 0, 0.8366024), & 0.5 < x < 1, 0 < y < 0.5. \end{cases} \quad (6.6)$$

For this problem, all the possible local wave patterns are detailed as follows:

- Between II and I:  $u_2$  and  $p_{12}$  are constants. All waves shown in  $\rho$ ,  $u_1$ ,  $p_{11}$  and  $p_{22}$  are the right-going rarefaction waves.
- Between III and II: The wave shown in  $\rho$  is a down-going contact discontinuity.  $u_2$  and  $p_{22}$  keep constant. The waves shown in  $u_1$  and  $p_{12}$  both contain a down-going shock wave and an up-going shock wave. The waves in  $p_{11}$  include a down-going shock wave, an up-going contact discontinuity and an up-going shock wave. However, the two shock wave jumps in  $p_{11}$  are both small and approximately equal to 0.0024262.
- Between III and IV: The wave in  $\rho$  is a left-going contact discontinuity.  $u_1$  and  $p_{11}$  keep constant. The waves in both  $u_2$  and  $p_{12}$  contain a left-going shock wave and a right-going shock wave. The waves in

$p_{22}$  include a left-going shock wave, a right-going contact discontinuity and a right-going shock wave. However, both two shock wave jumps in  $p_{22}$  are small and approximately equal to 0.0024262.

- Between IV and I:  $u_1$  and  $p_{12}$  are constants. All waves in  $\rho$ ,  $u_2$ ,  $p_{11}$  and  $p_{22}$  are the up-going rarefaction waves.

This problem is simulated up to  $t = 0.2$ . The contour plots with 40 equally spaced lines are presented in Figure 15. Similar with the 2D Riemann problem 1, due to the small shock jumps and only 40 contour lines being displayed, the shock waves in  $p_{11}$  and  $p_{22}$  seem to miss in Figures 15(d) and 15(f), which can be viewed by spacing many more contour lines as depicted in Figure 16.

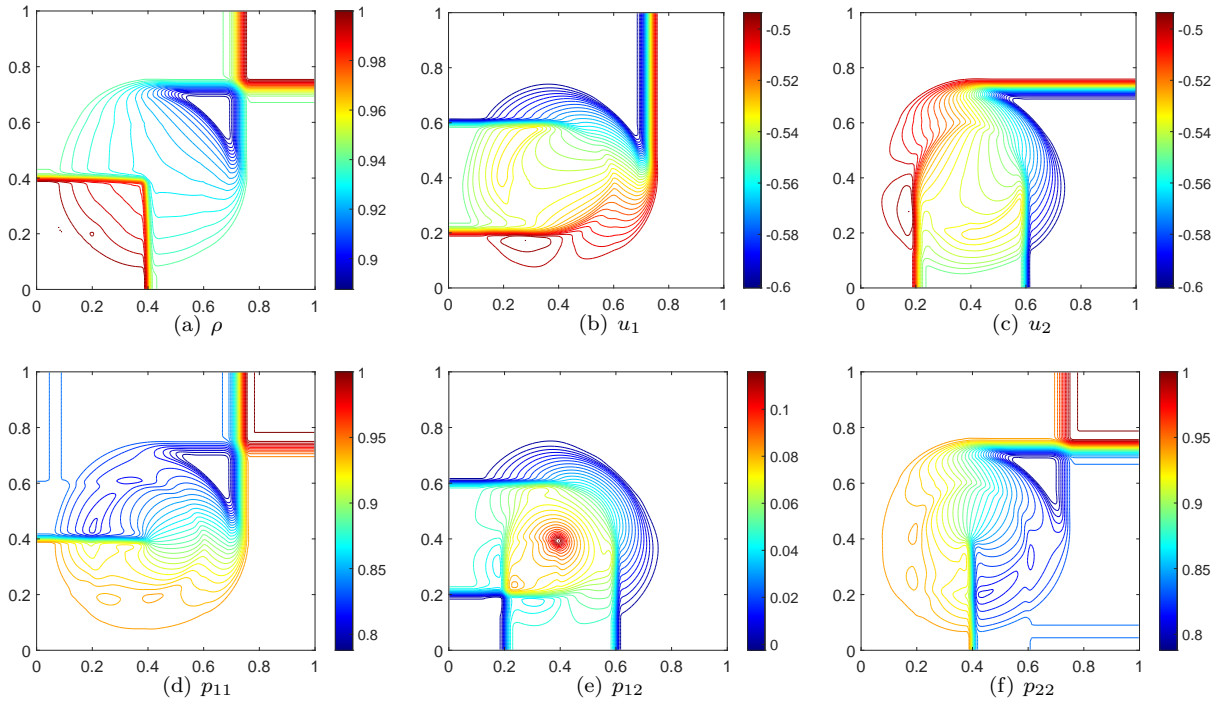


Figure 15: Example 6.6: The contour plots of solutions obtained by the GRP scheme for the 2D Riemann problem (6.6) on a mesh of  $200 \times 200$  cells. 40 equally spaced contour lines are displayed.

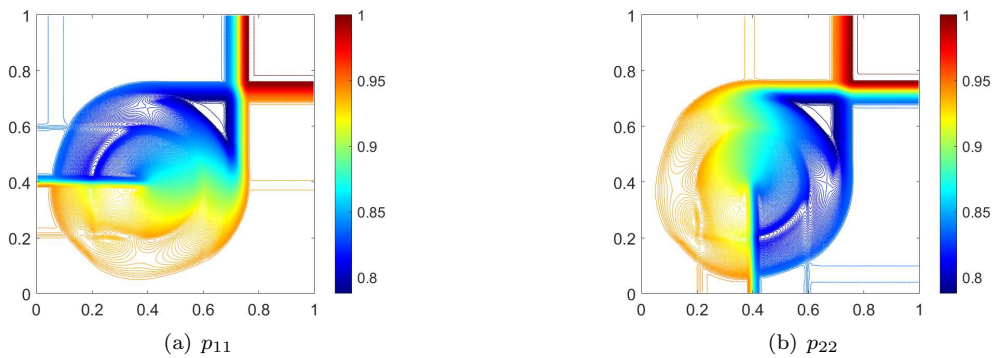


Figure 16: Example 6.6: The contour plots of  $p_{11}$  and  $p_{22}$  obtained by the GRP scheme for the 2D Riemann problem (6.6) on a mesh of  $200 \times 200$  cells. 400 equally spaced contour lines are displayed.

(iv) 2D Riemann problem 4:

$$(\rho, u_1, u_2, p_{11}, p_{12}, p_{22}) = \begin{cases} (1.0909, 0, 0, 1.0909, 0, 1.0909), & 0.5 < x < 1, 0.5 < y < 1, \\ (0.5065, 1.2024, 0, 0.3499, 0, 0.3499), & 0 < x < 0.5, 0.5 < y < 1, \\ (1.0909, 1.2024, 1.2024, 1.0909, 0, 1.0909), & 0 < x < 0.5, 0 < y < 0.5, \\ (0.5065, 0, 1.2024, 0.3499, 0, 0.3499), & 0.5 < x < 1, 0 < y < 0.5. \end{cases} \quad (6.7)$$

For this problem, all the possible local wave patterns are elaborated as follows:

- Between II and I: The waves in  $\rho$ ,  $u_1$ ,  $p_{11}$  and  $p_{22}$  all contain a left-going shock wave and a right-going shock wave. Besides, the waves in  $\rho$  and  $p_{22}$  both contain a right-going contact discontinuity.  $u_2$  and  $p_{12}$  are constants.
- Between III and II: All waves in  $\rho$ ,  $u_2$ ,  $p_{11}$  and  $p_{22}$  contain a down-going shock wave and an up-going shock wave. Besides, the waves in both  $\rho$  and  $p_{11}$  contain an up-going contact discontinuity.  $u_1$  and  $p_{12}$  are constants.
- Between III and IV: The wave patterns are similar with those between II and I.
- Between IV and I: The wave patterns are similar with those between III and II.

The final time is  $t = 0.15$ . The plots with 40 equally spaced contour lines of the primitive variables are presented in Figure 17.

From the above numerical results for the four 2D Riemann problems, one can find that the proposed GRP scheme obtains satisfactory results and captures these waves well, which include the shock wave, the rarefaction wave, the shear wave, the contact discontinuity and their interactions.

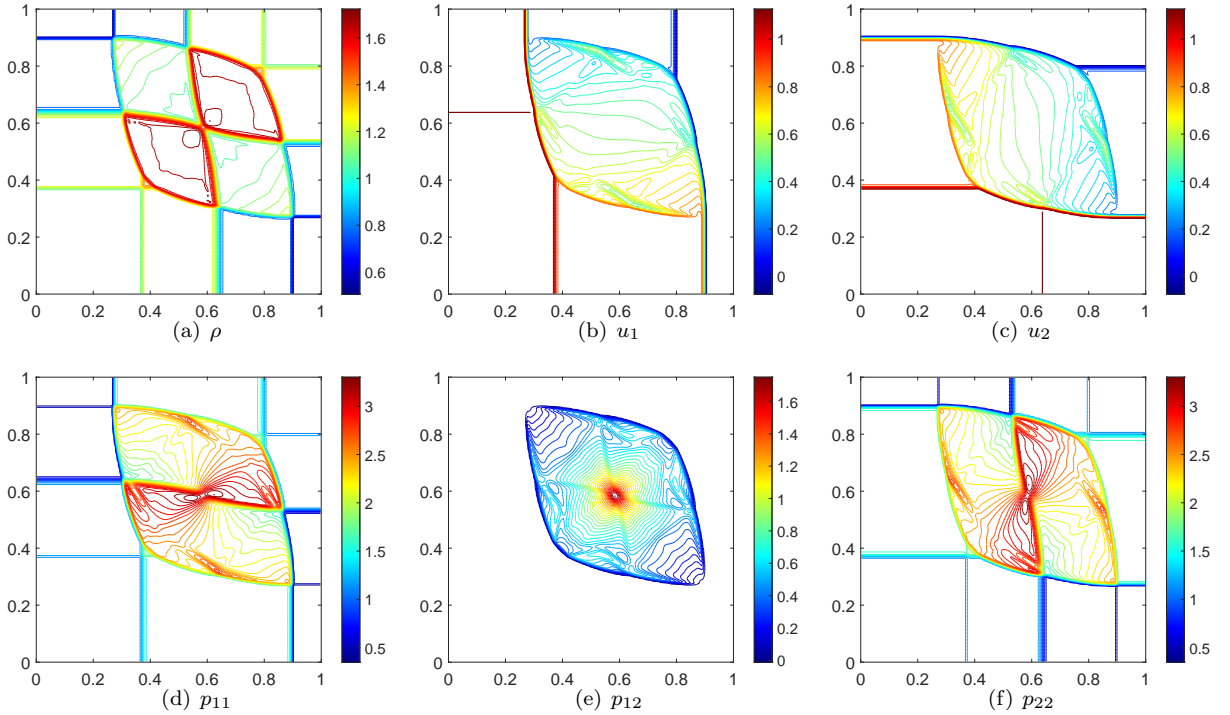


Figure 17: Example 6.6: The contour plots of solutions obtained by the GRP scheme for the 2D Riemann problem (6.7) on a mesh of  $200 \times 200$  cells. 40 equally spaced contour lines are displayed.

**Example 6.7.** *Uniform plasma state with 2D Gaussian source*

This test is applied to evaluate the influence of a Gaussian source term on a 2D plasma model [31, 39, 32]. The plasma is initially in a uniform state given by

$$(\rho, u_1, u_2, p_{11}, p_{12}, p_{22}) = (0.1, 0, 0, 9, 7, 9),$$

with the potential

$$W(x, y) = 25 \exp(-200((x-2)^2 + (y-2)^2))$$

over the spatial domain  $[0, 4]^2$ . The outflow boundary conditions are imposed. Figure 18 presents the numerical results at  $t = 0.1$ , obtained by the GRP scheme on a mesh consisting of  $200 \times 200$  cells. One can observe the anisotropic changes in the density due to the Gaussian source's influence.

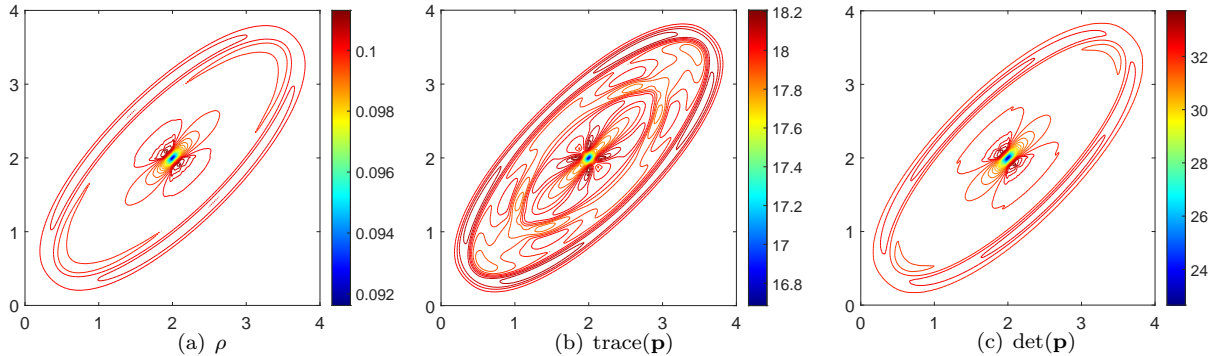


Figure 18: Example 6.7: The contour plots of the uniform plasma state with Gaussian source at time  $t = 0.1$  on a mesh of  $200 \times 200$  cells. 40 equally spaced contour lines are displayed.

**Example 6.8.** *Realistic simulation in two dimensions*

In this example [7, 31, 32], a plasma state within the domain  $[0, 100]^2$ , initially defined by

$$(\rho, u_1, u_2, p_{11}, p_{12}, p_{22}) = (0.109885, 0, 0, 1, 0, 1),$$

is examined. The potential is taken as

$$W(x, y) = \exp\left(\frac{-(x-50)^2 - (y-50)^2}{100}\right),$$

which exerts an influence solely in the  $x$ -direction with  $\mathbf{S}^y(\mathbf{U}) = 0$ . Outflow boundary conditions are implemented.

This problem originally aimed to study the effects of inverse Bremsstrahlung absorption (IBA) [7]. To simulate the IBA in an anisotropic plasma, we augment the energy equation for component  $E_{11}$  with an additional source term,  $v_T \rho W$ , where  $v_T$  denotes the absorption coefficient with  $v_T$  values of 0, 0.5, and 1.

By employing the GRP scheme, this problem is simulated up to  $t = 0.5$  on a mesh with  $200 \times 200$  cells. Figure 19 shows contour plots of  $\rho$ ,  $\text{trace}(\mathbf{p})$ , and  $\det(\mathbf{p})$  for  $v_T = 0.5$ . Figure 20 illustrates the 1D profiles of  $\rho$  and  $p_{11}$  along the line  $y = 50$ . An increase in the absorption coefficient,  $v_T$ , is observed to raise the pressure component  $p_{11}$  around the center. This, in turn, drives a more pronounced expulsion of particles from the region, leading to a reduction in density near the center. These observations are consistent with the results documented in [31, 39, 32].

**7. Conclusion**

This paper developed the second-order accurate direct Eulerian generalized Riemann problem (GRP) scheme for the ten-moment Gaussian closure equations with source terms. The generalized Riemann invariants associated with the rarefaction waves, the contact discontinuity and the shear waves are given, and the 1D exact

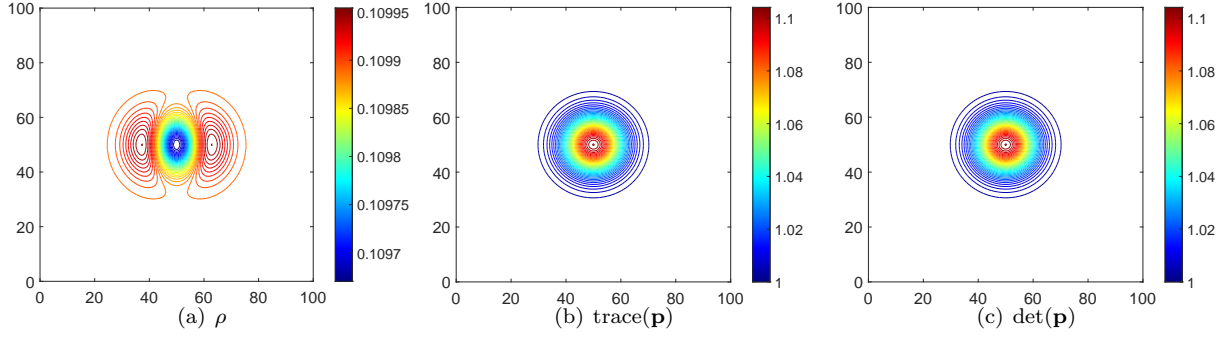


Figure 19: Example 6.8: The contour plots of the realistic simulation at time  $t = 0.5$  on the meshes of  $200 \times 200$  cells. 40 equally spaced contour lines are displayed.

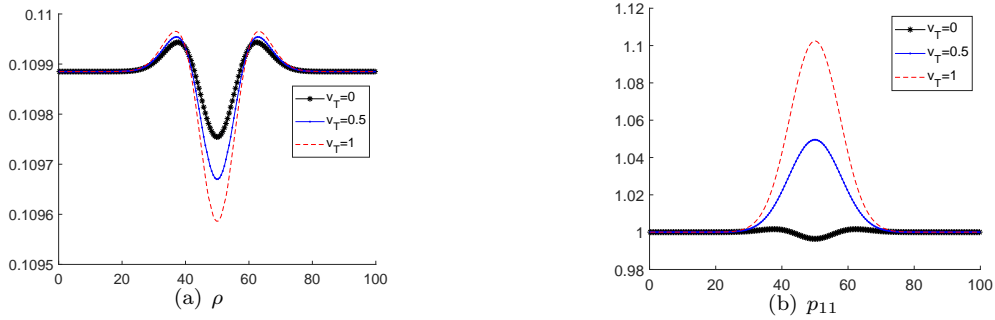


Figure 20: Example 6.8: Comparison of  $\rho$  and  $p_{11}$  for different absorption coefficient  $v_T = 0$ ,  $v_T = 0.5$  and  $v_T = 1$  along the line  $y = 50$ .

Riemann solver was obtained for the homogeneous system based on the characteristic analysis. By directly using two main ingredients, the generalized Riemann invariants and the Rankine-Hugoniot jump conditions, the left and right nonlinear waves of the local GRP were resolved in the Eulerian formulation, and the limiting values of the time derivatives of the primitive variables along the cell interface were also obtained. It was noted that compared to some other systems, such as the Euler equations [5], the shallow water equations [23], the radiation hydrodynamical equations [19] and the blood flow model [40] and so on, there were more physical variables and two more elementary waves (the left and right shear waves) for the ten-moment equations, which made the derivation of the GRP scheme much more complicated and nontrivial. Four 2D Riemann problems were constructed for the first time to verify the performance of the proposed GRP schemes. Some 1D and 2D numerical experiments were employed to demonstrate the accuracy and high resolution of the proposed GRP scheme.

## Acknowledgements

The works were supported by the National Key R&D Program of China (Project Number 2020YFA0712000 & 2020YFE0204200), and the National Natural Science Foundation of China (Nos. 12171227, 12326314, & 12288101).

## Appendix A. The right eigenvector matrix.

The right eigenvector matrix of the Jacobian matrix  $\frac{\partial \mathbf{F}(\mathbf{U})}{\partial \mathbf{U}}$  used in this paper is given by

$$\mathbf{R}(\mathbf{U}) = \begin{pmatrix} 0 & 2 & 0 & 2\rho p_{11} & 0 & 2\rho p_{11} \\ 0 & 2u_1 & 0 & -2p_{11}\sqrt{\rho}M_1 & 0 & 2p_{11}\sqrt{\rho}M_3 \\ 0 & 2u_2 & \sqrt{\rho p_{11}} & -2\sqrt{\rho p_{11}}M_2 & \sqrt{\rho p_{11}} & 2\sqrt{\rho p_{11}}M_4 \\ 0 & u_1^2 & 0 & p_{11}M_1^2 & 0 & p_{11}M_3^2 \\ 0 & u_1u_2 & \frac{1}{2}(u_1\sqrt{\rho p_{11}} - p_{11}) & \sqrt{p_{11}}M_1M_2 & \frac{1}{2}(u_1\sqrt{\rho p_{11}} + p_{11}) & \sqrt{p_{11}}M_3M_4 \\ 1 & u_2^2 & u_2\sqrt{\rho p_{11}} - p_{12} & M_2^2 + \det(\mathbf{p}) & u_2\sqrt{\rho p_{11}} + p_{12} & M_4^2 + \det(\mathbf{p}) \end{pmatrix},$$

where  $M_1 := \sqrt{3p_{11}} - u_1\sqrt{\rho}$ ,  $M_2 := \sqrt{3p_{12}} - u_2\sqrt{\rho p_{11}}$ ,  $M_3 := \sqrt{3p_{11}} + u_1\sqrt{\rho}$ , and  $M_4 := \sqrt{3p_{12}} + u_2\sqrt{\rho p_{11}}$ .

## Appendix B. Computing $\left(\frac{\partial u_1}{\partial t}\right)_{*K}$ , $\left(\frac{\partial p_{11}}{\partial t}\right)_{*K}$ and $\left(\frac{\partial \rho}{\partial t}\right)_{*K}$ ( $K = L, R$ ) for all possible cases.

In Subsection 5.1.1, only the case that the 1-rarefaction wave and the 6-shock wave is considered. Here, the computations of  $\left(\frac{\partial u_1}{\partial t}\right)_{*K}$ ,  $\left(\frac{\partial p_{11}}{\partial t}\right)_{*K}$  and  $\left(\frac{\partial \rho}{\partial t}\right)_{*K}$  for all possible cases are directly presented.

One can solve the following system

$$\begin{cases} a_1 \left(\frac{\mathcal{D}u_1}{\mathcal{D}t}\right)_* + b_1 \left(\frac{\mathcal{D}p_{11}}{\mathcal{D}t}\right)_* = d_1, \\ a_2 \left(\frac{\mathcal{D}u_1}{\mathcal{D}t}\right)_* + b_2 \left(\frac{\mathcal{D}p_{11}}{\mathcal{D}t}\right)_* = d_2, \end{cases}$$

to obtain the values of  $\left(\frac{\mathcal{D}u_1}{\mathcal{D}t}\right)_*$  and  $\left(\frac{\mathcal{D}p_{11}}{\mathcal{D}t}\right)_*$ , where

$$(a_1, b_1, d_1) = \begin{cases} (a_L^{\text{rare}}, b_L^{\text{rare}}, d_L^{\text{rare}}), & \text{1-rarefaction,} \\ (a_L^{\text{shock}}, b_L^{\text{shock}}, d_L^{\text{shock}}), & \text{1-shock,} \end{cases} \quad (a_2, b_2, d_2) = \begin{cases} (a_R^{\text{rare}}, b_R^{\text{rare}}, d_R^{\text{rare}}), & \text{6-rarefaction,} \\ (a_R^{\text{shock}}, b_R^{\text{shock}}, d_R^{\text{shock}}), & \text{6-shock.} \end{cases} \quad (\text{B.1})$$

Then utilizing (2.8) gives the values of  $\left(\frac{\partial u_1}{\partial t}\right)_{*K}$  and  $\left(\frac{\partial p_{11}}{\partial t}\right)_{*K}$  with  $K = L, R$ . The  $(a_K^{\text{rare}}, b_K^{\text{rare}}, d_K^{\text{rare}})$  and  $(a_K^{\text{shock}}, b_K^{\text{shock}}, d_K^{\text{shock}})$  ( $K = L, R$ ) in (B.1) are taken as

$$\begin{aligned} a_K^{\text{rare}} &= 1 + \delta_K \frac{u_{1,*}}{c_{*K}}, \quad b_K^{\text{rare}} = \frac{u_{1,*}}{3p_{11,*}} + \frac{\delta_K}{\rho_{*K}c_{*K}}, \\ d_K^{\text{rare}} &= \left[ \delta_K \frac{\rho_K^2 S'_{1,K}}{8c_{*K}^3} (3c_{*K}^2 + c_K^2) - (u_{1,K} + \delta_K c_K) \right] (u_{1,K} + \delta_K c_K) - \frac{1}{2} \left( 1 + \delta_K \frac{u_{1,*}}{c_{*K}} \right) W_x(0), \\ a_K^{\text{shock}} &= 1 + \delta_K \rho_{*K} (u_{1,*} - \sigma_K) \cdot \Phi_1^K, \quad b_K^{\text{shock}} = \frac{u_{1,*} - \sigma_K}{3p_{11,*}} + \delta_K \cdot \Phi_1^K, \\ d_K^{\text{shock}} &= L_\rho^K \cdot \rho'_K + L_{u_1}^K \cdot u'_{1,K} + L_{p_{11}}^K \cdot p'_{11,K} - \frac{1}{2} W_x(0) \cdot L_W^K, \end{aligned}$$

where

$$\begin{aligned} \delta_K &= \begin{cases} 1, & \text{if } K = L, \\ -1, & \text{if } K = R, \end{cases} \\ \sigma_K &= \frac{\rho_{*K} u_{1,*} - \rho_L u_{1,L}}{\rho_{*K} - \rho_K}, \quad \Phi_i^K = \Phi_i(p_{11,*}; p_{11,K}, \rho_K), \quad i = 1, 2, 3, \\ L_\rho^K &= -\delta_K (\sigma_K - u_{1,K}) \cdot \Phi_3^K, \quad L_{u_1}^K = \sigma_K - u_{1,K} + 3\delta_K p_{11,K} \cdot \Phi_2^K + \delta_K \rho_K \cdot \Phi_3^K, \\ L_{p_{11}}^K &= -\frac{1}{\rho_K} - \delta_K (\sigma_K - u_{1,K}) \cdot \Phi_2^K, \quad L_W^K = \delta_K \rho_{*K} (u_{1,*} - \sigma_K) \cdot \Phi_1^K + 1. \end{aligned}$$

The expressions of the functions  $\Phi_i$  ( $i = 1, 2, 3$ ) are given in (5.41).

For the 1-shock wave,  $\left(\frac{\partial \rho}{\partial t}\right)_{*L}$  is computed by

$$g_\rho^L \cdot \left(\frac{\partial \rho}{\partial t}\right)_{*L} + g_{u_1}^L \cdot \left(\frac{\mathcal{D}u_1}{\mathcal{D}t}\right)_* + g_{p_{11}}^L \cdot \left(\frac{\mathcal{D}p_{11}}{\mathcal{D}t}\right)_* = u_{1,*} \cdot f_L,$$

where

$$g_\rho^L = u_{1,*} - \sigma_L, \quad g_{u_1}^L = \rho_{*L} u_{1,*} (\sigma_L - u_{1,*}) \cdot H_1^L, \quad g_{p_{11}}^L = \frac{\sigma_L}{c_{*L}^2} - u_{1,*} \cdot H_1^L,$$

$$f_L = (\sigma_L - u_{1,L}) \cdot H_2^L \cdot p'_{11,L} + (\sigma_L - u_{1,L}) \cdot H_3^L \cdot \rho'_L - \rho_L (H_3^L + c_L^2 \cdot H_2^L) \cdot u'_{1,L} - \frac{1}{2} \rho_{*L} (\sigma_L - u_{1,*}) W_x(0) \cdot H_1^L$$

with  $H_i^L = H_i(p_{11,*}; p_{11,L}, \rho_L)$  ( $i = 1, 2, 3$ ). The expressions of the functions  $H_i$  ( $i = 1, 2, 3$ ) are given in (5.49).

For the 1-rarefaction wave,  $\left(\frac{\partial \rho}{\partial t}\right)_{*L}$  is given by (5.47).

For the 6-rarefaction wave, one has

$$\left(\frac{\partial \rho}{\partial t}\right)_{*R} = \frac{1}{c_{*R}^2} \left[ \left(\frac{\partial p_{11}}{\partial t}\right)_{*R} + \rho_R^2 S'_{1,R} \rho_{*R} u_{1,*} \frac{c_{*R}^3}{c_R^3} \right].$$

For the 6-shock wave,  $\left(\frac{\partial \rho}{\partial t}\right)_{*R}$  is given by (5.48).

### Appendix C. Computing $\left(\frac{\partial u_2}{\partial t}\right)_{*L}$ , $\left(\frac{\partial p_{12}}{\partial t}\right)_{*L}$ and $\left(\frac{\partial p_{22}}{\partial t}\right)_{*L}$ for the 1-shock wave.

For the 1-shock wave, one can first solve the system

$$\begin{cases} a_{3,L} \left(\frac{\mathcal{D}u_2}{\mathcal{D}t}\right)_{*L} + b_{3,L} \left(\frac{\mathcal{D}p_{12}}{\mathcal{D}t}\right)_{*L} = d_{3,L}, \\ a_{4,L} \left(\frac{\mathcal{D}u_2}{\mathcal{D}t}\right)_{*L} + b_{4,L} \left(\frac{\mathcal{D}p_{12}}{\mathcal{D}t}\right)_{*L} = d_{4,L}, \end{cases}$$

to get the values of  $\left(\frac{\mathcal{D}u_2}{\mathcal{D}t}\right)_{*L}$  and  $\left(\frac{\mathcal{D}p_{12}}{\mathcal{D}t}\right)_{*L}$ , then substituting them into (2.11) gives the values of  $\left(\frac{\partial u_2}{\partial t}\right)_{*L}$  and  $\left(\frac{\partial p_{12}}{\partial t}\right)_{*L}$ . In the above system,

$$\begin{aligned} a_{3,L} &= 2\rho_{*L}(u_{1,*} - \sigma_L), & a_{4,L} &= E_{11,*L} + \rho_{*L}(u_{1,*} - \sigma_L)^2 - \frac{1}{2}\rho_{*L}\sigma_L^2, \\ b_{3,L} &= 1 + \frac{\rho_{*L}(u_{1,*} - \sigma_L)^2}{p_{11,*}}, & b_{4,L} &= \left(E_{11,*L} - \frac{1}{2}\rho_{*L}u_{1,*}\sigma_L\right) \frac{u_{1,*} - \sigma_L}{p_{11,*}} + u_{1,*} - \frac{1}{2}\sigma_L, \\ d_{3,L} &= \frac{\mathcal{D}_{\sigma_L}\Gamma_{m_{2,L}}}{\mathcal{D}t} + \rho_{*L}u_{2,*L} \frac{\mathcal{D}_{\sigma_L}\sigma_L}{\mathcal{D}t} - u_{2,*L}(u_{1,*} - \sigma_L) \left(\frac{\mathcal{D}_{\sigma_L}\rho}{\mathcal{D}t}\right)_{*L} - \rho_{*L}u_{2,*L} \left(\frac{\mathcal{D}_{\sigma_L}u_1}{\mathcal{D}t}\right)_{*L} \\ &\quad + \frac{2\rho_{*L}p_{12,*L}(u_{1,*} - \sigma_L)^2}{3p_{11,*}^2} \left(\frac{\mathcal{D}p_{11}}{\mathcal{D}t}\right)_*, \\ d_{4,L} &= \frac{\mathcal{D}_{\sigma_L}\Gamma_{E_{12,L}}}{\mathcal{D}t} + E_{12,*L} \frac{\mathcal{D}_{\sigma_L}\sigma_L}{\mathcal{D}t} - \frac{1}{2}u_{1,*}u_{2,*L}(u_{1,*} - \sigma_L) \left(\frac{\mathcal{D}_{\sigma_L}\rho}{\mathcal{D}t}\right)_{*L} - \frac{1}{2}u_{2,*L} \frac{\mathcal{D}_{\sigma_L}p_{11,*}}{\mathcal{D}t} \\ &\quad - \left(2E_{12,*L} - \frac{1}{2}\rho_{*L}u_{2,*L}\sigma_L\right) \left(\frac{\mathcal{D}_{\sigma_L}u_1}{\mathcal{D}t}\right)_{*L} + \left(E_{11,*L} - \frac{1}{2}\rho_{*L}u_{1,*}\sigma_L\right) \frac{2p_{12,*L}(u_{1,*} - \sigma_L)}{3p_{11,*}^2} \left(\frac{\mathcal{D}p_{11}}{\mathcal{D}t}\right)_*, \end{aligned}$$

where

$$\begin{aligned} \frac{\mathcal{D}_{\sigma_L}\Gamma_{m_{2,L}}}{\mathcal{D}t} &= u_{2,L}(u_{1,L} - \sigma_L) \frac{\mathcal{D}_{\sigma_L}\rho_L}{\mathcal{D}t} + \rho_L u_{2,L} \frac{\mathcal{D}_{\sigma_L}u_{1,L}}{\mathcal{D}t} + \rho_L (u_{1,L} - \sigma_L) \frac{\mathcal{D}_{\sigma_L}u_{2,L}}{\mathcal{D}t} + \frac{\mathcal{D}_{\sigma_L}p_{12,L}}{\mathcal{D}t} - \rho_L u_{2,L} \frac{\mathcal{D}_{\sigma_L}\sigma_L}{\mathcal{D}t}, \\ \frac{\mathcal{D}_{\sigma_L}\Gamma_{E_{12,L}}}{\mathcal{D}t} &= \frac{1}{2}u_{1,L}u_{2,L}(u_{1,L} - \sigma_L) \frac{\mathcal{D}_{\sigma_L}\rho_L}{\mathcal{D}t} + \left(2E_{12,L} - \frac{1}{2}\rho_L u_{2,L}\sigma_L\right) \frac{\mathcal{D}_{\sigma_L}u_{1,L}}{\mathcal{D}t} - E_{12,L} \frac{\mathcal{D}_{\sigma_L}\sigma_L}{\mathcal{D}t} \\ &\quad + \left(E_{11,L} - \frac{1}{2}\rho_L u_{1,L}\sigma_L\right) \frac{\mathcal{D}_{\sigma_L}u_{2,L}}{\mathcal{D}t} + \frac{1}{2}u_{2,L} \frac{\mathcal{D}_{\sigma_L}p_{11,L}}{\mathcal{D}t} + \left(u_{1,L} - \frac{1}{2}\sigma_L\right) \frac{\mathcal{D}_{\sigma_L}p_{12,L}}{\mathcal{D}t}, \end{aligned}$$



$$\begin{aligned}\frac{\mathcal{D}_{\sigma_L}\sigma_L}{\mathcal{D}t} &= \frac{\mathcal{D}_{\sigma_L}u_{1,L}}{\mathcal{D}t} + \frac{\sqrt{2p_{11,*} + p_{11,L}}}{2\rho_L\sqrt{\rho_L}} \frac{\mathcal{D}_{\sigma_L}\rho_L}{\mathcal{D}t} - \frac{1}{\sqrt{\rho_L}(2p_{11,*} + p_{11,L})} \frac{\mathcal{D}_{\sigma_L}p_{11,*}}{\mathcal{D}t} - \frac{1}{2\sqrt{\rho_L}(2p_{11,*} + p_{11,L})} \frac{\mathcal{D}_{\sigma_L}p_{11,L}}{\mathcal{D}t}, \\ \left(\frac{\mathcal{D}_{\sigma_L}\rho}{\mathcal{D}t}\right)_{*L} &= H_1^L \cdot \frac{\mathcal{D}_{\sigma_L}p_{11,*}}{\mathcal{D}t} + H_2^L \cdot \frac{\mathcal{D}_{\sigma_L}p_{11,L}}{\mathcal{D}t} + H_3^L \cdot \frac{\mathcal{D}_{\sigma_L}\rho_L}{\mathcal{D}t}, \quad \left(\frac{\mathcal{D}_{\sigma_L}u_1}{\mathcal{D}t}\right)_{*L} = \left(\frac{\partial u_1}{\partial t}\right)_{*L} - \frac{\sigma_L}{3p_{11,*}} \left(\frac{\mathcal{D}p_{11}}{\mathcal{D}t}\right)_{*}, \\ \frac{\mathcal{D}_{\sigma_L}p_{11,*}}{\mathcal{D}t} &= \left(\frac{\mathcal{D}p_{11}}{\mathcal{D}t}\right)_{*} - \rho_{*L}(\sigma_L - u_{1,*}) \left[ \left(\frac{\mathcal{D}u_1}{\mathcal{D}t}\right)_{*} + \frac{1}{2}W_x(0) \right],\end{aligned}$$

with

$$\begin{aligned}\frac{\mathcal{D}_{\sigma_L}\rho_L}{\mathcal{D}t} &= (\sigma_L - u_{1,L})\rho'_L - \rho_L u'_{1,L}, \quad \frac{\mathcal{D}_{\sigma_L}u_{1,L}}{\mathcal{D}t} = (\sigma_L - u_{1,L})u'_{1,L} - \frac{p'_{11,L}}{\rho_L} - \frac{1}{2}W_x(0), \\ \frac{\mathcal{D}_{\sigma_L}u_{2,L}}{\mathcal{D}t} &= (\sigma_L - u_{1,L})u'_{2,L} - \frac{p'_{12,L}}{\rho_L}, \quad \frac{\mathcal{D}_{\sigma_L}p_{11,L}}{\mathcal{D}t} = (\sigma_L - u_{1,L})p'_{11,L} - 3p_{11,L}u'_{1,L}, \\ \frac{\mathcal{D}_{\sigma_L}p_{12,L}}{\mathcal{D}t} &= (\sigma_L - u_{1,L})p'_{12,L} - 2p_{12,L}u'_{1,L} - p_{11,L}u'_{2,L}.\end{aligned}$$

The value of  $\left(\frac{\partial p_{22}}{\partial t}\right)_{*L}$  is computed by

$$g_{p_{22}}^{*L} \left(\frac{\partial p_{22}}{\partial t}\right)_{*L} = f_{p_{22}}^{*L},$$

where

$$\begin{aligned}g_{p_{22}}^{*L} &= \frac{1}{2}(u_{1,*} - \sigma_L)^2, \\ f_{p_{22}}^{*L} &= u_{1,*}\tilde{f}_{p_{22}}^{*L} - \frac{(p_{11,*}p_{22,*L} - 4p_{12,*L}^2)(u_{1,*} - \sigma_L)\sigma_L}{6p_{11,*}^2} \left(\frac{\mathcal{D}p_{11}}{\mathcal{D}t}\right)_{*} - \frac{p_{12,*L}\sigma_L(u_{1,*} - \sigma_L)}{p_{11,*}} \left(\frac{\mathcal{D}p_{12}}{\mathcal{D}t}\right)_{*L}, \\ \tilde{f}_{p_{22}}^{*L} &= \frac{\mathcal{D}_{\sigma_L}E_{22,L}}{\mathcal{D}t} + E_{22,*L} \frac{\mathcal{D}_{\sigma_L}\sigma_L}{\mathcal{D}t} - \frac{1}{2}u_{2,*L}^2(u_{1,*} - \sigma_L) \left(\frac{\mathcal{D}_{\sigma_L}\rho}{\mathcal{D}t}\right)_{*L} - E_{22,*L} \left(\frac{\mathcal{D}_{\sigma_L}u_1}{\mathcal{D}t}\right)_{*L} \\ &\quad - (2E_{12,*L} - \rho_{*L}u_{2,*L}\sigma_L) \left(\frac{\mathcal{D}_{\sigma_L}u_2}{\mathcal{D}t}\right)_{*L} - u_{2,*L} \left(\frac{\mathcal{D}_{\sigma_L}p_{12}}{\mathcal{D}t}\right)_{*L},\end{aligned}$$

with

$$\begin{aligned}\frac{\mathcal{D}_{\sigma_L}E_{22,L}}{\mathcal{D}t} &= \frac{1}{2}u_{2,L}^2(u_{1,L} - \sigma_L) \frac{\mathcal{D}_{\sigma_L}\rho_L}{\mathcal{D}t} + E_{22,L} \frac{\mathcal{D}_{\sigma_L}u_{1,L}}{\mathcal{D}t} + (2E_{12,L} - \rho_L u_{2,L}\sigma_L) \frac{\mathcal{D}_{\sigma_L}u_{2,L}}{\mathcal{D}t} \\ &\quad + u_{2,L} \frac{\mathcal{D}_{\sigma_L}p_{12,L}}{\mathcal{D}t} + \frac{1}{2}(u_{1,L} - \sigma_L) \frac{\mathcal{D}_{\sigma_L}p_{22,L}}{\mathcal{D}t} - E_{22,L} \frac{\mathcal{D}_{\sigma_L}\sigma_L}{\mathcal{D}t}, \\ \left(\frac{\mathcal{D}_{\sigma_L}u_2}{\mathcal{D}t}\right)_{*L} &= \left(\frac{\mathcal{D}u_2}{\mathcal{D}t}\right)_{*L} - \frac{\sigma_L - u_{1,*}}{p_{11,*}} \left[ \left(\frac{\mathcal{D}p_{12}}{\mathcal{D}t}\right)_{*L} - \frac{2p_{12,*L}}{3p_{11,*}} \left(\frac{\mathcal{D}p_{11}}{\mathcal{D}t}\right)_{*} \right], \\ \left(\frac{\mathcal{D}_{\sigma_L}p_{12}}{\mathcal{D}t}\right)_{*L} &= \left(\frac{\mathcal{D}p_{12}}{\mathcal{D}t}\right)_{*L} - \rho_{*L}(\sigma_L - u_{1,*}) \left(\frac{\mathcal{D}u_2}{\mathcal{D}t}\right)_{*L}, \\ \frac{\mathcal{D}_{\sigma_L}p_{22,L}}{\mathcal{D}t} &= (\sigma_L - u_{1,L})p'_{22,L} - p_{22,L}u'_{1,L} - 2p_{12,L}u'_{2,L}.\end{aligned}$$

#### Appendix D. Computing $\left(\frac{\partial u_2}{\partial t}\right)_{*R}$ , $\left(\frac{\partial p_{12}}{\partial t}\right)_{*R}$ and $\left(\frac{\partial p_{22}}{\partial t}\right)_{*R}$ for the 6-rarefaction wave.

Denote  $\hat{\beta} := u_1 + c$ ,  $\varphi_1 := u_1 - c$ ,  $\varphi_2 := u_2 - \frac{\sqrt{3}p_{12}}{\sqrt{\rho p_{11}}}$  and  $\varphi_3 := \frac{p_{12}}{\rho^3}$ . For the 6-rarefaction wave, one can obtain the values of  $\left(\frac{\mathcal{D}u_2}{\mathcal{D}t}\right)_{*R}$  and  $\left(\frac{\mathcal{D}p_{12}}{\mathcal{D}t}\right)_{*R}$  by solving the following system

$$\begin{cases} a_{3,R} \left(\frac{\mathcal{D}u_2}{\mathcal{D}t}\right)_{*R} + b_{3,R} \left(\frac{\mathcal{D}p_{12}}{\mathcal{D}t}\right)_{*R} = d_{3,R}, \\ a_{4,R} \left(\frac{\mathcal{D}u_2}{\mathcal{D}t}\right)_{*R} + b_{4,R} \left(\frac{\mathcal{D}p_{12}}{\mathcal{D}t}\right)_{*R} = d_{4,R}, \end{cases}$$

where

$$\begin{aligned}
a_{3,R} &= 1 - \frac{\sqrt{3}\rho_{*R}u_{1,*}}{\sqrt{\rho_{*R}p_{11,*}}} + \frac{1}{c_{*R}} \left( \widehat{\beta}_{*R} + \frac{\widehat{\beta}_{*R} - \widehat{\beta}_R}{4} \varphi_{1,R} \right), \quad b_{3,R} = \frac{u_{1,*}}{p_{11,*}} - \frac{\sqrt{3}}{\sqrt{\rho_{*R}p_{11,*}}}, \\
d_{3,R} &= \left[ -\frac{\Pi_{2,R}}{2c_R} - \varphi'_{2,R} + \frac{\Pi_{2,R}}{8c_R} (\widehat{\beta}_{*R} - \widehat{\beta}_R) \right] \varphi_{1,R} + \frac{1}{2c_{*R}} \left( \widehat{\beta}_{*R} + \frac{\widehat{\beta}_{*R} - \widehat{\beta}_R}{4} \varphi_{1,R} \right) \left\{ \frac{2p_{12,*R}}{p_{11,*}} \left[ \left( \frac{\mathcal{D}u_1}{\mathcal{D}t} \right)_* + \frac{1}{2} W_x(0) \right] \right. \\
&\quad \left. + \frac{\rho_{*R}^2 p_{12,*R} S'_{1,R} c_{*R}}{2c_R p_{11,*}} \right\} - \frac{\sqrt{3}p_{12,*R}}{2\rho_{*R}\sqrt{\rho_{*R}p_{11,*}}} \left( \frac{\partial \rho}{\partial t} \right)_{*R} - \frac{\sqrt{3}p_{12,*R}}{2p_{11,*}\sqrt{\rho_{*R}p_{11,*}}} \left( \frac{\partial p_{11}}{\partial t} \right)_{*R} + \frac{2u_{1,*}p_{12,*R}}{3p_{11,*}^2} \left( \frac{\mathcal{D}p_{11}}{\mathcal{D}t} \right)_*, \\
a_{4,R} &= \frac{1}{\rho_{*R}^2} \left[ u_{1,*} - \frac{1}{2} \left( \widehat{\beta}_{*R} + \frac{\widehat{\beta}_{*R} + \widehat{\beta}_R}{4} \varphi_{1,R} \right) \right], \quad b_{4,R} = \frac{1}{\rho_{*R}^3} \left[ 1 - \frac{1}{2c_{*R}} \left( \widehat{\beta}_{*R} + \frac{\widehat{\beta}_{*R} + \widehat{\beta}_R}{4} \varphi_{1,R} \right) \right], \\
d_{4,R} &= \left[ -\frac{\Pi_{4,R}}{2c_R} - \varphi'_{3,R} + \frac{\Pi_{4,R}}{8c_R} (\widehat{\beta}_{*R} - \widehat{\beta}_R) \right] \varphi_{1,R} + \frac{3p_{12,*R}}{\rho_{*R}^4} \left( \frac{\partial \rho}{\partial t} \right)_{*R} + \frac{1}{2c_{*R}} \left( \widehat{\beta}_{*R} + \frac{\widehat{\beta}_{*R} - \widehat{\beta}_R}{4} \varphi_{1,R} \right) \\
&\quad \left\{ -\frac{3p_{12,*R}}{\rho_{*R}^3 c_{*R}} \left[ \left( \frac{\mathcal{D}u_1}{\mathcal{D}t} \right)_* + \frac{1}{2} W_x(0) \right] - \frac{p_{12,*R}}{p_{11,*}\rho_{*R}^3} \left( \frac{\mathcal{D}p_{11}}{\mathcal{D}t} \right)_* - \frac{3p_{12,*R} S'_{1,R}}{\rho_{*R} c_R} \right\},
\end{aligned}$$

with

$$\begin{aligned}
\Pi_{2,R} &= \frac{2}{\rho_R} p'_{12,R} - \frac{3p_{12,R}}{2\rho_R^2} \rho'_R - \frac{3p_{12,R}}{2\rho_R p_{11,R}} p'_{11,R}, \\
\Pi_{4,R} &= -\frac{c_R}{\rho_R^3} p'_{12,R} + \frac{p_{12,R}}{\rho_R^3} u'_{1,R} - \frac{p_{11,R}}{\rho_R^3} u'_{2,R} + \frac{3p_{12,R} c_R}{\rho_R^4} \rho'_R, \\
\varphi'_{2,R} &= u'_{2,R} - \frac{\sqrt{3}}{\sqrt{\rho_R p_{11,R}}} p'_{12,R} + \frac{\sqrt{3}p_{12,R}}{2\rho_R \sqrt{\rho_R p_{11,R}}} \rho'_R + \frac{\sqrt{3}p_{12,R}}{2p_{11,R} \sqrt{\rho_R p_{11,R}}} p'_{11,R}, \\
\varphi'_{3,R} &= \frac{1}{\rho_R^3} p'_{12,R} - \frac{3p_{12,R}}{\rho_R^4} \rho'_R, \quad S'_{1,R} = \frac{1}{\rho_R^3} (p'_{11,R} - c_R^2 \rho'_R).
\end{aligned}$$

After obtaining the values of  $\left( \frac{\mathcal{D}u_2}{\mathcal{D}t} \right)_{*R}$  and  $\left( \frac{\mathcal{D}p_{12}}{\mathcal{D}t} \right)_{*R}$ , one can get the values of  $\left( \frac{\partial u_2}{\partial t} \right)_{*R}$  and  $\left( \frac{\partial p_{12}}{\partial t} \right)_{*R}$  by (2.11).

The value of  $\left( \frac{\partial p_{22}}{\partial t} \right)_{*R}$  can be obtained from

$$\left( \frac{p_{11}}{\rho^4} \frac{\partial p_{22}}{\partial t} \right)_{*R} = -\frac{S'_{2,R}}{c_R} c_{*R} u_{1,*} - \left( \frac{p_{22}}{\rho^4} \frac{\partial p_{11}}{\partial t} \right)_{*R} + \left( \frac{2p_{12}}{\rho^4} \frac{\partial p_{12}}{\partial t} \right)_{*R} + \left( \frac{4 \det(\mathbf{p})}{\rho^5} \frac{\partial \rho}{\partial t} \right)_{*R},$$

where

$$S'_{2,R} = \frac{p_{11,R}}{\rho_R^4} p'_{22,R} + \frac{p_{22,R}}{\rho_R^4} p'_{11,R} - \frac{2p_{12,R}}{\rho_R^4} p'_{12,R} - \frac{4 \det(\mathbf{p}_R)}{\rho_R^5} \rho'_R.$$

## Appendix E. The sonic case when the $t$ -axis is located inside the 6-rarefaction wave.

For the sonic case that the  $t$ -axis is located inside the 6-rarefaction wave, one has

$$\begin{aligned}
\left( \frac{\partial u_1}{\partial t} \right)_0 &= \frac{1}{2} \left[ \widetilde{d}_{R,0} - \frac{1}{2} W_x(0) \right], \\
\left( \frac{\partial p_{11}}{\partial t} \right)_0 &= -\frac{\rho_0 c_0}{2} \left[ \widetilde{d}_{R,0} + \frac{1}{2} W_x(0) \right], \\
\left( \frac{\partial \rho}{\partial t} \right)_0 &= \frac{1}{c_0^2} \left[ \left( \frac{\partial p_{11}}{\partial t} \right)_0 - \frac{S'_{1,R}}{c_R} \rho_0^3 u_{1,0}^2 \right],
\end{aligned}$$

where

$$\widetilde{d}_{R,0} = -\frac{\rho_R^2 S'_{1,R}}{4c_R^3} u_{1,0} (3c_R^2 + u_{1,0}^2) - 2\varphi'_{1,R} u_{1,0} - \frac{1}{2} W_x(0),$$

with

$$\varphi'_{1,R} = u'_{1,R} - \frac{1}{\rho_R c_R} p'_{11,R} - \frac{\rho_R^2}{2c_R} S'_{1,R}.$$

The values of  $\left(\frac{\partial u_2}{\partial t}\right)_0$  and  $\left(\frac{\partial p_{12}}{\partial t}\right)_0$  are obtained by solving the following system

$$\begin{cases} \tilde{a}_{3,R,0} \left(\frac{\partial u_2}{\partial t}\right)_0 + \tilde{b}_{3,R,0} \left(\frac{\partial p_{12}}{\partial t}\right)_0 = \tilde{d}_{3,R,0}, \\ \tilde{a}_{4,R,0} \left(\frac{\partial u_2}{\partial t}\right)_0 + \tilde{b}_{4,R,0} \left(\frac{\partial p_{12}}{\partial t}\right)_0 = \tilde{d}_{4,R,0}, \end{cases}$$

where

$$\begin{aligned} \tilde{a}_{3,R,0} &= 1 - \frac{\hat{\beta}_R}{4}, \quad \tilde{b}_{3,R,0} = \frac{u_{1,0}}{p_{11,0}} \left(1 + \frac{\hat{\beta}_R}{4}\right), \quad \tilde{a}_{4,R,0} = \frac{\hat{\beta}_R c_0}{4\rho_0^2}, \quad \tilde{b}_{4,R,0} = \frac{1}{\rho_0^3} \left(1 + \frac{\hat{\beta}_R}{2}\right), \\ \tilde{d}_{3,R,0} &= \left(-\frac{\Pi_{2,R}}{2c_R} - \varphi'_{2,R} - \frac{\Pi_{2,R}\hat{\beta}_R}{8c_R}\right) \varphi_{1,R} + \frac{\hat{\beta}_R}{4} \left\{ \frac{2p_{12,0}}{p_{11,0}} \left[ \left(\frac{\partial u_1}{\partial t}\right)_0 + \frac{1}{2}W_x(0) \right] + \frac{S'_{1,R}}{c_R} \left(\frac{c\rho^2 p_{12}}{2p_{11}}\right)_0 \right\} \\ &\quad - \left(\frac{\sqrt{3}p_{12}}{2\rho\sqrt{\rho p_{11}}} \frac{\partial \rho}{\partial t}\right)_0 - \left(\frac{\sqrt{3}p_{12}}{2p_{11}\sqrt{\rho p_{11}}} \frac{\partial p_{11}}{\partial t}\right)_0, \\ \tilde{d}_{4,R,0} &= \left(-\frac{\Pi_{4,R}}{2c_R} - \varphi'_{3,R} - \frac{\Pi_{4,R}\hat{\beta}_R}{8c_R}\right) \varphi_{1,R} + \frac{\hat{\beta}_R}{4} \left\{ \left(\frac{3p_{12}}{\rho^3 u_1}\right)_0 \left[ \left(\frac{\partial u_1}{\partial t}\right)_0 + \frac{1}{2}W_x(0) \right] - \frac{3p_{12,0}}{\rho_0} \frac{S'_{1,R}}{c_R} \right\} + \left(\frac{3p_{12}}{\rho^4} \frac{\partial \rho}{\partial t}\right)_0, \end{aligned}$$

with  $\hat{\beta}_R = u_{1,R} + c_R$ .

The value of  $\left(\frac{\partial p_{22}}{\partial t}\right)_0$  is computed by

$$\left(\frac{p_{11}}{\rho^4} \frac{\partial p_{22}}{\partial t}\right)_0 = \frac{S'_{2,R}}{c_R} c_0^2 - \left(\frac{p_{22}}{\rho^4} \frac{\partial p_{11}}{\partial t}\right)_0 + \left(\frac{2p_{12}}{\rho^4} \frac{\partial p_{12}}{\partial t}\right)_0 + \left(\frac{4 \det(\mathbf{p})}{\rho^5} \frac{\partial \rho}{\partial t}\right)_0.$$

## References

## References

- [1] M. BEN-ARTZI, *The generalized Riemann problem for reactive flows*, Journal of Computational Physics, 81 (1989), pp. 70–101.
- [2] M. BEN-ARTZI AND J. FALCOVITZ, *A second-order Godunov-type scheme for compressible fluid dynamics*, Journal of Computational Physics, 55 (1984), pp. 1–32.
- [3] M. BEN-ARTZI AND J. FALCOVITZ, *Generalized Riemann Problems in Computational Fluid Dynamics*, Cambridge University Press, 2003.
- [4] M. BEN-ARTZI AND J. LI, *Hyperbolic balance laws: Riemann invariants and the generalized Riemann problem*, Numerische Mathematik, 106 (2007), pp. 369–425.
- [5] M. BEN-ARTZI, J. LI, AND G. WARNECKE, *A direct Eulerian GRP scheme for compressible fluid flows*, Journal of Computational Physics, 218 (2006), pp. 19–43.
- [6] C. BERTHON, *Numerical approximations of the 10-moment Gaussian closure*, Mathematics of Computation, 75 (2006), pp. 1809–1831.
- [7] C. BERTHON, B. DUBROCA, AND A. SANGAM, *An entropy preserving relaxation scheme for ten-moments equations with source terms*, Communications in Mathematical Sciences, 13 (2015), pp. 2119–2154.
- [8] B. BISWAS, H. KUMAR, AND A. YADAV, *Entropy stable discontinuous Galerkin methods for ten-moment Gaussian closure equations*, Journal of Computational Physics, 431 (2021), 110148.
- [9] S. L. BROWN, P. L. ROE, AND C. P. T. GROTH, *Numerical solution of a 10-moment model for nonequilibrium gasdynamics*, AIAA 12th Computational Fluid Dynamics Conference, San Diego, USA, AIAA-95-1677-CP, 1995.

- [10] J. CHENG, Z. DU, X. LEI, Y. WANG, AND J. LI, *A two-stage fourth-order discontinuous Galerkin method based on the GRP solver for the compressible Euler equations*, *Computers & Fluids*, 181 (2019), pp. 248–258.
- [11] C. DONG, L. WANG, A. HAKIM, A. BHATTACHARJEE, J. A. SLAVIN, G. A. DiBRACCIO, AND K. GERMASCHEWSKI, *Global ten-moment multifluid simulations of the solar wind interaction with mercury: from the planetary conducting core to the dynamic magnetosphere*, *Geophysical Research Letters*, 46 (2019), pp. 11584–11596.
- [12] Z. DU, *Generalized Riemann problem method for the Kapila model of compressible multiphase flows I: Temporal-spatial coupling finite volume scheme*, arXiv preprint, arXiv:2310.08241, 2023.
- [13] B. DUBROCA, M. TCHONG, P. CHARRIER, V. TIKHONCHUK, AND J.-P. MORREEUW, *Magnetic field generation in plasmas due to anisotropic laser heating*, *Physics of Plasmas*, 11 (2004), pp. 3830–3839.
- [14] EE HAN, J.Q. LI, AND H.Z. TANG, *An adaptive GRP scheme for compressible fluid flows*, *Journal of Computational Physics*, 229 (2010), pp. 1448–1466.
- [15] EE HAN, J.Q. LI, AND H.Z. TANG, *Accuracy of the adaptive GRP scheme and the simulation of 2-D Riemann problems for compressible Euler equations*, *Communications in Computational Physics*, 10 (2011), pp. 577–609.
- [16] Z. HUO AND Z. JIA, *A GRP-based tangential effects preserving, high resolution and efficient ghost fluid method for the simulation of two-dimensional multi-medium compressible flows*, *Computers & Fluids*, (2024), 106261.
- [17] Z. HUO AND J. LI, *A GRP-based high resolution ghost fluid method for compressible multi-medium fluid flows I: One-dimensional case*, *Applied Mathematics and Computation*, 437 (2023), 127506.
- [18] E. A. JOHNSON AND J. A. ROSSMANITH, *Ten-moment two-fluid plasma model agrees well with PIC/Vlasov in GEM problem*, in *Hyperbolic Problems: Theory, Numerics and Applications* edited by T.T. Li and S. Jiang, World Scientific, 2012, pp. 461–468.
- [19] Y.Y. KUANG AND H.Z. TANG, *Second-order direct Eulerian GRP schemes for radiation hydrodynamical equations*, *Computers & Fluids*, 179 (2019), pp. 163–177.
- [20] X. LEI AND J. LI, *A staggered-projection Godunov-type method for the Baer-Nunziato two-phase model*, *Journal of Computational Physics*, 437 (2021), 110312.
- [21] C. D. LEVERMORE, *Moment closure hierarchies for kinetic theories*, *Journal of Statistical Physics*, 83 (1996), pp. 1021–1065.
- [22] C. D. LEVERMORE AND W. J. MOROKOFF, *The Gaussian moment closure for gas dynamics*, *SIAM Journal on Applied Mathematics*, 59 (1998), pp. 72–96.
- [23] J. LI AND G. CHEN, *The generalized Riemann problem method for the shallow water equations with bottom topography*, *International Journal for Numerical Methods in Engineering*, 65 (2006), pp. 834–862.
- [24] J. LI AND Z. DU, *A two-stage fourth order time-accurate discretization for Lax–Wendroff type flow solvers I. Hyperbolic conservation laws*, *SIAM Journal on Scientific Computing*, 38 (2016), pp. A3046–A3069.
- [25] J. LI, Q. LI, AND K. XU, *Comparison of the generalized Riemann solver and the gas-kinetic scheme for inviscid compressible flow simulations*, *Journal of Computational Physics*, 230 (2011), pp. 5080–5099.
- [26] J. LI, T. LIU, AND Z. SUN, *Implementation of the GRP scheme for computing radially symmetric compressible fluid flows*, *Journal of Computational Physics*, 228 (2009), pp. 5867–5887.

- [27] J. LI AND Y. ZHANG, *The adaptive GRP scheme for compressible fluid flows over unstructured meshes*, Journal of Computational Physics, 242 (2013), pp. 367–386.
- [28] A. K. MEENA AND H. KUMAR, *Robust MUSCL schemes for ten-moment Gaussian closure equations with source terms*, International Journal on Finite Volumes, 14(2017), pp. 1–34.
- [29] A. K. MEENA AND H. KUMAR, *A well-balanced scheme for ten-moment Gaussian closure equations with source term*, Zeitschrift für angewandte Mathematik und Physik, 69 (2018), pp. 1–31.
- [30] A. K. MEENA AND H. KUMAR, *Robust numerical schemes for two-fluid ten-moment plasma flow equations*, Zeitschrift für angewandte Mathematik und Physik, 70 (2019), pp. 1–30.
- [31] A. K. MEENA, H. KUMAR, AND P. CHANDRASHEKAR, *Positivity-preserving high-order discontinuous Galerkin schemes for ten-moment Gaussian closure equations*, Journal of Computational Physics, 339 (2017), pp. 370–395.
- [32] A. K. MEENA, R. KUMAR, AND P. CHANDRASHEKAR, *Positivity-preserving finite difference WENO scheme for ten-moment equations with source term*, Journal of Scientific Computing, 82 (2020), p. 15.
- [33] J.-P. MORREEUW, A. SANGAM, B. DUBROCA, P. CHARRIER, AND V. TIKHONCHUK, *Electron temperature anisotropy modeling and its effect on anisotropy-magnetic field coupling in an underdense laser heated plasma*, Journal de Physique IV (Proceedings), 133(2006), pp. 295–300.
- [34] B. NKONGA AND P. CHANDRASHEKAR, *Exact solution for Riemann problems of the shear shallow water model*, ESAIM: Mathematical Modelling and Numerical Analysis, 56 (2022), pp. 1115–1150.
- [35] J. QIAN, J. LI, AND S. WANG, *The generalized Riemann problems for compressible fluid flows: Towards high order*, Journal of Computational Physics, 259 (2014), pp. 358–389.
- [36] J. QIAN AND S. WANG, *High-order accurate solutions of generalized Riemann problems of nonlinear hyperbolic balance laws*, Science China Mathematics, 66 (2023), pp. 1609–1648.
- [37] A. SANGAM, *An HLLC scheme for ten-moments approximation coupled with magnetic field*, International Journal of Computing Science and Mathematics, 2 (2008), pp. 73–109.
- [38] A. SANGAM, J.-P. MORREEUW, AND V. TIKHONCHUK, *Anisotropic instability in a laser heated plasma*, Physics of Plasmas, 14 (2007), 053111.
- [39] C. SEN AND H. KUMAR, *Entropy stable schemes for ten-moment Gaussian closure equations*, Journal of Scientific Computing, 75 (2018), pp. 1128–1155.
- [40] W. SHENG, Q. ZHANG, AND Y. ZHENG, *A direct Eulerian GRP scheme for a blood flow model in arteries*, SIAM Journal on Scientific Computing, 43 (2021), pp. A1975–A1996.
- [41] C.-W. SHU AND S. OSHER, *Efficient implementation of essentially non-oscillatory shock-capturing schemes, II*, Journal of Computational Physics, 83 (1989), pp. 32–78.
- [42] T.-T. LI, D. SERRE, AND H. ZHANG, *The generalized Riemann problem for the motion of elastic strings*, SIAM Journal on Mathematical Analysis, 23 (1992), pp. 1189–1203.
- [43] H. TANG AND T. TANG, *Adaptive mesh methods for one-and two-dimensional hyperbolic conservation laws*, SIAM Journal on Numerical Analysis, 41 (2003), pp. 487–515.
- [44] E. F. TORO, *Riemann Solvers and Numerical Methods for Fluid Dynamics: A Practical Introduction*, Springer Science & Business Media, 2013.
- [45] B. VAN LEER, *Towards the ultimate conservative difference scheme. II. monotonicity and conservation combined in a second-order scheme*, Journal of Computational Physics, 14 (1974), pp. 361–370.

- [46] J.F. WANG, H.Z. TANG, AND K.L. WU, *High-order accurate positivity-preserving and well-balanced discontinuous Galerkin schemes for ten-moment Gaussian closure equations with source terms*, arXiv preprint, arXiv:2402.15446, 2024.
- [47] L. WANG, K. GERMASCHEWSKI, A. HAKIM, C. DONG, J. RAEDER, AND A. BHATTACHARJEE, *Electron physics in 3-D two-fluid 10-moment modeling of Ganymede’s magnetosphere*, Journal of Geophysical Research: Space Physics, 123 (2018), pp. 2815–2830.
- [48] Y. WANG AND J. LI, *Stiffened gas approximation and GRP resolution for compressible fluid flows of real materials*, Journal of Scientific Computing, 95 (2023), p. 22.
- [49] Y. WANG AND S. WANG, *Arbitrary high order discontinuous Galerkin schemes based on the GRP method for compressible Euler equations*, Journal of Computational Physics, 298 (2015), pp. 113–124.
- [50] K. WU AND C.-W. SHU, *Geometric quasilinearization framework for analysis and design of bound-preserving schemes*, SIAM Review, 65 (2023), pp. 1031–1073.
- [51] K. WU AND H. TANG, *A direct Eulerian GRP scheme for spherically symmetric general relativistic hydrodynamics*, SIAM Journal on Scientific Computing, 38 (2016), pp. B458–B489.
- [52] K. WU, Z. YANG, AND H. TANG, *A third-order accurate direct Eulerian GRP scheme for one-dimensional relativistic hydrodynamics*, East Asian Journal on Applied Mathematics, 4 (2014), pp. 95–131.
- [53] K. WU, Z. YANG, AND H. TANG, *A third-order accurate direct Eulerian GRP scheme for the Euler equations in gas dynamics*, Journal of Computational Physics, 264 (2014), pp. 177–208.
- [54] J. XU, M. LUO, J. HU, S. WANG, B. QI, Z. QIAO, *A direct Eulerian GRP scheme for the prediction of gas-liquid two-phase flow in HTHP transient wells*, Abstract and Applied Analysis, 2013 (2013), 171732.
- [55] Z.C. YANG, P. HE, AND H.Z. TANG, *A direct Eulerian GRP scheme for relativistic hydrodynamics: one-dimensional case*, Journal of Computational Physics, 230 (2011), pp. 7964–7987.
- [56] Z.C. YANG AND H.Z. TANG, *A direct Eulerian GRP scheme for relativistic hydrodynamics: two-dimensional case*, Journal of Computational Physics, 231 (2012), pp. 2116–2139.
- [57] Y.H. YUAN AND H.Z. TANG, *Two-stage fourth-order accurate time discretizations for 1D and 2D special relativistic hydrodynamics*, Journal of Computational Mathematics, 38 (2020), pp. 768–796.
- [58] Q. ZHANG AND W. SHENG, *The generalized Riemann problem scheme for a laminar two-phase flow model with two-velocities*, Journal of Computational Physics, 506 (2024), 112929.
- [59] Z. ZHU, Q. CUI, AND G. NI, *A high-resolution scheme for axisymmetric hydrodynamics based on the 2D GRP solvers*, Computers & Fluids, 264 (2023), 105961.
- [60] L. ZOU, *Understand slope limiter—graphically*, arXiv preprint, arXiv:2102.04435, 2021.